19951117 001

Journal of

Rehabilitation
Research and Development

CONTENTS

Scientific/Technical Articles

LETTERS TO THE EDITOR SECTION

Interested readers are encouraged to engage in an exchange of information through this Section. Letters should relate specifically to material published in the *Journal of Rehabilitation Research and Development*. We request that the following information be supplied: full name of the author of the article, title of the article, Volume and Issue number, and the page number on which the article appeared. In addition, we request that the letter contain the full name and academic degree of the letter writer, along with the facility that the writer represents.

We hope to open up an ongoing dialogue between professionals as a means of exchanging information and sharing diverse opinions among disciplines.

Editor
Tamara T. Sowell

EDITOR'S NOTE

Due to circumstances beyond our control, this issue is being published two months later than originally planned. We apologize for any inconvenience this may have caused our authors and readers.

Editor
Tamara T. Sowell

Accesion For		
NTIS CRA&I		☒
DTIC TAB		☐
Unannounced		☐
Justification		
By		
Distribution /		
Availability Codes		
Dist	Avail and / or Special	
A-1		

Available at Government Printing Office Depositories for reading only.

Available in microfilm from University Microfilms International, Inc.

Indexed by:

DTIC QUALITY INSPECTED 5

DTIC QUALITY INSPECTED 5

Purpose and Scope

The *Journal of Rehabilitation Research and Development,* published quarterly, is a scientific rehabilitation research and development publication in the multidisciplinary field of disability rehabilitation. General priority areas are: Prosthetics and Orthotics; Spinal Cord Injury and Related Neurological Disorders; Communication, Sensory and Cognitive Aids; and Gerontology. The *Journal* receives submissions from sources within the United States and throughout the world.

Only original Scientific Rehabilitation Research and Development papers (including Preliminary Studies) will be accepted.

Technical Notes describing techniques, procedures, or findings of original scientific research may be submitted. Clinical Reports are of particular interest. These may be reports of an evaluation of a particular prototype developed, a new clinical technique, or any other topic of clinical interest. Letters to the Editor are encouraged. Books for Review may be sent by authors or publishers. The Editor will select reviewers.

Review Process

Scientific papers submitted to the *Journal* are subject to critical peer review by at least two referees, either editorial board members or ad hoc consultants, who have expertise in a particular subject. To ensure objectivity, anonymity will be maintained between the author(s) and the referees. The final decision as to a paper's suitability for publication rests with the Editor of the *Journal.*

Originality

A letter signed by all authors must confirm that the contribution has not been published by or submitted to another journal.

Instructions to Contributors

Manuscripts should meet the following requirements: 1) Original and in English; 2) Contain an Abstract, Introduction, Method, Results, Discussion, Conclusion, and References; 3) Typewritten, double-spaced with liberal margins, on good quality standard white paper; and, 4) A 3.5 or 5.25 in. (8.9 or 13.3 cm) non-returnable disk, preferably in IBM-PC format–generic ASCII text should accompany the hard copy. If using Macintosh, please so advise in cover letter. Manuscripts generally should not exceed 20 double-spaced typed pages.

Sponsorship: Source of funding must be included and should be listed on the cover page.

Abstracts: An Abstract of 150 words or less must be provided with the submitted manuscript. It should give the factual essence of the article and be suitable for separate publication in index journals.

Key Words: Three to ten key words, preferably terms from the Medical Subject Headings from *Index Medicus* should be provided.

Running Heads: A running head (short title) of fewer than 40 characters, including spaces, should be included.

Figures: Figures are for clarifying the text only, no more than six per article; list legends on a separate sheet and not on the artwork. Graphics (i.e., illustrations, schematics, charts, tables, graphs, etc.) must be camera-ready for printing in black and white, at a 3.5 in. (8.9 cm) width: internal labels must be set in professional type large enough to be read at that size. Avoid using extremely thin lines. Computer-generated graphics must be printed at a density of 300 or more dpi. Photos size: 5 x 7 in. (12.5 x 17.5 cm); photos should have good contrast. Color photos are not acceptable. List number and indicate TOP on typed label affixed to back of figure. Do not *write* on front or back of artwork.

References should be typed separately, double-spaced, and numbered consecutively in the order in which they are first mentioned in the text. References first cited in tables or figure legends should be numbered so that they will be in proper sequence with references cited in text. "Unpublished observations" or "personal communications," for which the author has secured permission of the person cited, should be treated as footnotes and not included in the numbering of the references. Authors are responsible for the accuracy of their references. Please follow these sample formats:

Article. Gilsdorf P, Patterson R, Fisher S. Thirty-minute continuous sitting force measurements with different support surfaces in the spinal cord injured and able-bodied. J Rehabil Res Dev 1991:28:33-8.

Chapter in a Book. Wagner KA. Outcome analysis in comprehensive rehabilitation. In: Fuhrer MJ, ed. Rehabilitation outcomes. Baltimore: Brookes Publishing Co., 1987:233-9.

Published Proceedings Paper. Kauzlarich JJ, Thacker JG. Antiskid wheelchair brake design. In: Proceedings of the 14th Annual RESNA Conference, Kansas City, MO. Washington, DC: RESNA Press, 1991:143-5.

Tables should not duplicate material in text or illustrations. They should be numbered consecutively with Arabic numerals cited in the text. Each table should be typed double-spaced and without vertical lines on a separate sheet and should have a brief title. Short or abbreviated column heads should be used and explained, if necessary, in footnotes.

Mathematical Formulas and Specialized Nomenclature: Traditional mathematical treatments should be extended by adding brief narrative notes of explanation and definitions of terms, as appropriate, to ensure that readers of other disciplines gain the fullest understanding of the material presented. The **Metric System** is requested for use in all quantities in text, tables, and figures.

Permissions and Copyright

Articles published and their original illustrations (unless borrowed from copyright sources) are in public domain. Borrowed illustrations must contain full information about previous publication and credit to be given. Authors must obtain permission to reproduce figures, signed release forms for use of photographs containing identifiable persons, and submit originals of those signed documents with the manuscript.

Review of Proofs

Galley proofs will be sent to the first-named author, unless otherwise requested. To avoid delays in publication, galleys should be checked immediately and returned to the publishers by express mail within five working days. **If not received within the prescribed time, it will be assumed that no changes are needed.**

Reprints Policy/Procedures

The VA will provide 100 reprints free of charge to the first-named author (or other designated corresponding author) of published articles at the time of *Journal* distribution.

Manuscripts should be submitted to:

Editor, *Journal of Rehabilitation Research and Development*
Scientific and Technical Publications Section (117A)
103 South Gay Street—5th floor
Baltimore, MD 21202-4051
Telephones: (410)962-1800, 962-2777
Fax: (410)962-9670
e-mail: pubs@balt-rehab.med.va.gov

BACK ISSUE ORDER FORM

The following back issues and reprints of the *Journal of Rehabilitation Research and Development and Rehabilitation R&D Progress Reports* are available on request, free of charge, when in stock. Check any you wish to receive.

____ Annual Supplement (*PR 1988*)
____ Vol. 26 No. 2 (1989)
____ Vol. 26 No. 3 (1989)
____ Annual Supplement (*PR 1989*)
____ Vol. 27 No. 2 (1990)
____ Vol. 27 No. 3 (1990)
____ Vol. 27 No. 4 (1990)
____ Vol. 28 No. 3 (1991)
____ Vol. 28 No. 4 (1991)
____ Vol. 29 No. 1 (1992) + *JRRD* Index: Vol. 28
____ Vol. 29 No. 2 (1992)
____ Vol. 29 No. 3 (1992)
____ Vol. 29 No. 4 (1992)
____ Vol. 30 No. 1 (1993)
____ Vol. 30 No. 2 (1993)
____ Vol. 30 No. 3 (1993)
____ Vol. 30 No. 4 (1993)
____ Vol. 31 No. 1 (1994) + *JRRD* Index: Vol. 30
____ Vol. 31 No. 2 (1994)
____ Vol. 31 No. 3 (1994)
____ Vol. 31 No. 4 (1994)
____ Vol. 30-31 Annual Supplement (*PR 92-93*) (1994)
____ Vol. 32 No. 1 (1995) + *JRRD* Index Vol. 31
____ Vol. 32 No. 2 (1995)
____ Vol. 32 Annual Supplement (*PR 94*) (1995)

Clinical Publications:
____ Clinical Supplement No. 2 (Choosing A Wheelchair System)
____ Clinical Guide (Physical Fitness/Lower Limb Loss)

Name: _____

Address: _____
　　　　　　　　　Street

_____
　　　City　　　　　　　　　　　State

_____
　　　　　　　Country

Label ID Number: _____

Apt. # _____

Zip Code _____

Postal Code _____

Please mail this form with your request to:
Scientific and Technical Publications Section (117A)
Rehabilitation Research and Development Service
103 South Gay Street
Baltimore, MD 21202-4051

Fax orders accepted:
(410) 962-9670
e-mail: pubs@balt-rehab.med.va.gov

CONTENTS

Scientific/Technical Articles

Contents continued

Clinical Report

Departments

GUEST EDITORIAL

Biomaterials in the 21st Century?

When asked by our Editor to write a guest editorial on Biomaterials for this issue, I began to look for a theme that would crystallize my thoughts. The 21st century is less than 5 years away. That is approximately the time scale of many research projects sponsored by the VA Rehabilitation Research and Development Service. Thus, I face the same challenge that researchers do in trying to develop new or improve already existing materials in the quest for improving our quality of health, extending life spans, or freeing us from pain—where do we go from here?

At present, the biomaterials scientist has the entire gamut of appropriate materials to choose from—metals, alloys, ceramics, polymers, composites—the choice being predicated on a number of factors: location, function, compatibility, availability. Of course, always in mind is the dual concern—the material(s) do not act inimically on the body and vice versa, the body does not affect the material(s) inimically. Thus, we now have joint implants made of various combinations of metals or composites used with ceramics and/or polymers to restore function when it is lost due to accident or pathology; the metals and composites providing the appropriate stiffness and rigidity to support loads; the ceramics and polymers providing low friction surfaces for joint movement. We have sight and sound restored in many instances by the use of biomaterials. Where function involves some sort of stimulus, as in pacemakers or cochlear implants, the electrical systems and the leads must be properly encapsulated in biocompatible materials able to withstand the body's inimical environment for long periods of time. It is similar for synthetic heart valves and vascular replacements. Artificial skin combining synthetic materials with the naturally occurring biopolymer, collagen, saves the lives of burn patients. Many drugs, whose use is required for a specific target (e.g., pills for birth control or nitroglycerin tablets for angina), are taken systemically, which means larger doses than might be required on site. External patches over the heart, which release small amounts of the drug continuously, keep the condition under control. Implantable time-release systems *in situ* for birth control mean significantly lower dosages
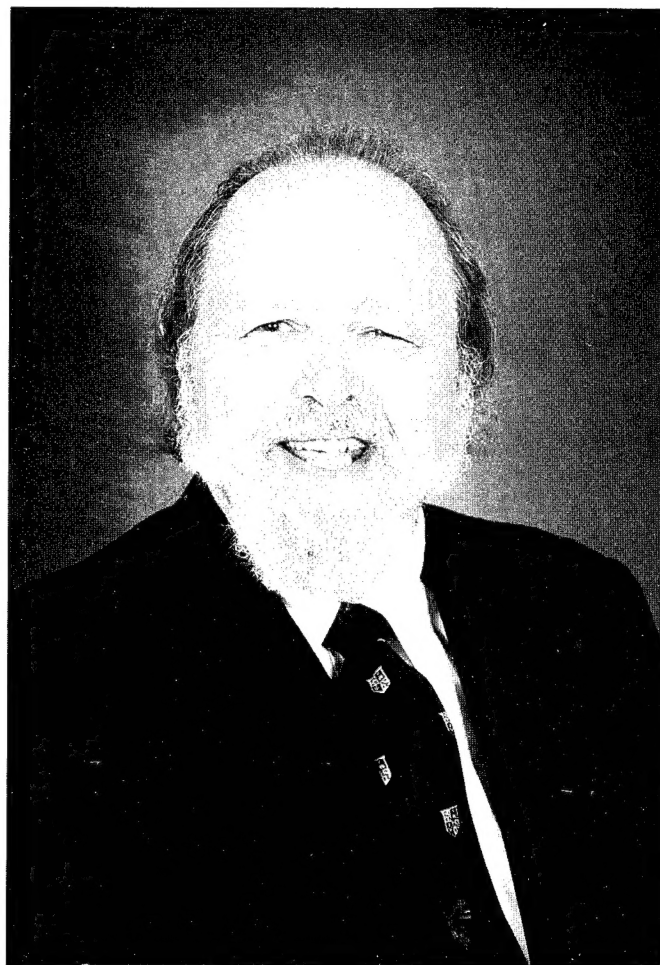
J. Lawrence Katz, Ph.D.
Professor of Biomedical Engineering
Case Western Reserve University
Cleveland, OH

are possible; thus reducing the potential for side effects. Other areas of time-released drug delivery are being developed at present.

In the area of limb prostheses, new composite materials, lighter but with appropriate stiffness and rigidity, are being developed. Direct skeletal attachment of arm and leg prostheses also involves the biomaterials scientist, as stability and longevity of the bone-biomaterials interface in direct skeletal attachment of prostheses is a complex problem

requiring significant research and clinical studies. Dudley Childress, PhD, addressed this issue, in part, in his Guest Editorial in Vol. 30 No. 2, 1993, pp. vii–viii of this *Journal.*

I have covered only a small part of the exciting areas in which biomaterials play a significant role in our lives. However, in the midst of all the glow, a dark shadow has appeared affecting the future in many areas of biomaterials use. Recent law suits on the use of silicone breast implants (often based on very little scientific evidence) have resulted in large settlements. This has, in fact, caused Dow-Corning, producers of medical grade silicone, to declare bankruptcy, solely because of this issue. However, this is not the worst of it. Other major producers of medical grade polymers, used in all manner of implants, now have adopted a policy of not making any polymers of medical grade available for either clinical use or research. The amount of polymers needed for medical purposes is a minute portion of the production of these companies, while law suit settlements can be the major portion of their legal problems. Clearly, any use of such polymers for medical purposes produced by these companies is now prohibited. This is a serious problem that must be addressed and solved by our nation, or the use of biomaterials in the 21st century will be seriously inhibited. Even now, key clinical areas requiring the use of polymers, such as vascular grafts, hydrocephalic shunts, etc., will be severely affected. Research areas, such as the artificial heart program, requiring blood compatible biomaterials, will also suffer setbacks.

We have touched on the past and the present. These help establish the bases for future innovations in biomaterials design and use setting the stage for Biomaterials in the 21st Century. The purely synthetic and generic materials are the museum pieces of the 20th century. Advances and new innovations in scientific instrumentation and techniques for studying material properties and function down to the atomic and molecular level are providing new insights into material-tissue interactions involving interfaces, adhesive

characteristics, compatibility, etc., that will permit the design of "tailor-made" materials for specific uses. The ability to study the interaction between blood components and various synthetic material surfaces using scanning force microscopy utilizing a variety of probes should lead to blood-compatible materials for all sorts of applications. Acoustic microscopy at gigahertz frequencies (billions of cycles/sec) is providing information on elastic properties at sub-micrometer resolution. This information, coupled with electron microscopy for structural studies, could lead to the understanding of how certain tissues, such as bone, are resorbed and regenerated in response to forces. It might then be possible to combine mechanical and biological methods for the regeneration of such tissues rather than use synthetic materials. Natural tissues are also a part of biomaterials research. When tissue regrowth is not a solution, the techniques mentioned above, along with other material procedures, will lead the way to developing biomimetic materials. Biomimetics is the development of synthetic material systems based on information derived from biological systems. Regeneration of natural tissues and biomimetics will be two of the key areas of biomaterials research in the 21st century.

I paraphrase a statement made many years ago by a famous wit—it is very difficult to make predictions, especially about the future. Artificial organs, such as heart, pancreas, kidney, etc.; synthetic blood; regeneration of bone and cartilage; synthetic tendons and ligaments; direct skeletal attachment; artificial vision; spinal fixation; external orthoses and prostheses; pacemakers; vascular grafts; timed drug release; joint replacements, etc.; all depend on biomaterials research. Many are in clinical use at present but are continually undergoing improvement. Many now exist only in the research laboratory or in the minds and notebooks of scientists and clinicians. I predict all these and many other biomaterials usages not listed above will be our heritage in the 21st century.

J. Lawrence Katz, Ph.D.

RETIREMENT OF DR. MED. RENÉ BAUMGARTNER

Dr. med. René Baumgartner, one of the world's leading orthopaedic surgeons in the field of prosthetics and rehabilitation, has recently retired from the medical faculty of the University of Münster in Münster, Germany. Dr. Baumgartner has been Director of the University Clinic for Technical Orthopaedics and Rehabilitation in Münster for many years. At Münster, he has followed in the great tradition of Dr. Hepp and Dr. Kuhn. On July 14, 1995, Dr. Baumgartner delivered his farewell lecture entitled, "From the artificial hand of Goetz von Berlichingen until today."

Dr. Baumgartner has been a prolific writer in the prosthetics field and it is hoped that he will continue to write and practice after his departure from Münster. He is presently finishing a new book on upper extremity amputation and prosthetics care. He is the author of *Amputation und Prothesenversorgung der unteren Extremitat* (Amputation and Prosthetics Management of the Lower Extremity) published by Ferdinand Enke Verlag of Stuttgart, and has a new book on the foot: Die orthopädietechnische Versorgung des Fusses (Technical Orthopaedic Management of Feet), published by Georg Thieme Verlag of Stuttgart. Highly regarded internationally through his writing, he is also known because of his service as Secretary General of the first World Congress of the International Society for Prosthetics and Orthotics (ISPO) in Montreux, Switzerland during 1974.

Not only has Baumgartner continued the Hepp/Kuhn tradition of excellence in prosthetics and rehabilitation at Münster, but he, Dr. Ernst Marquardt (at Heidelberg), and others of their generation continued the advancements begun originally in Germany by Drs. Ferdinand Sauerbruch, Konrad Biesalski, and Max Lebsche. In 1915, Sauerbruch was perhaps the first person to introduce the "clinic team" concept to the prosthetics field and many people regard Biesalski as the father of the rehabilitation concept. René Baumgartner is a man of this line and stature. It is to be hoped that his successor and other young orthopedists in technical orthopaedics and rehabilitation in Germany will follow in his footsteps.

Although Dr. Baumgartner officially retired in February, he will continue duties in Münster until September 1995. In October, he and his wife, Antoinette, plan to move to Switzerland. In 1996, they hope to visit in the USA and Canada. We hope this highly cultured man, this man of depth, compassion, and humor, will visit North America frequently. We have much to learn from him.

Dudley S. Childress, Ph.D.
Director, Northwestern University,
Prosthetics Research Laboratory, Chicago, IL;
Director of Prosthetic Research, VA Medical Center,
Lakeside, Chicago, IL

ERRATA

In Vol. 32 No. 2, page 198, in the Publications of Interest section, the address of the *Contact* for number 176 is incorrect, and should read as follows:

> *Contact*: Dennis A. Chakkalakal, PhD, VA Medical Center,
> 4101 Woolworth Ave., Omaha, NE 68105

In the same issue, on page 204, in the Calendar of Events section, the date, city, and contact listed for the ASHA meeting are incorrect. The listing should read as follows:

> **December 7-10, 1995**
> **American Speech-Language-Hearing Association**
> **(ASHA)** Annual Convention, Orlando, Florida
> *Contact*: Cheryl Russell, ASHA, 10801 Rockville Pike, Rockville, MD
> 20852; Tel (301) 897-5700

Also on page 204 of the same issue, the first listing under 1996 is incorrect. The meeting site for the annual convention of the American Academy of Orthopaedic Surgeons is incorrectly listed. The listing should read as follows:

> **February 22-27, 1996**
> **American Academy of Orthopaedic Surgeons Annual**
> **Convention (AAOS),** Atlanta, Georgia
> *Contact*: AAOS, 6300 North River Road, Rosemont, IL
> 60018-4226; Tel: 708-823-7186; Fax: 708-823-8031

Editor
Tamara T. Sowell

JACQUELIN PERRY, M.D. IS HONORED

Jacquelin Perry, MD, world renowned orthopaedic surgeon, Director of the Pathokinesiology Laboratory at Rancho Los Amigos Medical Center in Downey, California and member of the Editorial Board of the *Journal of Rehabilitation Research and Development*, has received a memorable tribute from the medical center with which she has been associated for many years.

A building at Rancho Los Amigos Medical Center has been dedicated to Dr. Perry and has been named "The Jacquelin Perry Neuro-Trauma Institute and Rehabilitation Center" (JPI).

JPI is a new three-story hospital scheduled to open in the early part of 1996. The Institute will house the neuro-trauma "cluster" consisting of the Spinal Cord Injury, Adult Brain Injury, Pressure Management, and Urology Services.

This addition will allow Rancho to provide "cutting edge" quality care along with the features afforded by a new and modern state-of-the-art building.

Dr. Perry is the foremost leader in the field of gait analysis and pathokinesiology. She has been a long-standing supporter of VA rehabilitation research and development, as well as being instrumental in the early management of post-polio victims.

We applaud Rancho Los Amigos Medical Center for their appreciation and recognition of this outstanding physician.

Tamara T. Sowell
Editor

Clinical Relevance for the Veteran

SUMMARY OF SCIENTIFIC/TECHNICAL PAPERS IN THIS ISSUE

Plantar Pressures with Total Contact Casting.
Jacqueline J. Wertsch, MD;
Lawrence W. Frank, MD; Hongsheng Zhu, PhD;
Melvin B. Price, DPM, PT; Gerald F. Harris,
PhD, PE; Henry M. Alba, MD *(p. 205)*

Purpose of the Work. When a person does not have normal feeling on the bottom of the foot, he/she can develop sores and ulcerated areas on the foot. One of the treatments that has been used is total contact casting. The purpose of this study was to examine how much casting reduces the pressure on the bottom of the foot. **Subjects.** Plantar pressures were collected from six individuals during walking normally and with a total contact cast. **Procedures.** A portable microprocessor-based data-acquisition system was used to record the pressure under the foot with each step. **Results.** The study results showed that total contact casting does reduce high pressure areas on the sole of the foot. **Relevance to Veteran Population.** This study helps define how total contact casting can aid in the management of the individual who has ulcerations on the bottom of his/her foot.
Jacqueline J. Wertsch, MD

A Small and Lightweight Three-Channel Signal-Conditioning Unit for Strain-Gage Transducers: A Technical Note.
Joan E. Sanders, PhD; Lezley M Smith, MSE;
Francis A. Spelman, PhD *(p. 210)*

Purpose of the Work. In Rehabilitation Medicine, biomechanical force measurements on human subjects as they walk are important. For example, force measurements between a residual limb and prosthetic socket during walking potentially provide insight applicable to the design of better prosthetic limbs. Typically, so as not to interfere with a subject's normal motion, it is important that the instrumentation be small and lightweight. The pur-pose of this work was to develop a small and lightweight amplifier for force transducers used in biomechanical assessment. **Procedures.** The dimensions of the unit are 4.5 cm × 3.0 cm × 2.5 cm and an approximate mass of 15 grams. In evaluation studies, it was shown to perform reliably with low noise. **Results.** The unit is being used with normal and shear interface stress transducers to measure interface stresses on persons with lower limb amputation as they walk. **Relevance to Veteran Population.** The device enhances researchers' capabilities to collect relevant biomechanical data, information that potentially can be used to enhance the quality of prosthetic componentry and treatment strategies for the veteran and general populations.
Joan E. Sanders, PhD

Skin Response to Mechanical Stress: Adaptation Rather Than Breakdown—A Review of Literature.
Joan E. Sanders, PhD and Barry S. Goldstein,
MD, PhD *(p. 214)*

Purpose of the Work. Oftentimes, understanding of medical problems in one discipline can be improved by understanding related issues in other disciplines. New ideas are generated which often lead to new perspectives and approaches to medical challenges. The purpose of this review paper is to assemble work in the literature on the adaptation of skin to repetitive mechanical stress. **Procedures.** Papers from disciplines such as Comparative Anatomy and Biomechanics are discussed and put in perspective of how the findings are of relevance to Rehabilitation Medicine. The work is particularly relevant for prosthesis-users and wheelchair-users because their skin must be encouraged to adapt to become load-tolerant before excessive or prolonged weight-bearing is initiated. **Relevance to Veteran Population.** This review provides numerous examples of skin adaptation and provides insight, at a micro-level, of the adaptation process. It sets new directions for scientific research toward a better understanding of skin adaptation and toward developing new therapies to encourage the adaptation processes so that skin breakdown is avoided.
Joan E. Sanders, PhD

Phase Plane Analysis of Stability in Quiet Standing.
Patrick O. Riley, PhD; Brian J. Benda, MS; Kathy M. Gill-Body, MS, PT; David E. Krebs, PhD, PT *(p. 227)*

Purpose of the Work. The Purpose of this work was to determine if center of gravity and center of pressure phase plane (velocity versus displacement) plots provide insight into the dynamic aspect of balance control. **Subjects/Procedures.** We analyzed the standing balance control of 11 healthy subjects and 15 subjects with bilateral vestibular hypofunction (BVH). We altered the base of support and visual information. AP, lateral, and combined stability parameters were calculated based on the root mean square variance of velocity and displacement. **Results.** The phase plane plots and parameters showed changes in stability as base of support was altered or visual input was removed, and revealed stability differences between the control and BVH groups. **Relevance to Veteran Population.** We conclude that phase plane plots are useful in characterizing balance control. Impairment of balance control adversely affects the safety and functional status of many elderly persons including veterans.
Patrick O. Riley, PhD

Asymmetry in Walking Performance and Postural Sway in Patients With Chronic Unilateral Cerebral Infarctions.
Ekaterina B. Titianova, MD, PhD and Ina M. Tarkka, PhD *(p. 236)*

Purpose of the Work. Hemiparetic stroke patients show various degrees of impairments in posture, gait, and voluntary movements. This study was designed to analyze the relationship between gait asymmetry in stroke patients and the ability of the patients to walk with different speeds. **Subjects/Procedures.** Twenty ambulatory patients with chronic infarction in one side of the brain were studied. Gait with five different speeds and standing posture were studied. Results were compared to similar studies performed on age-matched healthy subjects. **Results.** All patients had more asymmetric gait than the normal subjects. Increased lateral sway during standing was indicative of a narrow range of walking velocities among the patients. Interestingly, the overall gait asymmetry did not predict the ability

of a patient to use a range of velocities. Patients with lesions in the right side of the brain seemed to have less walking abilities than patients with lesions in the left side of the brain. **Relevance to Veteran Population.** Gait studies using the methods described in this paper allow objective evaluation of endurance and its development during recovery. Also, subtle changes in the different phases of gait, swing, and stance can be recognized and analyzed. Results may help in adjusting assistive devices.
Ina M. Tarkka, PhD

Strain-Based Fatigue Analysis of Wheelchairs on a Double Roller Fatigue Machine.
J. David Baldwin, PhD and John G. Thacker, PhD *(p. 245)*

Purpose of the Work. Like many other structures, wheelchairs are subjected to loads that vary in time. Such loading is known to cause failure by metal fatigue at intensities significantly lower than the static strength of the structure. The goal of this project was to record the stress variation in wheelchair frames as they were tested on a double roller fatigue machine. From these data, the stress histories could be analyzed and fatigue life estimates could be made. **Subjects/Procedures.** Two wheelchairs, one manual, the other power, were used in this study. Using strain gages, the stresses at three frame locations on each wheelchair were measured as the chairs were run on a double roller fatigue machine. Data were collected by a computer-controlled data acquisition system. The strain histories were used in two ways. First, the strains were converted to von Mises stresses, which were evaluated in terms of maximum and minimum values. Second, the strains were used directly in a strain-based fatigue analysis to compute an estimate of the life to failure for each strain gage location on the frame. **Results.** The stress histories indicated that the frame tubes near their crossing point were the most highly stressed points on the structure. Surprisingly low stresses were recorded in the frame behind the front casters. The fatigue life estimates also indicated the cross tubes as points of anticipated failure. There was a great deal of variability in the life estimates, however, for nominally identical strain histories, indicating the need for multiple replications of the load history record. **Relevance to Veteran Population.** The procedures described here

should guide manufacturers in preparing their wheelchairs for standard fatigue tests and evaluating the structural integrity of their wheelchairs in terms of fatigue life estimates.
J. David Baldwin, PhD

Power Wheelchair Range Testing and Energy Consumption During Fatigue Testing.
Rory A. Cooper, PhD; David P. VanSickle, MS; Steven J. Albright, BS; Ken J. Stewart, BS; Margaret Flannery, BS; Rick N. Robertson, PhD
(p. 255)

Purpose of the Work. The purpose of this study was to evaluate the feasibility of three methods of estimating power wheelchair range. Another significant purpose was to compare the current draw on pavement to current draw on an ISO Double Drum Tester at one meter per second. **Procedures.** Tests were performed on seven different unloaded power wheelchairs, and loaded with an ISO 100 kg test dummy. Each of the chairs was configured per the manufacturer's specifications, and tires were properly inflated. Experienced test technicians were used for the tennis court tests and treadmill tests. An ISO 100 kg test dummy was used for the ISO Double Drum Test. Energy consumption was measured over a distance of 1500 meters for each of the three test conditions. The rolling surface was level in all cases. **Results.** The range of a power wheelchair depends on many factors, including battery type, battery state, wheelchair/rider weight, terrain, the efficiency of the drive train, and driving behavior. The predicted range for the tennis court test at maximum speed ranges from a low of 23.6 to a high of 57.7 km. The range of the power wheelchair can be improved by the use of wet lead acid batteries in place of gel lead acid batteries. **Relevance to Veteran Population.** Power wheelchairs provide an important means of mobility for many physically impaired veterans. Wheelchair standards provide a means for clinicians and veterans to compare and contrast various products. The range that a power wheelchair can travel on a single charge is an important factor to consider when selecting a power wheelchair. This study examined factors related to providing consistent and reliable test methods for estimating range. When manufacturers and test laboratories apply these methods, they will attain results suitable for comparison. This information will make it simpler for veterans and clinicians to select the appropriate power wheelchair for each veteran.
Rory A. Cooper, PhD

An Augmented Computer Vision Approach for Enhanced Image Understanding.
Malek Adjouadi, PhD; John Riley, ME; Frank Candocia, ME; Jean Andrian, PhD; Habibie Sumargo, ME *(p. 264)*

Purpose of the Work. The work presented here constitutes an approach in exploiting image information acquired by the camera(s) in order to yield useful three-dimensional (3-D) descriptions of the viewed environment. A primary objective sought is the development of algorithms that seek efficient and reliable guidance cues with the intent to improve the mobility needs of individuals who are blind. **Procedures.** A mathematical framework is provided pertaining to the development of suitable 3-D descriptions of the viewed real world. **Results.** The research efforts have thus far yielded imaging techniques which (*a*) provided guidance cues on simple indoor and outdoor scenes, (*b*) detect drop-offs or depressions, (*c*) discriminate upright objects from flat objects, and other debris, and (*d*) identify important objects such as stairs, crosswalks, and shadows (false alarms) under different situations. The concepts of spatially and spectrally augmented computer vision toward enhanced analysis and understanding refer, respectively, to 1) the inclusion of the stereo disparity measure (1/2-D) along with the (2-D) images, together yielding the augmented (2 1/2-D) representation, and 2) the implementation of the multiresolution concept of the wavelet theory to analyze and assess in detail the local properties of images. **Relevance to Veteran Population.** To yield purposeful 3-D views of the environment.
Malek Adjouadi, PhD

Plantar pressures with total contact casting

Jacqueline J. Wertsch, MD; Lawrence W. Frank, MD; Hongsheng Zhu, PhD; Melvin B. Price, DPM, PT; Gerald F. Harris, PhD, PE; Henry M. Alba, MD

Clement J. Zablocki VA Medical Center, Milwaukee, WI 53295; Medical College of Wisconsin, Milwaukee, WI 53201; Rehabilitation Institute of Chicago, Chicago, IL 60611; Marquette University, Milwaukee, WI 53233

Abstract—Total contact casting has been used to aid in the healing of plantar neurotrophic ulcerations. The efficacy of total contact casts in promoting ulcer healing is presumably due to a reduction in the load over high pressure areas with pressure redistribution over the entire surface of the foot. The purpose of this study was to quantify the effectiveness of total contact casting in reducing plantar pressures. A portable microprocessor-based data-acquisition system was used for recording plantar pressures. Plantar pressures were collected from six nondisabled individuals with and without total contact casting at cast-walking cadence. In our study, there was a decrease in plantar loading under the metatarsal heads (first, fourth, fifth), the great toe, and the heel. The average decrease was 32% under the fifth metatarsal, 63% under the fourth metatarsal, 69% under the first metatarsal, 65% under the great toe, and 45% under the heel. Our study quantitatively showed that total contact casting does reduce vertical plantar pressures in high load areas.

Key words: *casts, diabetic neuropathies, gait, plantar pressure.*

INTRODUCTION

Total contact casts have been used for decades to promote healing of plantar ulcerations secondary to neuropathy. This technique was originally described in the 1930s by Dr. Joseph Kahn in patients with Hansen's disease (1). Dr. Paul Brand expanded the application of total contact casting to neuropathic ulceration in diabetes mellitus which has been pursued by Dr. Helm and her colleagues (2–4). Total contact casting has been used not only in diabetic neuropathies but also in plantar ulcerations due to alcoholic neuropathy, syringomyelia, tabes dorsalis, yaws, spina bifida, and Charcot-Marie-Tooth disease (5,6). Dr. Myerson and associates demonstrated that the total contact cast provided safe, reliable, and cost-effective treatment for neuropathic ulcers of the foot (7).

The efficacy of total contact casts in promoting ulcer healing is presumably due to reduction of the load over high pressure areas via pressure redistribution over the entire surface of the foot. This concept has not been proven, however. Kominsky hypothesized that there may be two additional factors contributing to plantar unloading (8). First, the total contact cast forces the patient to shorten the stride length and the walking velocity is decreased which diminishes the vertical forces on the foot. Second, the cast eliminates the motion at the ankle joint in the sagittal plane, which in turn decreases the propulsive phase of the gait cycle. Certainly, the most direct effect that the total contact cast has on

the foot is its ability to increase the plantar surface area.

Although total contact casts have been used for decades, only limited studies have been done to quantify changes in plantar pressures. Dr. Dorey studied the effect of a short leg walking cast on the pressures between the cast and leg/foot in the static stance phase by a pneumatic pressure device (9). He found that the walking cast did spread out the weight across the arch and at the edges of the foot. Birke and colleagues investigated plantar pressures inside total contact walking casts for 36 steps using discrete pressure transducers at four sites on the plantar surface: first, third, and fifth metatarsal heads and the heel. They found a relative decrease in plantar pressures over the first and third metatarsal heads (10). Since an oscillographic recorder was used for their study, relative plantar pressures were reported in mm chart deflection instead of absolute pressure values. The purpose of this study was to quantify the changes in plantar pressures over an extended period of continuous cast walking.

METHODS

System Description

The data collection system consisted of eight resistive pressure transducers of 0.5 mm thickness and 11 mm diameter (Interlink Electronics, Santa Barbara, CA 93105) connected to a lightweight microprocessor-based portable pressure recording module carried by the subject in a backpack (11). Transducers were backed by a rigid metal plate to prevent bending artifact and dynamically calibrated with a load cell as the reference. Eight transducers were securely taped over the first, second, fourth, and fifth metatarsal heads, medial and lateral midfoot, calcaneal midline, and plantar aspect of the great toe of the left foot. These positions are common sites of plantar ulceration (12) and have easily palpated anatomical landmarks for consistent application. Consistent transducer location during data collection was assured by inspection of the foot before and after every stage of data collection. The system is capable of continuously sampling 14 channels of pressure data for 7 min at a 35-Hz sample rate. The recorded data are downloaded into a microcomputer through a parallel interface for data processing, analysis, and display.

Subjects

Six males (physicians, residents, and engineers) ranging in age from 25 to 40 years were studied. All subjects were free of gait abnormalities, lower extremity deformaties, edema, ulcers, and vascular disease. All subjects had normal plantar sensation as determined by a threshold Semmes–Weinstein monofilament test (13). This project was approved by the hospital's Human Subject Review Board.

Casting Technique

A total contact cast was applied according to the protocol described by Coleman et al. (14), modified by the application of a fiberglass reinforced outer shell for early weightbearing. The cast was applied with the subject in the prone position on the casting table with the knee flexed at 90°, the ankle joint in pronation and at 90°, and the forefoot in the neutral position. Foam padding (Reston™, 3M Medical-Surgical Division, St. Paul, MN 55144) was applied and placed over the toes to prevent interdigital maceration. A standard stockinette tube was used to cover the foot and leg and carefully trimmed to avoid folds. Both malleoli were covered with disks of 1/4-inch (0.625 cm) orthopedic felt (Zimmer Inc, Warsaw, IN 46580) fixed with paper casting tape. An anterior strip of 1/4-inch (0.625 cm) orthopedic felt was placed over the tibial crest and dorsum of foot. One roll of fast setting plaster (Specialist™, Johnson & Johnson Products, New Brunswick, NJ 08903) was applied, carefully rubbed into all contours of the foot and leg, and allowed to set. Another roll of plaster was applied with five layers of splinting over the plantar surface and toe areas. A 1/4-inch (0.625 cm) plywood board was placed over the plantar surface of the cast. This board extended from the metatarsal heads to mid-heel with the arch of the foot between the plaster layer and plywood board carefully filled in with plaster. A rubber walking heel (Zimmer Inc, Warsaw, IN 46580) was placed at approximately 40 percent of heel-to-toe distance. Two additional 4 in × 4 yd (1.25 cm x 3.66 m) rolls of fiberglass casting material (Zim-Flex™, Zimmer Inc.) were applied for extra strength and early weightbearing.

Test Protocol

Subjects wore extra depth shoes (PW Minor, Batavia, NY 14020) at all times during data collec-

207

WERTSCH, et al. Plantar Pressure/Total Contact Casts

tion except when casted. For each test, the subject walked a total of 720 m (6 laps of 30 m/lap × 4). A total of four sets of plantar pressure data was taken per subject. First, the subject walked at a spontaneous self-selected cadence. After this initial trial a total contact cast was applied. Weightbearing was not allowed for 3 to 4 hrs setting time to assure sufficient hardening of the plaster inner shell. The subject then walked the course with the total contact cast at a comfortable self-selected cadence. After cast removal, data were obtained at the casted cadence with pacing from a metronome. Final data were taken at the initial uncasted cadence, again with pacing via metronome. Pressure data were sampled at a rate of 35 samples per sec.

Data Analysis

Pressure data were collected over four laps of a 30 m course during straight line, steady state walking only. Effects of acceleration and deceleration within 5 m of turnaround points were controlled by rejecting data collected during these periods. Data were taken using the distances and acclimatization as used by Zhu et al. (11) previously. Excluded data included 5 m of deceleration and acceleration at the end points of the course correlated with the timing recorded on a stopwatch separate of the machine. Raw data were inspected for obvious errors. Peak plantar pressures were processed from raw pressure-time data. Data were compiled and analyzed using the student's T-test ($p = 0.05$). Data comparison included analysis of peak pressures at each of the pressure points both with and without the total contact cast at a cast walking cadence. Statistical significance of the pressure differences between total contact cast and non-total contact cast walking was calculated.

RESULTS

Table 1 shows the average peak plantar pressures during both walking with total contact cast and normal walking at casting cadences under the heel; lateral and medial midfoot; first, fourth, and fifth metatarsals; and great toe of the left foot. The range of peak pressures are from 115 kPa to 1082 kPa for normal walking and from 101 kPa to 905 kPa for cast walking. Intersubject standard variations were also shown in the table. Data from the

Table 1.

Peak plantar pressures (kPa) during cast and normal walking.

Sensor Locations	Normal Walking	Cast Walking
Heel	1020 ($\pm$761)	905 ($\pm$673)
Lateral midfoot	262 ($\pm$186)	224 ($\pm$95)
Medial midfoot	115 ($\pm$180)	101 ($\pm$54)
5th metatarsal	273 ($\pm$56)	179 ($\pm$24)
4th metatarsal	440 ($\pm$185)	160 ($\pm$69)
1st metatarsal	602 ($\pm$280)	286 ($\pm$281)
Hallux	1082 ($\pm$566)	333 ($\pm$294)

*kPa = kilopascals (10^3 N/m^2).
Normal walking is at casted cadence.

second metatarsal head were rejected because of failure of the sensor connectors.

Table 2 shows the percentage differences between cast walking and normal walking at cast cadence. There was an average decrease of 32.2 percent (4.7–48.2 percent) in plantar pressures under the fifth metatarsal in all subjects when walking with the cast. There was an average decrease of 63.2 percent (53.5–69.8 percent) in plantar pressures under the fourth metatarsal in all subjects when walking with the cast. There was an average decrease of 65.3 percent (6.5–87.4 percent) in plantar pressures under the great toe in all subjects when walking with the cast. In 5/6 of the subjects, the first metatarsal was unloaded by an average of 68.6 percent (37.8–84 percent). In 4/6 of the subjects, the heel was unloaded by an average of 44.5 percent. In half of the subjects, there was an increase in loading under lateral midfoot with the cast; in the other half, there was a decrease in lateral midfoot loading. In 4/6 of the subjects, the medial midfoot was not loaded during normal walking, but was loaded 59–195 kPa when walking with the total contact cast. The other two subjects did have medial midfoot loading (296–392 kPa) during normal walking. Interestingly, these two subjects showed a decrease in midfoot loading (50–117 kPa) with the cast.

DISCUSSION

Dr. Paul Brand has hypothesized that a difference between the sensate and insensate gait is that

Table 2.
Differences in plantar pressures during cast walking and normal walking (%).

Subjects	Heel	L midfoot	M midfoot	Sensor locations 5th meta.	4th meta.	1st meta.	Hallux
1	− 70.6	+ 47.0		− 48.2	− 53.5	+ 12.8	− 81.9
2	− 5.4	− 48.1	− 83.1	− 34.4	− 69.8	− 81.5	− 6.5
3	+ 681.3	− 0.8	− 70.2	− 47.1	− 63.1	− 37.8	− 76.3
4	− 81.9	− 37.9		− 4.7	− 66.3	− 84.0	− 87.4
5	− 19.9	+ 30.7		− 23.0	− 62.0	− 79.3	− 54.8
6	+ 34.6	+ 122.1		− 36.0	− 64.3	− 60.4	− 84.6

Normal walking is at casted cadence.

over time the sensate will begin to limp to avoid repetitious overloading of a section of the foot (2). The insensate do not get sufficient sensory feedback from the foot and thus do not develop this protective limp. Thus, the insensate can excessively load areas repetitively with resultant tissue damage. Many investigators have shown that diabetic patients produce high pressures over areas of plantar ulceration (15–19). It has been suggested that neurotrophic foot lesions may be due to the lack of this adaptive, protective limp.

Short leg walking total contact casts have been advocated by Brand and Coleman for plantar ulcerations on insensitive feet (14). Dr. Phala Helm et al. studied their clinical efficacy and found that 72.7 percent of their diabetic patients showed healing of their neuropathic ulcerations in an average of 38.3 days (3). Other studies have shown total contact casting resulting in mean healing times ranging from 37.8 to 43.6 days (20–22). Helm et al. also studied the recurrence of neuropathic ulceration following healing in a total contact cast in a 6-year prospective study (4). The main reasons for ulcer recurrence were patient compliance, persistent destructive plantar pressures, unvaried walking patterns, and osteomyelitis. Total contact walking casts have the advantage of increased patient compliance (86.4 percent) over other treatments such as frequent dressing changes, bed rest, and hospitalization (3). Other methods used to treat plantar ulcerations report longer healing times. Molded insoles were reported by Holstein et al. to have a mean healing time of 3.6 months (23). Mueller et al. have shown traditional dressing techniques to have a mean healing time of 65 days (21). The Scotchcast below-ankle boot with pre-cut windows over ulcer

sites has a mean healing time of 3 months, and also has other disadvantages including window edema, and potential damage to healthy tissue surrounding ulcer sites if windows are not trimmed properly (24). Contact casts cost less than dressing supplies over the normal course of treatment, minimize income loss due to inability to work, and minimize interference in activities of daily life. Since casting is an outpatient treatment, use of this technique also reduces hospitalization costs.

Studies by Soames and Zhu et al. have shown an effect of cadence on ground reaction forces (25–27). Soames discovered a positive correlation between increasing cadence and vertical ground reaction force. Since most subjects walk at a slower cadence when wearing the cast, it is important to quantify the contribution of slowed cadence to pressure reduction. To eliminate this effect of cadence on plantar pressures, we used the freely chosen cast cadence for both cast walking and non-cast walking.

The efficacy of total contact casts in promoting ulcer healing is presumably due to a reduction of the load over high pressure areas with pressure redistribution over the entire surface of the foot. In our study, there was a decrease in plantar loading under the metatarsal heads (first, fourth, fifth), the great toe, and the heel. The average decrease was 32 percent under the fifth metatarsal, 63 percent under the fourth metatarsal, 69 percent under the first metatarsal, 65 percent under the the great toe, and 45 percent under the the heel. Our study quantitatively showed that total contact casting does reduce vertical plantar pressures. Shear forces may also play a significant role in plantar ulceration. The effect of total contact casting on plantar shear stress

209

WERTSCH, et al.   Plantar Pressure/Total Contact Casts

is unknown. Further studies are in progress to determine the effects of total contact casting on plantar shear stress.

ACKNOWLEDGMENTS

REFERENCES

1. Khan JS. Treatment of leprous trophic ulcers. Leprosy in India 1939:11:19–21.
2. Brand PW. The diabetic foot. In: Ellenberg M, Rifkin H, eds. Diabetes mellitus. Garden City, NY: Medical Examination Publishing 1983:829–49.
3. Helm PA, Walker SC. Pulliam G. Total contact casting in diabetic patients with neuropathic foot ulcerations. Arch Phys Med Rehabil 1984:65(11):691–3.
4. Helm PA, Walker SC, Pullium GF. Recurrence of neuropathic ulceration following healing in a total contact cast. Arch Phys Med Rehabil 1991:72:967–70.
5. Brenner MA. An ambulatory approach to the neuropathic ulceration. J Am Pod Assoc 1974:64:862.
6. Laing PW, Cogley DI, Klenerman L. Neuropathic foot ulceration treated by total contact casts. J Bone Joint Surg 1991:74–B(1):133–6.
7. Myerson M, Papa J, Eaton K, Wilson K. The total-contact cast for management of neuropathic plantar ulceration of the foot. J Bone Joint Surg 1992:74–A(2):261–9.
8. Kominsky SJ. The ambulatory total contact cast. In: Frykberg RG, ed. The high risk foot in diabetes mellitus. New York: Churchill Livingstone 1991:449–61.
9. Dorey LR. Short leg walking casts: pressure and volume studies. Orthopaedic Seminar 1970:3:69–75.
10. Birke JA, Sims DS, Buford WL. Walking casts: effect on plantar foot pressures. J Rehabil Res Dev 1985:22(3):18–22.
11. Zhu H, Harris GF, Wertsch JJ, Tompkins WJ, Webster JG. A microprocessor-based data acquisition system for measuring plantar pressures from ambulatory subjects. IEEE Trans Biomed Eng 1991:38(7):710–4.
12. Shipley DE. Clinical evaluation and care of the insensitive foot. Phys Ther 1979:59(1):13–8.
13. Birke JA, Sims DS. Plantar sensory threshold in the ulcerative foot. Leprosy Rev 1986:57:261–7.
14. Coleman WC, Brand PW, Birke JA. Total contact casting: a therapy for plantar ulceration on insensitive feet. J Am Pod Assoc 1984:74(11):548–52.
15. Pollard JP, Le Quesne LP. Method of healing diabetic forefoot ulcers. Br Med J 1983:286:436–7.
16. Ctercteko GC, Dhanendran M, Hutton WC, Le Quesne LP. Vertical forces acting on the feet of diabetic patients with neuropathic ulceration. Br J Surg 1981:68:609–14.
17. Stokes IAF, Farris FB, Hutton WC. The diabetic neuropathic ulcer and loads on the foot in diabetic patients. Acta Orthop Scand 1975:46:839–47.
18. Boulton AJM, Hardisty CA, Betts RP, et al. Dynamic foot pressure and other studies as diagnostic and management aids in diabetic neuropathy. Diabetes Care 1983:6(1):26–33.
19. Pollard JP, Le Quesne LP. Forces under the foot. J Biomed Eng 1983:5:37–40.
20. Sinacore DR, Mueller MJ, Diamond JE, et al. Diabetic plantar ulcers treated by total contact casting: a clinical report. Phys Ther 1987:67(10):1543–9.
21. Mueller MJ, Diamond JE, Sinacore DR, et al. Total contact casting in treatment of diabetic plantar ulcers: controlled clinical trial. Diabetes Care 1989:12(6):384–8.
22. Boulton AJM, Bowker JH, Gadia M, et al. Use of plaster casts in the management of diabetic neuropathic foot ulcers. Diabetes Care 1986:9(2):149–52.
23. Holstein P, Larsen K, Sager P. Decompression with aid of insoles in treatment of diabetic neuropathic ulcers. Acta Orthop Scand 1976:47:463–8.
24. Burden AC, Jones GR, Jones R, Blandford RL. Use of the 'scotchcast boot' in treating diabetic foot ulcers. Br Med J 1983:286:1555–7.
25. Soames RW, Richardson RPS. Stride length and cadence: their influence on ground reaction forces during gait. In: Winter DA, Norman RW, Wells RP, Hayes KC, Patla AE, eds. Biomechanics IX–A. Champaign, IL: Human Kinetics Publishers, 1986:406–10.
26. Soames RW. Foot pressure patterns during gait. J Biomed Eng 1985:7(2):120–6.
27. Zhu H, Harris GF, Wertsch JJ. The effect of walking cadence on plantar pressures. Arch Phys Med Rehabil 1991:72:834.

A Technical Note

A small and lightweight three-channel signal-conditioning unit for strain-gage transducers: A technical note

Joan E. Sanders, PhD; Lezley M. Smith, MSE; Francis A. Spelman, PhD

Center for Bioengineering, Regional Primate Research Center, University of Washington, Seattle, WA 98195

Abstract—A small and lightweight signal conditioning unit for use with strain-gage transducers is described. The unit provides bridge-balancing, amplification, and filtering for three channels of Wheatstone bridge circuits. The electronics are housed within a 4.5 cm × 3.0 cm × 2.5 cm box that allows connection to a transducer and to a cable that extends to power supplies and a data storage facility. Evaluation tests showed the signal conditioning unit had low noise (0.356 μV, peak-to-peak, referenced to input) with crosstalk between channels of less than 0.02% of the peak-to-peak input signal. The signal conditioning unit has application in biomechanics where a small and lightweight unit is needed; for example, skin/support interface stress measurements in prosthetics and orthotics research.

Key words: *instrumentation amplifier, prosthetics, signal conditioning, strain-gage transducer.*

INTRODUCTION

Strain-gage transducer applications in biomechanics research can require a small and lightweight

signal conditioning unit. A signal conditioning unit typically provides bridge-balancing, amplification, and filtering for each channel of the transducer and should be positioned as near to the transducing element as possible to avoid noise pickup. Typical cases where a small lightweight unit is required are portable applications where instrumentation must be carried by a moving human or animal subject. For example, skin/support interface stress transducers in prosthetics and orthotics require an unobtrusive unit so that the subject's gait is not altered by the presence of the instrumentation. In addition to being small and lightweight, the unit must be sufficiently durable to withstand the mechanical motion induced during ambulation and the manipulation during application and removal.

Some portable commercial signal conditioning units are available. For example, the 1B31 and 1B32 by Analog Devices (Norwood, MA) provide bridge balancing, amplification, and filtering for a single channel. However, the mounting card is large (11.4 cm × 10.5 cm). Other commercial units offer low noise and excellent performance (e.g., Vishay Amplifier, Micromeasurements Group, Raleigh, NC) but include a power supply within the signal conditioning unit, making it large and heavy. For biomedical applications where it is preferable to house the power supply several centimeters from the transducer, and connect it via a cable (e.g., batteries

211

SANDERS, et al. Signal Conditioner for Strain-Gage Transducers

in a waist belt or a stationary power unit), the availability of commercial products is limited.

In the biomedical literature, several instrumentation amplifier circuits for multichannel applications are described. Most of them are for collecting physiological data such as EEG (1–3) or ECG (4,5). Though the circuits performed well, they were custom-designed for specific applications, fixed in configuration, and thus lacked the versatility for easy change of gain and filter settings. Also, because the circuits had many components, they were large. Discrete fabrication technology was used, increasing the cost and reducing the versatility of the signal conditioning unit.

In this technical note, a small, lightweight three-channel signal conditioning unit for a strain-gage transducer is described. Thirteen modules have been used to record from 13 three-channel strain-gage transducers. The unit allows bridge balancing and changes in gain and filter cut-off frequencies. It is sufficiently durable to withstand mechanical motion induced during ambulation.

METHODS

The signal conditioning unit is a 4.5 cm × 3.0 cm × 2.5 cm box housing electronics for conditioning data from three channels (Figure 1). The unit is designed to be connected to three full Wheatstone bridge circuits, a circuit typically used in strain-gage force transducers. In force measurement systems, three channels are common, one for each of the three orthogonal directions.
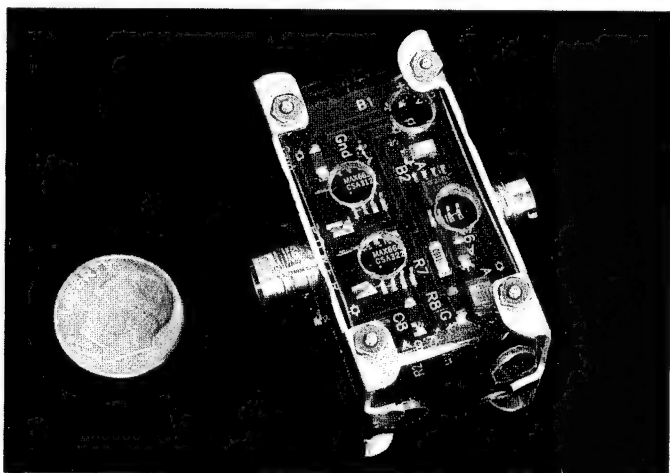
Bridge balancing, amplification, low-pass filtering, and power regulation are performed by low-power surface mount electronic circuitry on boards housed in the unit. A schematic is shown in **Figure 2,** and a list of the principal components is given in **Table 1.** The potentiometers to balance the Wheatstone bridges are accessible through holes in the plastic housing. For amplification, two AD620 instrumentation amplifiers (Analog Devices) are used in cascade. Gains ranging from 0 to 10,000 are possible; gains of 667 V/V, 2604 V/V, or 5538 V/V are typically used. The gain is set by switching R4, R5, or R6 into the circuit. After the second stage amplifier, there is a single-pole, low-pass, passive RC filter set at a cut-off frequency of 106 Hz, a value typical for gait analysis studies. Power regulators are used for the three DC levels for the bridge voltage, positive supply rail, and negative supply rail to limit noise into the bridge and amplifier integrated circuits.

The signal conditioning circuitry for the three-channel unit is on two surface mount boards of dimension 3.7 cm × 2.3 cm × 0.1 cm. A commercial software package (Tango-PCB, Accel Technologies, Inc., San Diego, CA) was used to lay out the boards.

The mechanical housing of the signal conditioning unit was designed to be lightweight and stable but was easily disassembled for access to the boards. A schematic is shown in **Figure 3.** Each of the two aluminum side plates holds one connector, a 12-pin (FR-12S-4, Microtech, Inc., Boothswyn, CT) that connects to the transducer, or a 7-pin (Microtech ER-7S-4) that attaches to a cable extending to power supplies and a data acquisition system. The connectors are modified by making a groove into the connector, then epoxying an external retainer ring (Q-RE-6 and Q-RE-5, Small Parts Inc., Miami Lakes, FL) into the groove to act as a lip that a set screw can hold to the aluminum frame. For four sides of the box, a plastic frame is made by heating a butyrate tube until it is molten and then forming it onto a 3.8 cm × 1.9 cm aluminum block. Holes are made in the walls to allow access to the potentiometers to balance the bridges. Four threaded rods extend through the plastic housing, aluminum plates, and boards to hold the unit together. Once constructed, the unit weighs approximately 15 grams.

Figure 1.
An assembled 3-channel signal conditioning unit.
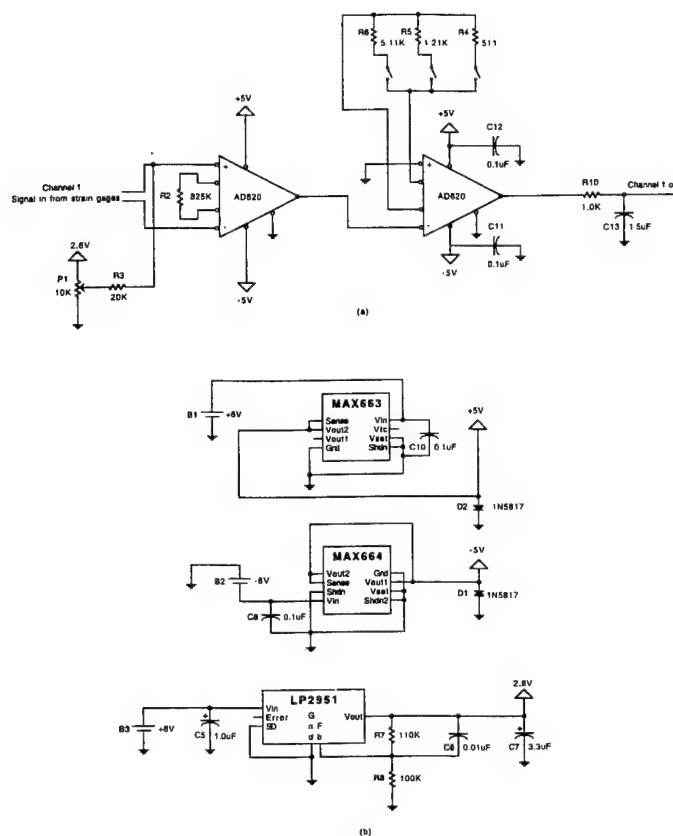
Figure 2.
Electronic schematics of the signal conditioning circuitry: (a) bridge-balancing,
amplification, and filtering for one channel; (b) regulated supply circuits for a
signal conditioning unit. B1, B2, and B3 are batteries.

Table 1.
Electronic componentry used in the three-channel signal-conditioning unit.

Component	Supplier	Part Number
IC amplifier	Analog Devices, Norwood, MA	AD620
Amplifier regulators	Maxim, Sunnyvale, CA	MAX663, MAX664
Bridge regulators	National Semiconductor, Santa Clara, CA	LP2951

RESULTS

Evaluation tests were conducted to determine
the noise, crosstalk, and bandwidth for the signal
conditioning unit. All tests were conducted at the
intermediate gain setting of 2604 V/V. Results
showed that for an input signal of 2.0 mV peak-to-
peak the measured noise referenced to the output

was more than 75dB below the signal of interest.
Using a spectrum analyzer, the circuit demonstrated
a flat passband that had a 3 dB roll-off at 100 Hz.
The group delay in the passband was 500-600 μs,
measured at the cutoff frequency. The delay was
constant for a decade below the cutoff frequency.
Crosstalk to the two off channels when a 2.0 mV
peak-to-peak sine wave was input to the third

213

SANDERS, et al. Signal Conditioner for Strain-Gage Transducers
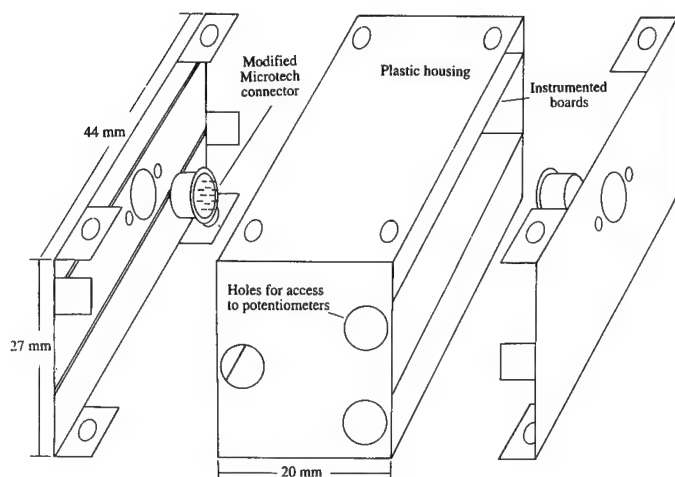
Figure 3.
Mechanical layout of the signal conditioning unit housing. The fasteners to attach the connectors to the aluminum housing and those to hold the unit together are not shown.

channel averaged 0.407 μV peak-to-peak, 0.02 percent of the input signal. The current consumption of a three-channel unit was 30 mA when it was connected to a four-arm bridge where each arm was of 350 ohms resistance.

The signal conditioning unit has been used repeatedly with interface stress transducers mounted on the prosthetic sockets of subjects with amputation. After several hours of ambulation testing, the units showed no degradation in performance and no parts were found loosened.

DISCUSSION

A simple and lightweight unit for conditioning three channels from a strain-gage transducer is described in this technical note. The unit has application principally in force measurement, where force is to be measured in three orthogonal direc-

tions simultaneously. Several units have been used to measure triaxial forces from many locations simultaneously.

Evaluation testing of the unit showed good performance. The on-board regulators minimized noise on the supply lines, a common source of poor circuit performance. Mechanical motion has minimal effect on performance because the unit is small and lightweight and the boards are well-stabilized in the box. The wires extending from the connectors to the boards are the principal sources of noise and crosstalk. However, these levels introduce minimal error to the signal.

The signal conditioning unit has potential use in rehabilitation medicine and other biomedical fields where a small and lightweight unit is required.

REFERENCES

1. Duffy FH. Topographic display of evoked potentials: clinical applications of brain electrical activity mapping (BEAM): evoked potentials. Ann NY Acad Sci 1982:388:183–96.
2. Gruzelier JD, Liddiard D, David L, Wilson L. Topographic mapping of electrocortical activity in schizophrenia during directed nonfocussed attention recognition memory and motor programming. In: Pfurtscheller G, Lopez Da Silva FH, eds. Functional brain imaging. Lewiston, NY: Hans Huber Publishers Inc., 1988:181–6.
3. Duff TA. Topography of scalp recorded potentials by stimulation of the digits. Electroenceph Clin Neurophysiol 1980:49:452–60.
4. Reed EJ, Grinbergen CA, Van Oosterom A. A low-cost 64 channel microcomputer based data acquisition system for bedside registration of body surface maps. In: Proceedings of the 11th International Congress on Electrocardiology, Caen, France, 17-20 July, 1984:37–8.
5. Spekhorst H, SippensGroenewegen A. Body surface mapping during percutaneous transluminal coronary angioplasty: QRS changes indicating regional conduction delay. Circ 1990:81:840–9.

Skin response to mechanical stress: Adaptation rather than breakdown—A review of the literature

Joan E. Sanders, PhD; Barry S. Goldstein, MD, PhD; Daniel F. Leotta, MSEE
*Center for Bioengineering and Department of Rehabilitation Medicine, University of Washington,
Seattle, WA 98195; Seattle VA Medical Center, Seattle, WA 98108*

Abstract—The abnormal loading of skin and other surface tissues unaccustomed to bearing large mechanical forces occurs under many circumstances of chronic disease or disability. A result of abnormal loading is breakdown of the body wall tissues. An effective rehabilitation program avoids the pathological processes that result in skin trauma and breakdown and encourages load-tolerance and adaptation, changes in the body wall so that the tissues do not enter an irreversible degenerative pathological process. In the past, prevention has been the principal approach to the challenge of maintaining healthy skin and avoiding breakdown; therefore, relatively little is described in the rehabilitation literature about skin adaptation. However, adaptation has been investigated in other fields, particularly biomechanics and comparative anatomy. The purpose of this paper is to assemble the research to date to present the current understanding of skin response to mechanical stress, specifically addressing load cases applicable to rehabilitation. Factors important to tissue response are considered and their effects on adaptation and breakdown are discussed.

Key words: *adaptation, bedsores, decubitus, pressure sores, prevention, skin breakdown.*

INTRODUCTION

One of the common manifestations of chronic disease and disability is the abnormal loading of skin and other surface tissues unaccustomed to bearing large mechanical forces. There are many general etiologies, including paralysis, altered sensation, altered level of consciousness, prolonged bedrest and sitting, and the use of an orthosis or prosthesis.

A result of abnormal mechanical loading of surface tissues is breakdown. Though breakdown might appear initially as only a slight reddening of the skin, it can develop into a significant injury that damages tissues through the entire thickness of the body wall. Changes in color of the skin, blisters, bruises, and excoriations often develop and are signs of early breakdown. If loading continues unchanged in an area that demonstrates early breakdown, irreversible injury and necrosis might occur. More extensive pressure ulcers develop which extend deeper into subcutaneous tissues, sometimes into joint or body cavities. Typically, these more extensive ulcers require debridement of necrotic tissues followed by prolonged periods of pressure relief. Both conservative and surgical treatment programs are then employed to debride the pressure ulcer and allow healing of tissues.

The principal approach in the past to the challenge of maintaining healthy skin and avoiding breakdown has been prevention. For example, patients restricted to bedrest, a subject population at high risk of pressure ulcer formation, will be turned frequently by the nursing staff to relieve prolonged pressure. Mattresses designed to cyclically change the distribution of pressure have been developed.

Address all correspondence and requests for reprints to: Joan E. Sanders, PhD, Assistant Professor, Center for Bioengineering, Box 357962, University of Washington, Seattle, WA 98195; e-mail: sanders@limbs.bioeng.washington.edu.

215

SANDERS, et al. Skin Response to Mechanical Stress

Similarly, custom-designed wheelchair cushions are manufactured to help distribute the load more evenly. Further, patients in wheelchairs are taught to conduct pressure releases regularly to prevent breakdown. Patients with altered sensation use timers to indicate when pressure releases should be conducted, and they undergo extensive educational programs to encourage effective prevention practices. For patients with limb deficiencies, orthoses and prostheses are custom-designed so as to distribute forces properly at the body support interface in a manner that avoids skin breakdown. Thus, current prevention programs are designed to reduce force levels and loading durations below those that cause breakdown.

Ideally, tissue pressure management and prevention programs would eliminate all skin breakdown. However, attempting to reduce force levels and durations conflicts with life and functional activities. Mechanical forces and/or load durations are now induced in regions that do not typically bear such high loads. For example, in spinal cord injury (SCI) patients, the sacral and ischial regions are subjected to large pressures during sitting. Persons with below-knee amputation will typically expose the antero-distal regions of their residual limbs to excessive normal and shear stresses due to interaction with the prosthetic socket during ambulation. It is important to recognize that the load levels are much higher than those typically borne by the tissues at these sites. Frequently, breakdown occurs, particularly during the early weightbearing period, and results in increased costs, prolonged hospitalization, increased morbidity and mortality, lost time at work and home, and psychological trauma.

Scope and Cost of Skin Breakdown. The scope and cost of skin breakdown in the US are staggering. Research studies show a prevalence of decubitus ulcers in 11 percent of the hospitalized population and in 20 percent of nursing home residents at any given time (1). For patients in nursing homes, the prevalence of pressure sores (of Grade 2 or greater) ranges from 7 to 35 percent (2), resulting in a four-fold increase in mortality (3). In SCI patients, pressure ulcer incidence is as high as 42 to 85 percent in some centers (4). Amputees using prosthetic limbs are also at risk of breakdown, as a result of the mechanical forces at the residual limb-socket interface. Over 43,000 new major amputations are performed per year in the US (5), with 58 percent of

them on patients between the ages of 21 and 65 years (trauma, cancer, congenital). Thus, there is a significant patient population of young people with amputation, a group likely to conduct strenuous activities when using their prosthetic limbs. For those persons with amputation over 50 years old, vascular causes are the etiology in 89 percent of the cases (6). Their skin is typically at high risk of breakdown.

From a financial standpoint, direct medical expenses associated with curing skin that has broken down are tremendous. As an example, the "average" cost of pressure sore treatment was $120,000 per sore in 1987 (7). Total costs for treating pressure sores in the US, including medical and surgical care, hospital bed occupancy, lost time from work, nursing home care, home health care, special equipment, and transportation, are estimated to exceed $3–$7 billion per year (8). Thus, it is clear that skin breakdown induces much hardship and expense, and treatments to avoid breakdown are needed.

Adaptation. Individuals with a chronic disease or disability frequently have conditions that affect body position and mobility. Abnormal loads in areas that are not primarily designed for weightbearing are encountered in these individuals. Therefore, maintenance of skin integrity is one of the primary goals following the onset of a severe disabling condition.

Rehabilitation programs typically focus on prevention and education to avoid the pathological processes that result in skin breakdown. Prevention measures involve the application of interface surfaces (mattresses, cushions, liners) and frequent pressure reliefs to avoid sustained pressures in one position. It is interesting to note that skin and body wall tolerance for sustained pressures typically increases over time (9). Perhaps effective treatment is not exclusively a matter of prevention, reducing the force levels and durations, but also a matter of adaptation or changing of the tissue itself. It is desirable to induce a rehabilitation process that involves adaptation of tissues rather than merely preventing breakdown.

Clinical treatments designed specifically to encourage skin adaptation and avoid breakdown do exist (10–12). A mobilization program for an individual with SCI who has undergone myocutaneous flap surgery for a pressure sore is an excellent example. Postoperatively, the surgical area is not

stressed for approximately 3 weeks. During this period, there is no weightbearing and no range of motion so as to avoid compression and tension on the flap. Subsequently, a typical program might involve several short periods of weightbearing while in bed. The duration of each period will be increased each day after successful completion of the previous day's program. Range of motion and progressive tensile forces will be placed on the surgical region during this same period of time. Finally, a sitting program will begin that also involves progressive increase in weightbearing duration.

Though some clinical treatments designed to encourage adaptation exist, numerous basic and clinical questions remain. How dependent are adaptive changes in the body wall to the magnitude and duration of the applied load? Is response dependent on the direction of the stress, for example, whether pressure, shear, or tension? Without answers to these questions, rational interventions to prevent breakdown and stimulation of adaptation will remain limited.

There is a growing body of biomechanical and comparative anatomical literature that clarifies some of the confounding issues in this area. The purpose of this paper is to review that literature, particularly information addressing skin adaptation to mechanical stress. Factors important to tissue response are considered and their effects on adaptation and breakdown discussed.

Adaptation involves the entire body wall, including loose connective tissue, fat, fascia, and muscle in addition to skin. In this paper, however, we have concentrated on skin and underlying tissue adaptation to mechanical stress, since skin is the most dynamic tissue of the body wall and offers great adaptation potential.

Functional Anatomy of the Body Wall

A presentation of the functional anatomy of the skin and underlying tissue is required for the reader who is less familiar with the anatomy of the body wall. A cross section of skin, with important components labeled, is shown in **Figure 1**. Skin is composed of two principal layers, the epidermis and the dermis, joined by a distinct structure, the dermal-epidermal junction.

The *epidermis,* the outermost and nonvascular layer of the skin, is a cellular layer that varies in
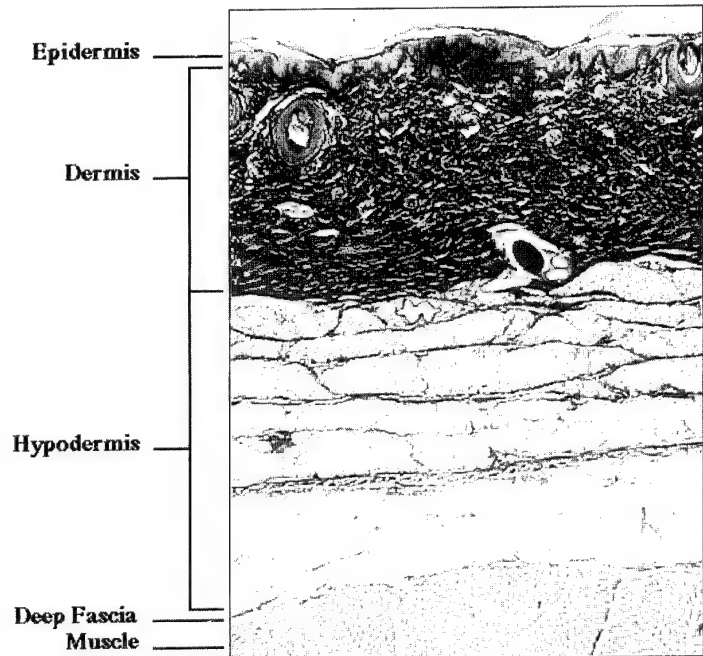
Figure 1.
A cross section of pig skin showing the different layers.

thickness from 0.07 mm to 0.12 mm, except on the palms and soles, where it varies from 0.8 mm to 1.4 mm (13). The epidermis serves to protect against physical and ultraviolet injury, to provide a relatively impermeable barrier to water and chemicals, and to establish a first line of resistance to microbial penetration.

The turnover of the epidermis contributes to the maintenance of its mechanical tolerance. Turnover is achieved by migration of the cells from their origin at the basement membrane, at the separation between the epidermis and dermis, toward the skin surface; this process takes approximately 28 days. As they migrate, cells die, lose their nuclei, and become more pancake-shaped with larger diameters but thinner cross sections, such that the surface area of a cell at the most external layer of the epidermis, the stratum corneum, is approximately 25 times that of one at the basement membrane.

As the cells migrate from the base to the surface of the epidermis, the process of keratinization (the synthesis and deposition of a specific fibrous scleroprotein, keratin, that fills the cytoplasm of the epithelial cells) occurs. Eventually, the epithelial cells die and only the keratin remains. During this process, the keratin molecules are reinforced by

217

SANDERS, et al.   Skin Response to Mechanical Stress

formation of several disulfide bonds. This results in a layer of keratin molecules that are strong, insoluble, and resistant to enzymes and breakdown.

Attachments between cells contribute to the mechanical strength of the epidermis, and they are achieved via the desmosomes (bipartite structures consisting of plaque-like local differentiations on the surfaces of opposing cell membranes). A feltwork of fine filaments spans the gap between the plaques of the two cells. Tonofilaments in the cytoplasm converge on the desmosomal plaque; thus, desmosomes also serve as sites of attachment of the cytoskeleton to the cell surface.

The *dermal-epidermal junction* (DEJ) is an important interface of mechanical attachment between these two distinctly different layers of the skin: the epidermis and the dermis. It is composed of a basement membrane that is wavy in shape with finger-like projections that extend into the dermis. Anchoring filaments (type VII collagen) extend from the dermal side of the basement membrane to plaques (types IV and VII collagen) within the papillary dermis. It has been proposed that attachment of the basement membrane with the underlying collagen fiber matrix (types I and III collagen) is achieved via intertwining of the collagen fibers with the network created by the anchoring filaments and plaques (14).

The DEJ has at least three major functions: it provides a permeable barrier between the vascular dermis and the avascular epidermis; it provides contact between the epidermal cells and the macromolecules within the DEJ, which contact is thought to influence the epidermal cells during their differentiation, growth, and repair; and the DEJ is important for adherence of the epidermis to the underlying tissues. The major point of weakness of the DEJ is considered to be its sublayer, the lamina lucida (15).

The *dermis* is the connective tissue matrix of the skin, providing structural strength, storing water, and interacting with the epidermis. In humans, dermal thickness varies from 1 mm to 3 mm. Its principal components include elastin (0.2 to 0.6 percent by volume; 4 percent by dry weight), collagen (27 to 39 percent by volume; 75 to 80 percent by dry weight), glycosaminoglycans (0.03 to 0.35 percent by volume), water (60 to 72 percent by volume), and cells. Each component has important functions.

Elastin is a fibrous protein that forms a meshlike network in skin. It gives skin its mechanical integrity at low loads, as demonstrated by elastin degradation that causes skin to lose its recoil capability at low force levels (16). Fiber diameters of elastin are approximately 1–3 μm. Each elastin fiber is made up of microfibrils of 10–12 nm diameter. Elastin is produced by fibroblasts.

Collagen is the principal fibrous load-bearing component in skin and provides mechanical integrity at higher load levels. Collagen fiber diameters range from 2–15 μm in skin. Fibers are made up of fibrils, which themselves are approximately 20–100 nm in diameter. Collagen molecules within the fibrils are arranged in a staggered array such that there is a 1/4 length overlap between adjacent molecules, a structure which gives fibrils a striated appearance under the electron microscope. Attachments between collagen molecules are achieved via crosslinks, covalent bonds between lysine residues of constituent collagen molecules. Collagen production involves fibroblast cells.

Collagen remodeling occurs in normal skin, during stress, in pathologic situations, and during wound healing. This remodeling is dependent upon the shifting equilibrium of collagen synthesis and collagen catabolism. The degradation of collagen is initiated by several collagenase enzymes secreted by fibroblasts, epidermal cells, and granulocytes. The enzyme collagenase is representative of a group of connective tissue metalloproteinases responsible for collagen breakdown. Conversely, tissue inhibitors of the metalloproteinases (TIMP) exist. These macromolecules are thought to regulate collagen breakdown (17).

Evidence is accumulating that there is altered skin collagen synthesis and metabolism following SCI. There is evidence that there are qualitative and quantitative changes in skin collagen below the level of injury and as a function of time post-injury (18–21).

Glycosaminoglycans, principally dermatan sulfate, hyaluronic acid, and chondroitin sulfate make up the ground substance surrounding the fibrous components and, with water, contribute to the viscoelastic nature of skin. Glycosaminoglycans are covalently linked to peptide chains to form high-molecular-weight complexes called proteoglycans.

Cells within the dermis include fibroblasts, macrophages, mast cells, and leukocytes. Fibro-

blasts are the principal cells responsible for the creation of collagen, elastin, and glycosaminoglycans. Fibroblasts also play a role in wound healing in that they help to align collagen fibrils with the direction of principal mechanical stress, contributing to closure and strengthening of a healing wound (22).

The vasculature of human skin is composed of two distinct parts, the nutritional capillaries and the thermoregulatory blood vessels. The nutritional capillaries are organized into vertical capillary loops in the papillary dermis, providing nutrients to the upper dermis and basement membrane. The thermoregulatory vessels are larger, deeper vessels that run parallel with the skin surface, assisting in heat transfer to and from the skin.

Subcutaneous Tissue. The skin is connected to the underlying bones or deep fascia by a layer of areolar tissue that varies widely in character in different sites and between species. This layer is well developed in humans and has been named subcutaneous tissue, superficial fascia, or panniculus adiposus.

The limbs and body wall are wrapped in a tough membrane of fibrous tissue called the deep fascia. It varies widely in thickness, although in general it is arranged as an irregular, dense, collagenous, relatively avascular network. The deep fascia serves for attachment of the skin by way of fibrous strands in the subcutaneous tissue. In most areas of the body, underlying muscles are free to glide beneath the deep fascia.

The underlying muscular layer of the body wall consists of skeletal muscles bound together by loose areolar tissues and tougher connective tissue sheaths. The membranous envelope surrounding the entire muscle, the epimysium, is tougher in composition and resembles deep fascia; whereas the delicate endomysium between the individual muscle cells is composed of loose, vascular connective tissues. Muscle tissue is an extremely well-vascularized, aerobic tissue composed of parallel, non-branching striated muscle cells.

Evolutionary and Developmental Adaptation

A correlation between the structural design and mechanical demands in skin is suggested in the evolutionary and developmental literature. The observations are important because they demonstrate changes in structure to sustain high magnitude or prolonged mechanical loads. There are two excellent reviews on the subject (23,24).

Several important findings have been made regarding this correlation.

- Collagen fibers in altricious animals have the same limiting diameter at birth and recommence growth after birth, probably as a consequence of postnatal exercise (24). In contrast, precocious animals, capable of locomotion immediately after birth, contain collagen fibrils which are sufficiently developed at birth to withstand the applied mechanical stresses. The form of the collagen fibril diameter distribution of tendon at birth reflects the degree of development of the animal at this stage of life.
- The ultimate tensile strengths of connective tissues and skin are positively correlated with the mass-average diameter of the collagen fibrils (25).
- Collagen fibril diameter distributions are a function of both the applied stress and its duration. The mechanical properties of a connective tissue are strongly correlated with the collagen fibril diameter distribution (24,26). In general, those skins subjected to increased tensional loads (rat tail skin, trout skin, dorsal skins of mammals) contain collagen fibrils of larger diameter than those skins with lower tension. Collagen fibril diameters were smallest in those skins bearing compression. For example, in guinea pigs fibril diameters were twice as large on the dorsum, a region subjected to tension, than were those of the footpad, a region subjected to high compression or pressure.
- Mammalian and avian body skins generally contain relatively sharp unimodal distributions of fibril diameters consistent with a "passive" mechanical role. Whereas reptilian and fish skins have bimodal distributions of fibril diameters compatible with an "active" biomechanical role typical of those animals with exotendinous skin attributes (26).
- The mechanical properties of a connective tissue are strongly correlated with the type and amount of glycosaminoglycans (23). This positive correlation exists in comparing skins from different sites within an animal, in comparing different species, and in comparing skins at various stages of development (23,27). For example, in altrucial animals, there is a greater content of hyaluronic acid, a proteoglycan functionally designed for its hydrophilic properties but not particularly strong. In precocial animals,

219

SANDERS, et al. Skin Response to Mechanical Stress

their more mature skins at birth contain a greater proportion of sulfated proteoglycans (keratin sulfate), glycosaminoglycans designed to withstand greater mechanical forces.

To summarize: it is possible to make reasonable predictions about the type of force to which connective tissues are subjected by examination of the morphological and biochemical features of 1) the glycosaminoglycan composition and content; 2) the collagen fibril diameter distribution and the mode of packing; 3) the histological staining reaction of the collagen fibers by the Masson trichrome stain; and 4) the axial periodicity of the collagen fibrils (23,24,26).

Short-term Response To Mechanical Stress

The evolutionary relationships between structure and function described above suggest that continual loading induces structural changes in skin that improve load-tolerance. In the short-term, it is also desirable to encourage adaptive changes that increase load-tolerance. However, in the short-term it is also desirable to avoid degradatory processes that result in skin breakdown. Both breakdown and adaptation of skin to mechanical stress are addressed below. The literature on the topic can be divided by loading configuration: pressure, shear and friction, and tension.

Pressure. Pressure is a uniformly distributed force applied perpendicular to the skin surface. The effect of prolonged pressure on the skin of weight-bearing areas has been hypothesized as a major pathophysiologic factor in the development of pressure ulcers. Numerous animal studies and measurements in humans have been conducted in an attempt to demonstrate a pressure-time relationship for skin breakdown (animals: 28–32; humans: 33–36). Most of these investigations discuss the generally accepted model of pressure-induced ischemia leading to tissue necrosis.

In the animal models, external loads were applied to the skin and the tissue response assessed. Various outcomes have been measured including erythema, inflammation, reversible damage, irreversible breakdown, alterations in blood flow, transcutaneous oxygen tension, and temperature, to name a few. Different tissues of the body wall (i.e., epidermis, dermis, subcutaneous layer, and muscle) have been examined. Dinsdale (37), for example, applied

pressures from 45 to 1500 mmHg (6 kPa to 195 kPa) in normal and paraplegic swine for various durations and examined pathomorphological changes over time. He demonstrated epidermal and dermal alterations that preceded pressure ulcers, particularly at higher pressures for longer durations. Husain (32) demonstrated ischemic histologic changes in underlying muscles at 100 mmHg (13 kPa) for 2 hours. Complete muscle necrosis was demonstrated at 100 mmHg (13 kPa) for 6 hours. The changes included venous sludging, venous thrombosis, edema, cellular extravasation, decrease or loss of muscle striations, hyalinization of fibers, neutrophilic infiltration, and phagocytosis by neutrophils and macrophages. Kosiak (31) demonstrated that pressures of 70 mm Hg (9 kPa) for 2 hours resulted in pathologic changes within muscle and that lower pressures of 35 mmHg (5 kPa) for 4 hours resulted in no changes. A clinically accepted relationship between pressure and duration, particularly over bony prominences, has been accepted (38).

The results suggest an important concept. Application of pressures for low or moderate durations is acceptable for intact skin. Damage might occur but is reversible. An equilibrium between breakdown and regeneration is established. Beyond a certain period of time or level of force, however, catabolic processes overcome reparative mechanisms and the net result is tissue breakdown. Thus, attention should be paid to the pressure-time relationship for skin breakdown, and threshold values for pressure and time at which injury occurs should not be exceeded.

A second important concept that has emerged from the research in animal models is that deeper tissues are more vulnerable to injury than skin. Daniel, et al. (28), Groth (29), and Nola and Vistnes (39) all demonstrated the earliest pathologic changes in muscle: with increasing pressure, ulceration progressed in a superficial manner toward the skin.

The pressure-duration relationship is affected by a multitude of intrinsic and extrinsic factors. Moisture, for example, places skin at greater risk for breakdown. A suggested explanation comes from the biomechanics literature. The stiffnesses of both the stratum corneum and the dermis decrease with increased humidity and temperature (40–42) probably because of a reduced load-supporting contribution from the stratum corneum in the epidermis and the glycosaminoglycans in the dermis. The skin

undergoes greater elongation, requiring the collagen to undergo greater strain, and possibly putting cells and the vasculature interspersed among the collagen fibers under greater concentrated stresses and risk of trauma.

Aging, smoking, and immobility are also important factors affecting the pressure-duration relationship (43,44). The thickness of skin decreases with age (45,46). As a result of a reduction in elastin, the elastic range of the skin is decreased. Collagen, proteoglycan, and water content, as well as blood supply, have all been shown to decrease with age, indicating a general atrophy of the body wall. Smoking is also an important risk factor for skin breakdown and is suggested to be related to decreased blood supply to the skin. Immobility results in prolonged pressure over bony prominences and this places an individual at high risk for skin breakdown. Paralysis combines immobility with muscle atrophy. Part of the problem is that the loss of sensation causes the individual to load the skin for extended periods of time without performing pressure reliefs regularly. However, neurogenic skin is also thinner than normal, indicating that a loss of constituents, possibly those important to load-tolerance discussed above, has occurred.

The location of the applied pressure on the skin relative to underlying bone has also been shown clinically to be relevant to the pressure-time relationship. Individuals who are supine in bed for prolonged periods typically break down over the occiput, scapulae, sacrum, and heels; whereas, an individual side-lying will break down over the greater trochanter and the malleoli. If sitting for prolonged periods, such as following a SCI, breakdown typically occurs over bony prominences (i.e., the ischial tuberosity and the sacrum). Persons with below-knee amputation commonly experience problems over the anterior residual limb surface, where skin is directly over bone, as opposed to posteriorly, where there is a thick layer of subcutaneous tissue and muscle. The high sensitivity of skin over bony prominences is explained mechanically. Stresses are concentrated in a very small connective tissue region between the bone and the surface; thus, high stresses and stress gradients, which threaten skin viability, occur. The threshold for injury is thus lower at thin skin sites over bone, and excessive loading should be avoided.

There is evidence that suggests skin can adapt if proper clinical treatments are conducted. Clinical practices dictate some loose rules for adaptation to loading under pressure (10–12). A good example is postsurgical treatment for a myocutaneous flap that has been transferred from an area that did not have much weightbearing. Inspection and palpation are the principal diagnostic tests used to evaluate the progression of skin adaptation. Inspection includes an assessment of erythema, detection of visible open wounds in the skin, and identification of ischemic changes. Palpation allows assessment of edema, and fluid collection in deep tissue layers. The SCI patient will initially lie on the affected region for short periods. If skin redness quickly disappears upon unloading, then another loading period will be conducted. If skin redness persists, then the site will be rested. Bogginess and pitted tissue are likely indicators of tissue breakdown beginning beneath the skin surface. The goal in postoperative treatment of a myocutaneous flap is for continuous sitting from morning until evening with pressure releases several times each hour.

Though descriptions for the early signs of skin breakdown (bogginess, fluid regions) are noted, clinical evaluation for signs of skin adaptation are lacking. Animal studies from the literature, however, provide some insight into structural changes that take place in skin subjected to repeated compression. Though no studies have been reported on skin, studies on tendon do exist. Tendon is a tissue made up of the same types of collagen and glycosaminoglycans as found in skin. In tendon previously under tension but then subjected to pressure, increases in glycosaminoglycan content during remodeling occur (47). In particular, hyaluronic acid and chondroitin sulfate content were found to increase. When tension was restored, the hyaluronic acid and chondroitin sulfate contents returned to normal values. These findings are consistent with the evolutionary changes described above for skin, though changes described in the tendon studied occurred over a relatively short time period. Thus, the literature suggests increases in hyaluronic acid and chondroitin sulfate are indicative of skin adaptation to pressure. Clinically, these changes might be apparent as a change in skin mechanical properties which possibly could be perceived during palpation assessment.

221

SANDERS, et al. Skin Response to Mechanical Stress

Shear and Friction. Shear stress occurs when a force is applied in the plane of the skin surface. Friction occurs when there is displacement between the skin and the supporting surface. For example, a patient with SCI who tilts up in bed from a supine position induces shear stresses in the sacral region over the bone. When there is slip between the skin and the bed, friction is induced. Persons using prosthetic limbs experience shear stresses at the residual limb–socket interface because the socket is designed to bear much of the weight on the sides of the residual limb rather than distally. "Pistoning," displacement of the residual limb relative to the socket, causes frictional loads.

The importance of avoiding shear stress in SCI patients has been addressed. Inducing shear stress at thin skin sites over bone will put excessive tension in the skin, increasing the risk of injury compared with the no-shear case. Effects on blood flow occlusion have been demonstrated. Bennett developed an apparatus to measure the applied pressure, shear, and pulsatile arteriolar blood flow on the palm of the hand near the thumb of human subjects (48). Results showed that at a sufficiently high level of shear, the pressure necessary to produce occlusion was half that required when little shear was present.

A number of clinical and animal studies have been conducted in an attempt to establish a load-time relationship for the threshold of breakdown from frictional stress. Naylor conducted systematic studies of blister formation in response to friction. A machine was used to rub the skin on the anterior tibial surface at a constant speed and with constant perpendicular force, and the frictional forces were recorded (49). Naylor utilized multiple loading regimes with various materials to quantify thresholds of blister formation. He investigated the work needed to produce a blister, defined as the product of the frictional force and the number of rubs. Results on human subjects demonstrated that the lower the frictional force, the greater the amount of work required to rupture the epidermis. In other words, given the choice of receiving a high number of rubs at a low force or a low number of rubs at a high force, the skin is more tolerant of the case of a high number of rubs under low force. Changes in material of the loading head, speed of rubbing, and dermal perfusion did not appear to alter the number of rubs required to produce a blister. Sulzberger, et al. (50) also used a machine to rub the skin, and found a large variation among sites in the work required to produce blisters when the frictional forces were low. It was demonstrated that less time and work were required to produce a blister over thin skin than thick skin, an expected result because of the adapted load-tolerant structure of thick skin. Blisters form more quickly if the skin is heated rather than cooled (51). The frictional force on the skin depends on the amount of moisture at the skin surface. A small amount of water on the skin surface increases the frictional force compared with a dry surface. A large amount of water on the surface decreases the frictional force compared with a dry surface (52).

The above findings are important because they suggest rules for clinical practice. Given a choice of inducing a high force at a low repetition rate rather than a low force at a high repetition rate, the latter should be chosen. For example, an amputee walking up a flight of stairs would put skin at lower risk if he or she were to take one stride per stair rather than one stride per two stairs. A further suggested rule for clinical practice deduced from the shear force literature described above is that a small amount of sweat at the interface will increase frictional forces and increase susceptibility to breakdown. Thus, individuals that sweat often should take precautions to remove the sweat layer frequently or wear materials that absorb sweat well. In addition, if possible, frictional forces should be applied to thick skin sites instead of thin skin locations. Thus, skin structure should be inspected clinically to determine potential regions for load tolerance.

Other researchers have identified important parameters that affect the magnitude of the frictional force at the interface: relevant work because of the significance of force magnitude to tissue response as demonstrated in Naylor's studies described above. Interface materials have been studied by Jagoda, et al. (53), who compared blister formation in a group of Marines in training using different combinations of socks and powders. A green military issue sock worn over a white athletic sock was more effective at preventing blisters than a green issue sock alone or an athletic sock over a nylon sock.

Jagoda found other interesting results. The likelihood of blister formation depended on the running habits of the individual. Those who normally ran more than 30 miles per week were less likely to develop blisters than those who ran less than 10 miles per week, suggesting an adaptive response of the skin on the feet to continual running. In addition, incidence of blisters was highest in the early stages of training, indicating that adaptive changes took time to occur.

Histologically, examination of skin that has broken down under friction has been conducted. A mechanical system to apply an approximately constant normal force and a cyclic shear force to the skin surface was used (49,50). Rubbing was conducted until breakdown occurred. Results demonstrated that friction blisters occurred within the epidermis, as a result of shearing between the epidermis and deeper anchored layers, which creates a zone of damage or cleavage (50). In response to repeated rubbing, the skin becomes red, there is slight flaking of the stratum corneum, and finally the epidermis ruptures suddenly, producing sharp pain and a crater in the skin. Histologically, necrosis of prickle cells, formation of small intra-epidermal vesicles which coalesce to form larger vesicles, and edema in the dermis around blood vessels are observed (49).

The response, blister or abrasion, depends on the structure of the skin and its location on the body. Blister formation requires firm attachment to tissues below and a tough superficial layer. Differential movement of upper layers over lower ones produces shearing which results in a cleft that fills with fluid (54). The tear or cleft appears consistently at the same area in the epidermis: below the granular layer, or stratum granulosum, and above the basal layer, or stratum spinosum (53). Application of a tourniquet or elevation of the loaded region relative to the heart eliminates filling of the blister but the cleft still appears. Friction blisters generally occur only on the palms and soles where the overlying stratum corneum is thick enough to form a roof on the blister. On thinner skin, friction results in an abrasion rather than a fluid-filled pocket. In response to high friction levels, blister formation can occur in several minutes (acute response). If friction levels are below a certain threshold, adaptive thickening of the skin (epidermal hypertrophy) results instead of injury, and

thickening can increase over the course of weeks to months (chronic response).

Adaptation to shear can occur and is encouraged clinically. An ambulation protocol for a person with lower limb amputation is an example. Although the timing of postoperative weightbearing varies among practitioners and patients, increasing weightbearing begins very early postoperatively. Gentle weightbearing might begin as early as 1–2 days postoperatively to stimulate wound healing and begin proprioceptive feedback. The program then progresses with longer durations and increased forces during weightbearing activities. Activities progress through the following stages, progressively stressing the residual limb: gentle touch weightbearing, weight shifting, walking in parallel bars, ambulating with adaptive aids, and finally ambulating without adaptive aids.

An adaptive response to frictional loading is the formation of calluses. Calluses are even thickenings of the keratinized layer of the epidermis which form in response to repeated frictional loads. There is much variability in individual response, with some people tending to blister in response to slight friction, while others immediately develop a callus (55). Damp skin tends to blister, while dry skin tends to develop callosities. An explanation is that the damp skin produces higher friction, above the breakdown threshold for the skin compared with frictional forces induced in dry skin. Thickening of the horny layer, the outermost layer of the epidermis, has been observed in response to ultraviolet light, mechanical, chemical, electrical, and thermal stimulation (56,57).

Other epidermal adaptation studies to friction have been conducted to investigate the processes underlying the epidermal hypertrophy described above and the time course of the response. In mouse ears subjected to frictional loading by a rotating brush, increases in epidermal thickness, mitotic activity, cell sizes, and cell numbers were demonstrated (58,59). The rate of migration of cells from the basement membrane to the stratum corneum was two to three times higher than in the control (59). Several loading regimes were applied. Higher levels of friction (over 10 days) resulted in ulceration followed by epidermal thickening; healing was observed at days 3–4 despite continued application of friction. The 10-day severe friction group showed similar but more accentuated changes than the

223

SANDERS, et al.   Skin Response to Mechanical Stress

35-day moderate friction group (hypertrophy of both stratum corneum and other layers: thickening of stratum Malpighii, increased cells in stratum spinosum and stratum granulosum). Increased cellularity in the dermis was also noted. Changes in the 7-day moderate application group were no different from the 14–35 day groups, indicating that the principal changes in epidermal structure take place within several days. The response is interpreted as a means to maintain the structure of the stratum corneum under stressed condition. In the case of severe friction, the epidermis is able to eventually withstand the original stimulus without damage. Another animal study by Carter (60) based on the brushing of the gums of rats reported an increase in the height of the epithelial papillae (measured as difference between maximum and minimum thickness of epidermis) in the stressed tissue.

The results suggest mechanisms and processes for adaptation to frictional stress. The cells at the basement membrane increase in size, density, and speed of transport across the epidermis, increasing thickness of the stratum corneum layer. The thickened stratum corneum means that there is a greater volume through which to distribute the shear load between the skin surface and immediately above the basement membrane. With a greater volume of stratum corneum, shear stress gradients are lower; thus, the skin is at lower risk of failure.

Tension. Tensile loading occurs when skin is pulled in the plane of its surface. For example, closure of a wound with a suture induces tension across the wound. Swelling induces tensile forces in the skin. Tension also occurs when shear stress is present, for example, near adherent scar tissue or at the distal region of a residual limb as the prosthesis is donned.

Results from interface stress studies on persons with amputation support the importance of tension. Prosthetic socket design practice emphasizes the need to design socket indentations on the tibial flares and posterio-proximally so as to avoid loading the antero-tibial crest region. Interface shear stress studies by Sanders, et al. (61) produced an interesting finding concerning anterior shear stress and skin tension. Sanders found that anterior shear stresses had a high horizontal force component. In other words, the shear stresses were directed away from the crest of the tibia such that skin over the tibial

crest, a region that was not in direct contact with the socket, was put under tension. Excessive tension, and thus tissue injury, could result in skin that was not even in contact with the socket surface. These findings indicate the importance of the distribution of the applied shear stress on the tibial flare regions and that it influences tension in the skin.

Investigators conducting clinical and animal studies have searched for rules on the threshold for breakdown from tension. The research has been conducted principally with reference to the healing wound. The rate at which surgical wounds initially gain tensile strength is slow. The breaking strength of an incisional wound by the end of the postoperative third week has been demonstrated to be only about 20 percent of intact skin (62). The slow rate of gain in tensile strength is explained physiologically. During the initial weeks, granulation tissue formation is occurring, a period in which a loose matrix of collagen and proteoglycans are synthesized and angiogenesis occurs. However, there is then a rapid increase in tensile strength over the following 3 weeks (postoperative fourth to sixth weeks). The increase in tensile strength is thought to be secondary to collagen deposition, collagen remodeling, and, finally, alteration of crosslinks (22).

Factors that affect skin tension have been demonstrated in rehabilitation practice. The shape of the apex angle of the prosthetic socket to control tibial flare shear stress and thus tension over the tibial crest is an excellent example. As a second example, in treatment of SCI patients undergoing myocutaneous flap surgery, during the operative procedure as well as the perioperative period, tension is avoided by having the patient rest in bed. Slow progressive range of motion is conducted postoperatively, putting tension on the wound.

Clinically, encouragement of skin adaptation to tension is practiced. Tissue expansion procedures commonly used to provide skin for reconstructive surgery provide an example. Sacs inserted beneath the skin are slowly inflated over periods of weeks to months, putting the skin in biaxial tension and increasing its surface area. Once sufficient skin is grown using this method, the defect is removed and the skin closed.

Studies on animals have provided some insight into the physiological changes during tissue expansion. In the epidermis, increases in thickness, mitotic activity in basal cells, and undulations of the

basement membrane were noted (63). In the dermis, a decreased thickness, an increased number of active fibroblasts, and an overall increase in the amount of collagen were reported. The papillary and reticular layers were filled with thick bundles of collagen fibers, and elastic tissues were thickened and compacted (64). Thus, results suggest that while a redistribution of the collagen matrix occurred which increased the skin surface area and thereby relieved skin tension, it was also evident that the makeup of the collagen matrix was modified into a more robust structure.

Tissue adaptation in other collagenous tissues provides insight into collagen adaptation. A model developed by Flint (65) allowed study of changes in tendon, a collagenous tissue that has some of the same collagen types as skin, for different loading configurations. The release of normal distractive forces from the rabbit Achilles tendon resulted in the disaggregation of collagen fibers and increased quantities of nonsulfated proteoglycans. Subsequent tendon repair and restoration of continuity reversed these changes with the reappearance of collagen fibers, decreased quantities of nonsulfated and increased quantities of sulfated proteoglycans. The influence of tension on tendon composition was also examined in regions of tendon under tension versus those subjected to compression (66). Again in this model, surgical manipulations altered the physical forces acting on the tendon and changes were observed as new functional demands were placed on the tendon. Specifically, the type and amount of proteoglycans were found to be a function of loading parameters (tension vs. weightbearing).

Other investigations support a change in structure to appropriately meet new functional demands in tendons and ligaments. In exercised versus control animals, physical training (weeks to months) was found to induce increased mean collagen diameter, fibril number, and fibril cross-sectional area (67). Birefringence measurements have indicated a reorganization of the extracellular matrix components into a structure with greater alignment and more intense molecular packing, accompanied by an increase in tensile strength (68). In swine tendons, exercise resulted in higher resistance to applied loads due to an increase in tensile properties and mass (69). Crosslinking density is correlated with tensile strength of tendons (70), and a shift in the types of crosslinks in response to exercise has been demonstrated (71).

Thus skin, tendon, and ligament studies all suggest, in response to increased tensile forces, increases in collagen fibril diameters, collagen crosslinking, and sulfated proteoglycans.

CONCLUSION

The knowledge gained concerning skin response to mechanical stress from clinical experience and from basic science studies to date emphasize an important concept. Rather than considering "breakdown" as an endpoint, we should instead consider "adaptation" as the endpoint. In other words, our goal in clinical treatment should be to encourage the skin to adapt to become load-tolerant to the high force levels it will be subjected to for the life of the individual with the chronic disease or disability. Adaptation is not optional, it is critical. A new structure that will tolerate the abnormally high force levels the skin will be subjected to must be generated.

Studies from the biomechanical and comparative anatomy literature investigating skin and related collagenous tissues indicate two important concepts. First, skin adaptation occurs. Second, the adaptations are different for different directions and durations of applied mechanical loads. Skin structure and bioprocesses are modified according to the mechanical demands placed on the skin. A goal of rehabilitation treatment should be to encourage the skin to adapt to become load-tolerant to the force levels it will be subjected to for the life of the individual.

REFERENCES

1. Sanders SL. Pressure ulcers, part I: prevention strategies. J Am Acad Nurse Prac 1992:4(2):63–70.
2. Allman RM, Laprade CA, Noel LB, et al. Pressure sores among hospitalized patients. Ann Intern Med 1986:105(3):337–42.
3. Norton D, McLaren R, Exton-Smith AN. An investigation of geriatric nursing problems in hospital. 2nd ed. Edinburgh: Churchill Livingstone, 1975:193–238.
4. Richards JS. Pressure ulcers in spinal cord injury: psychosocial correlates. Sci Dig 1981:3:11–8.
5. Kay HW, Newman JD. Relative incidences of new amputations: statistical comparison of 6000 new amputees. Orthot Prosthet 1975:29(2):3–16.

225

SANDERS, et al. Skin Response to Mechanical Stress

6. Sanders GT. Lower-limb amputations: a guide to rehabilitation. Philadelphia: FA Davis, 1986.

7. Wharton G, Milani J, Dean L. Pressure sore profile: cost and management (Abstract). In: Proceedings of the American Spinal Injury Association meeting 1987:115-9.

8. Maklebust J, Mondoux L, Sieggreen M. Pressure relief characteristics of various support surfaces used in prevention and treatment of pressure ulcers. J Enterostom Ther 1986:13:85-9.

9. Yarkony GM. Aging skin, pressure ulcerations, and spinal cord injury. In: Whiteneck GG, Charlifue SW, Gerhart KA, et al., eds. Aging with spinal cord injury. New York: Demos, 1993:39-52.

10. Griffiths BH. Advances in the treatment of decubitus ulcers. Surg Clin North Am 1963:43:245-60.

11. Herceg SJ, Harding RL. Surgical treatment of pressure ulcers. Arch Phys Med Rehabil 1978:59(4):193-200.

12. Daniel RK, Faibisoff B. Muscle coverage of pressure points: the role of myocutaneous flaps. Ann Plast Surg 1982:8:446-52.

13. Fawcett DW. A textbook of histology. 11th ed. Philadelphia: W.B. Saunders Company, 1986.

14. Briggaman RA. Biochemical composition of the epidermal-dermal junction and other basement membrane. J Invest Dermatol 1982:78(1):1-6.

15. Briggaman RA, Wheeler CE. The epidermal-dermal junction. J Invest Dermatol 1975:65(1):71-84.

16. Daly CH. The role of elastin in the mechanical behavior of human skin. 8th ICMBE, Chicago, IL, 1969:18-7.

17. Devlin TM, ed. Textbook of biochemistry with clinical correlations. 3rd ed. New York: Wyley Liss, 1972:61-6.

18. Claus-Walker J, Kretzer FL. Insensitive skin properties of spinal cord injured patients. Arch Phys Med Rehabil 1981:62:521.

19. Rodriguez GP. Lysyl hydroxylase activity: relationship to skin collagen metabolism in spinal cord injury patients. Final report, Mary Switzer Fellowship, National Institute of Handicapped Research, August, 1985.

20. Rodriguez GP, Glaus-Walker J. Measurement of hydroxylysine glycosides in urine and its application to spinal cord injury. J Chromatogr 1984:308:65-73.

21. Rodriguez GP, Claus-Walker J, Kent MC, Garza HM. Collagen metabolite excretion as a predictor of bone- and skin-related complications in spinal cord injury. Arch Phys Med Rehabil 1989:70:442-4.

22. Clark RA. Cutaneous tissue repair: basic biologic considerations. J Am Acad Dermatol 1985:13(5):701-25.

23. Flint MH, Craig AS, Reilly HC, Gillard GC, Parry DAD. Collagen fibril diameters and glycosaminoglycan content of skins—indices of tissue maturity and function. Conn Tissue Res 1984:13:69-81.

24. Parry DAD, Barnes GRG, Craig AS. A comparison of the size distribution of collagen fibrils in connective tissues as a function of age and a possible relation between fibril size distribution and mechanical properties. Proc R Soc Lond B Biol Sci 1978:203:305-21.

25. Bailey AJ, Peach CM, Fowler. In: Balazs EA, ed. The chemistry and molecular biology of the intercellular matrix. Vol. 1. New York: Academic Press, 1970:385-404.

26. Craig AS, Eikenberry EF, Parry DAD. Ultrastructural organization of skin: classification on the basis of mechanical role. Conn Tiss Res 1987:16:213-23.

27. Flint MH, Gillard GC, Merrilees MJ. In: Parry DAD, Creamer LK, eds. Connective tissue proteins: scientific, industrial, and medical aspects. Vol. 2. London: Academic Press, 1980:107-19.

28. Daniel RK, Priest DL, Wheatley DC. Etiologic factors in pressure sores: an experimental model. Arch Phys Med Rehabil 1981:62:492-8.

29. Groth KE. Klinische beobachtungen und experimentelle studien uber die entstehung des dekubitus. Acta Chir Scand 1942:87(Supp 76):198-200.

30. Dinsdale SM. Decubitus ulcers: role of pressure and friction in causation. Arch Phys Med Rehabil 1974:55(4):147-52.

31. Kosiak M. Etiology of decubitus ulcers. Arch Phys Med Rehabil 1961:42:19-29.

32. Husain T. An experimental study of some pressure effects on tissues, with reference to the bed-sore problem. J Path Bact 1953:66:347-58.

33. Reswick JB, Simoes N. Application of engineering principles in management of spinal cord injured patients. Clin Orthop 1975:112:124-9.

34. Reddy NP, Cochran GVB. Interstitial flow as a factor in decubitus ulcer formation. J Biomech 1981:14(12):879-81.

35. Patterson RP, Fisher SV. Pressure and temperature patterns under the ischial tuberosities. Bull Prosthet Res 1980:10-34:5-11.

36. Newson TP, Rolfe P. Skin surface PO_2 and blood flow measurements over ischial tuberosity. Arch Phys Med Rehabil 1982:63(11):553-6.

37. Dinsdale SM. Decubitus ulcers in swine: light and electron microscopy study of pathogenesis. Arch Phys Med Rehabil 1973:54:51-6.

38. Krouskop TA, Noble PC, Garber SL, et al. The effectiveness of preventive management in reducing the occurrence of pressure sores. J Rehabil Res Dev 1983:20(1):74-83.

39. Nola GT, Vistnes LM. Differential response of skin and muscle in the experimental production of pressure sores. Plast Reconstr Surg 1980:66:728-33.

40. Wildnauer RH, Bothwell JW, Douglass AB. Stratum corneum biomechanical properties. I: influence of relative humidity on normal and extracted human stratum corneum. J Invest Dermatol 1971:56(1):72-8.

41. Papir YS, Hsu K-H, Wildnauer RH. The mechanical properties of the stratum corneum. I. The effect of water and ambient temperature on the tensile properties of newborn rat stratum corneum. Biochim Biophys Acta 1975:399:170-80.

42. Daly CH. The biomechanical characteristics of human skin (Thesis). Strathclyde, Scotland: University of Strathclyde, 1966.

43. Lamid S, El Ghatit AZ. Smoking, spasticity and pressure sores in spinal cord injured patients. Am J Phys Med 1983:62:300-6.

44. Exton-Smith AN. Prevention of pressure sores: monitoring mobility and assessment of clinical condition. In: Kenedi RM, Cowden JM, Scales JT, eds. Bedsore biomechanics. Baltimore: University Park Press, 1975:133–9.

45. Lavker RM, Zheng PS, Dong G. Morphology of aged skin. Clin Geriatr Med 1989:5(1):53–67.

46. Lavker RM, Zheng P, Dong G. Aged skin: a study by light, transmission electron, and scanning electron microscopy. J Invest Dermatol 1987:88(3):44s–51s.

47. Reid T, Flint MH. Changes in glycosaminoglycan content of healing rabbit tendon. J Embryol Exp Morphol 1974:31:489–95.

48. Bennett L, Kavner D, Lee BK, Trainor FA. Shear vs pressure as causative factors in skin blood flow occlusion. Arch Phys Med Rehabil 1979:60:309–14.

49. Naylor PFD. Experimental friction blisters. Br J Dermtol 1955:67:327–42.

50. Sulzberger MB, Cortese TA, Fishman L, Wiley HS. Studies on blisters produced by friction. I. results of linear rubbing and twisting technics. J Invest Dermatol 1966:47(5):456–65.

51. Cortese TA, Griffin TB, Layton LL, Hutsell TC. Experimental friction blisters in macaque monkeys. J Invest Dermatol 1969:53:172–7.

52. Naylor PFD. The skin surface and friction. Br J Dermatol 1955:67:239–48.

53. Jagoda A, Madden H, Hinson C. A friction blister prevention study in a population of marines. Mil Med 1981:146:42–4.

54. Akers WA, Sulzberger MB. The friction blister. Mil Med 1972:137:1–7.

55. Whitfield A. On the development of callosities, corns and warts. Br J Dermatol 1932:44:580–5.

56. Rubin L. Hyperkeratosis in response to mechanical irritation. J Inv Dermatol 1949:13:313–5.

57. Brand P. Repetitive stress on insensitive feet. US Public Health Service Hospital, Carville, LA, 1975.

58. Mackenzie IC. The effects of frictional stimulation on mouse ear epidermis. I. Cell proliferation. J Invest Dermatol 1974:62:80–5.

59. Mackenzie IC. The effects of frictional stimulation on mouse ear epidermis. II. Histologic appearance and cell counts. J Invest Dermatol 1974:63:194–8.

60. Carter SB. The masticatory mucosa and its response to brushing; findings in the merion rat, meriones libycus, at different ages. Br Dent J 1956:101:76–9.

61. Sanders JE, Daly CH, Burgess EM. Interface shear stresses during ambulation with a prosthetic limb. J Rehabil Res Dev 1992:29(4):1–8.

62. Levenson SM, Geever EF, Crowley LV, et al. The healing of rat skin wounds. Ann Surg 1965:161:293–308.

63. Baker SR. Fundamentals of expanded tissue. Head Neck 1991:13:327–33.

64. Argenta LC, Marks MW, Pasyk KA. Advances in tissue expansion. Clin Plast Surg 1985:12:159–171.

65. Flint M. Interrelationships of mucopolysaccharide and collagen in connective tissue remodelling. J Embryol Exp Morphol 1972:27(2):481–95.

66. Gillard GC, Reilly HC, Bell-Booth PG, Flint MH. The influence of mechanical forces on the glycosaminoglycan content of the rabbit flexor digitorum profundus tendon. Conn Tiss Res 1979:7:37–46.

67. Michna H, Hartmann G. Adaptation of tendon collagen to exercise. Int Orthop 1989:13(3):161–5.

68. Vilarta R, Vidal BC. Anisotropic and biomechanical properties of tendons modified by exercise and denervation: aggregation and macromolecular order in collagen bundles. Matrix 1989:9:55–61.

69. Woo SLY, Ritter MA, Amiel D, et al. The biomechanical and biochemical properties of swine tendons—long term effects of exercise on the digital extensors. Connect Tissue Res 1980:7:177–83.

70. Birk SW, Silver FH, Trelstad RL. Matrix assembly. In: Hay ED, ed. Cell biology of the extracelluar matrix. New York: Plenum Press, 1991.

71. Curwin SL, Vailas AC, Wood J. Immature tendon adaptation to strenuous exercise. J Appl Physiol 1988:65:2297–301.

Phase plane analysis of stability in quiet standing

Patrick O. Riley, PhD; Brian J. Benda, MS; Kathy M. Gill-Body, MS, PT; David E. Krebs, PhD, PT
Biomotion Laboratory, Massachusetts General Hospital, Boston 02114

Abstract—We analyzed the standing balance control of 11 healthy subjects and 15 subjects with bilateral vestibular hypofunction (BVH) using phase plane (velocity versus displacement) plots. We hypothesized that maintaining postural stability requires control of both the position and momentum of the center of gravity (CG) and infer that it is advantageous to use both velocity and displacement data to characterize balance control. Phase plane plots provide insight into this dynamic aspect of balance control. We evaluated phase plane plots based on whole body CG and center of pressure (CoP). We varied stability by altering the base of support and visual information. Three different foot placements were used: feet wide apart, feet together, and semitandem stance. Feet together standing was performed with eyes open and with eyes closed. The phase plane plots show changes in stability as base of support is altered or visual input is removed and reveal stability differences between the control and BVH groups. The root mean square variance of velocity and displacement was used to quantify the phase plane information. This parameter showed significant differences between activities and between groups. We conclude that phase plane plots that combine displacement and velocity information are more useful in characterizing balance control than displacement or velocity alone.

Key words: *balance, center of gravity, center of pressure, force plates, phase plane, posture, vestibular.*

INTRODUCTION

Deficits of posture and balance control can severely limit activities of daily living. Such deficits also can lead to falls, a major source of morbidity and mortality in the elderly population (1,2). Many sensory and motor system pathologies adversely affect balance control, including balance impairment associated with vestibular system pathologies. Vestibular physical therapy treatments have been developed to improve the function and quality of life of persons with vestibular pathologies such as bilateral vestibular hypofunction (BVH). Objective measures of balance control are needed to assess the effectiveness of these treatments (3,4). In addition, BVH provides a model of balance impairment where the sensory deficit is quite well characterized. Defining the relationship between the sensory system pathology and resulting functional impairment will permit improved analytical and conceptual models of the balance control system and provide insight into the less understood forms of balance impairment.

Balance testing is commonly done using force plates and some measure of center of pressure (CoP) movement called postural sway (5–9). Several different parameters are used to quantify postural sway: linear measures, such as mean sway path (10–12), area measures, such as sway area (9,11–15), and velocity measures, such as mean sway velocity (5,6). We hypothesize that maintaining postural stability requires not only control of the body center of gravity (CG) position but also control of its momentum. We expect, therefore, that measures that incorporate both position and velocity of the CG or

CoP will be more useful in characterizing balance control than displacement measures alone.

A phase plane plot is developed by plotting the time derivative of a parameter against that parameter. A phase plane plot with CG velocity as the ordinate and CG displacement as the abscissa characterizes both CG displacements and CG velocity or momentum. Such plots can provide insight into both the static and dynamic aspects of balance control.

CoP movement is assumed to reflect CG movement, but this is not strictly true (16). We have explored the relationship between CoP and CG kinematics and confirmed that a reasonable approximation of CG kinematics can be derived from measurements of CoP displacement if the standing posture is quasi-static, such as quiet standing in healthy controls (17). While CG kinematics are of primary interest on theoretical grounds, CoP displacements are more readily and economically measured, accounting for their widespread use. Only a force plate is required to measure CoP movement, while a kinematic data acquisition system and a whole body model are required to obtain CG kinematics (18). Because CoP measures are so prevalent in balance control research and are widely used clinically for both diagnosis and treatment, we also present here phase plane plots based on CoP displacements.

METHODS

We estimated the body CG displacements using whole body kinematic data acquired with a four-camera SELSPOT II™/TRACK® kinematic data acquisition system. The kinematic data and subject-specific anthropometric data were incorporated into our 11-segment whole body model (18) to estimate the body CG kinematics. The subjects stood on two force plates in the approximate center of our viewing volume. Their sagittal planes were aligned approximately with our laboratory global X and Y (vertical) axes. The CG kinematics were expressed as displacements from the initial position in the laboratory global coordinate system. Anterior/posterior displacements correspond to movements along the global X axis: lateral displacements correspond to movements along the global Z axis.

The CoP was measured using two Kistler™ force plates. The subjects stood with one foot on each force plate to permit individual ground reaction forces and centers of pressure to be measured. This information was needed for detailed analysis of trials in which the subject had to take a step to maintain balance control. The combined CoP was calculated from the individual force plate CoPs and the known force plate locations and orientations. CoP displacements were also measured in the laboratory global coordinate system using the same convention used for CG displacement. Force plate data were obtained at 153 Hz in synchrony with the kinematic data.

Data sets were 7 seconds long. We desired to compare force plate and kinematic data directly and 7 seconds was the longest whole body kinematic data set that could be obtained at the time of this study. Derivatives were estimated using a fifth-order Lagrangian estimator. The middle 6 seconds of data were used for analysis to avoid startup transients in the derivative estimates.

To compare the phase plane plots quantitatively, we used a set of unitless parameters to characterize the size of the anterior/posterior (AP) and lateral (Lat) phase plane distributions. The parameters were based on the root mean square variance of the position and velocity components. For AP movement, the parameter was calculated using Equation 1a. For lateral movement the parameter was given by Equation 1b.

$$\sigma_{AP_r} = \sqrt{\sigma_{AP_d}^2 + \sigma_{AP_v}^2} \qquad [1a]$$

$$\sigma_{Lat_r} = \sqrt{\sigma_{Lat_d}^2 + \sigma_{Lat_v}^2} \qquad [1b]$$

Where:

σ_{AP_r} and σ_{Lat_r} are the directional stability parameters.

σ_{AP_d} and σ_{Lat_d} are the standard deviations of the displacements.
and

σ_{AP_v} and σ_{Lat_v} are the standard deviations of the velocities.

Directional parameters were calculated for each phase plane plot, that is, for CG, CoP and TF displacements and velocities. A combined stability parameter was then calculated using Equation 1c.

$$\sigma_r = \sqrt{\sigma_{AP_r}^2 + \sigma_{Lat_r}^2} \qquad [1c]$$

Analysis of variance (ANOVA) was used to determine whether the parameters were significantly related to group (control versus BVH) and test conditions.

The subjects were told to stand as still as possible. The base of support was varied by controlling foot placement. The wide base of support (FW: feet wide, the baseline measure) was obtained by placing the feet parallel and approximately 30 cm apart at the midheel; the eyes were open. The narrow base of support was obtained by placing the feet side by side with a separation of approximately 1 cm; in this condition, the subjects were tested both with eyes open (EO) and with eyes closed (EC). For semitandem stance (ST) the feet were 1 cm apart, with the heel of the forward (dominant) foot even with the toe tip of the hind foot. Foot dominance was determined by asking the subjects to pretend to kick a ball. In all cases, the feet were parallel to each other and to the sagittal plane.

Eleven non-BVH control subjects and 15 subjects with BVH were evaluated and compared. The control subjects were in good general health with no neurological or orthopedic conditions that would affect balance control. The BVH patients were diagnosed based on testing conducted in the Jenks Vestibular Laboratory at the Massachusetts Eye and Ear Infirmary that included sinusoidal vertical axis rotational (SVAR) tests showing vestibulo-ocular reflex (VOR) gains of ≥ 3 SDs below normal. The BVH subjects had no other condition that might affect balance control. Informed consent was obtained from all subjects. Subject descriptive parameters are presented in **Table 1.**

Pearson correlation coefficients were used to evaluate the relationship between stability parameters σ_r for repeat tests within a session and the relationship between AP and lateral parameters. Two-factor repeated measures ANOVA was used to assess the between group and between conditions discriminating power of the combined stability parameters. For each combined stability parameter, one-way repeated measures ANOVA was used to access the between-group discrimination for each test condition and the between-condition discriminating power for each group. The level of significance was set at 0.05.

RESULTS

Phase Plane Plot Comparison

Figures 1a and **2a** show a set of lateral CG and lateral CoP phase plane plots representing seven standing trials from a test session of a typical control subject. The seven plots in **Figure 1a** show the lateral CG velocity plotted against the lateral CG displacement. In this analysis, the initial CG position was taken to be zero and all subsequent data points are displacements from that initial position. Lateral CoP kinematics for the same seven standing trials are shown in **Figure 2a.**

Figures 1b and **2b** are the corresponding plots for a typical BVH subject that provide a clear pictorial indication of the difference in stability between the normal and BVH subject in all conditions except the FW baseline. The larger areas shown in these plots indicate the greater variability in both position and velocity for the BVH subject. The second ST trial **(Figure 2b/6)** is of particular interest as it shows the effect of a transient loss of

Table 1.
Subject parameters.

	N	Sex		Age (yr)	Height (m)	Weight (kg)	BMI (kg/m2)
Control Mean	11	7M	4F	50.25	1.71	69.17	23.40
Control SD				22.63	0.09	11.29	2.09
BVH Mean	15	4M	11F	66.01	1.68	65.54	23.40
BVH SD				15.72	0.11	11.50	3.46

BVH = bilateral vestibular hypofunction; BMI = body mass index.

Figure 1a.
Lateral CG Phase Plane Plots for two sets of seven standing posture control trials of the typical control subject.

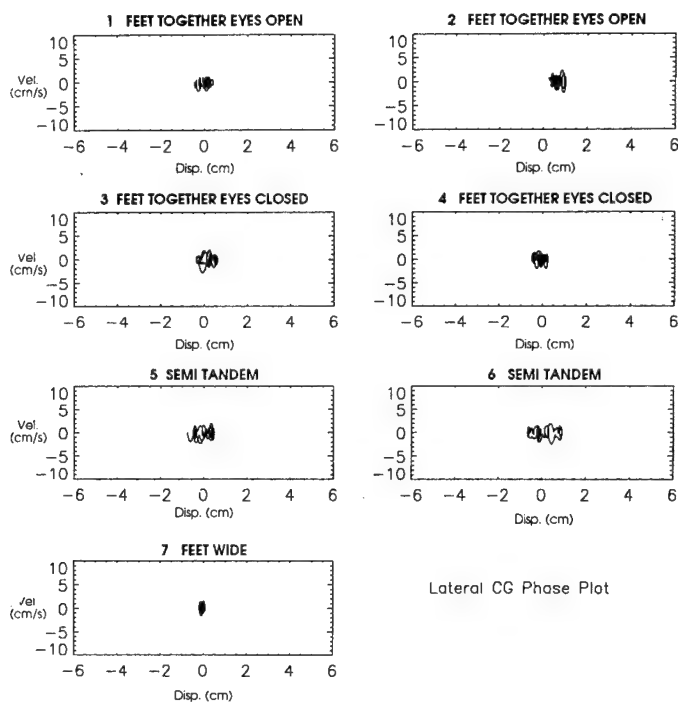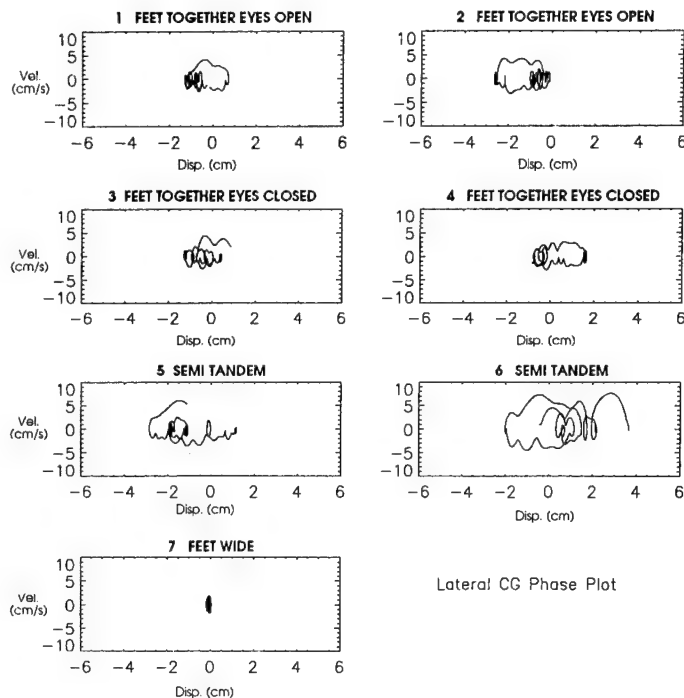**Figure 1b.**
Lateral CG Phase Plane Plots for two sets of seven standing posture control trials of the typical BVH subject.
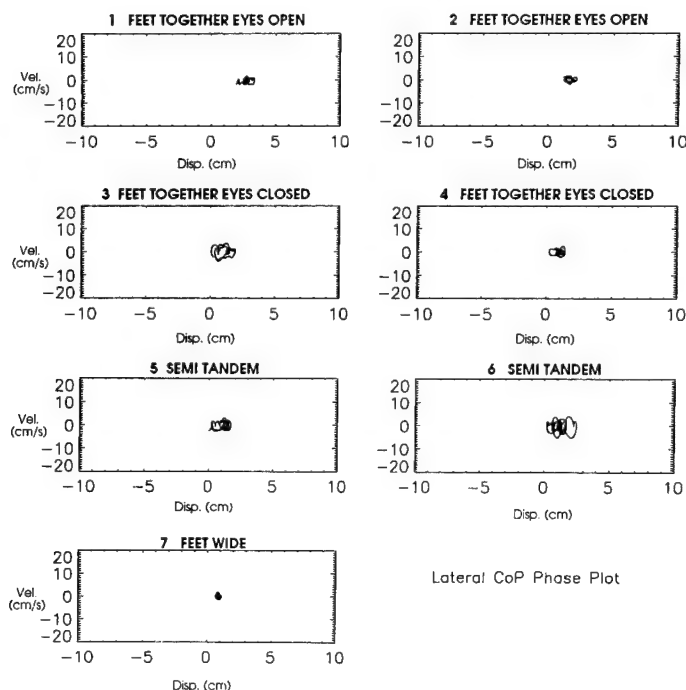
Figure 2a.
Lateral CoP Phase Plane Plots for two sets of seven standing posture control trials of the control subject in Figure 1a.
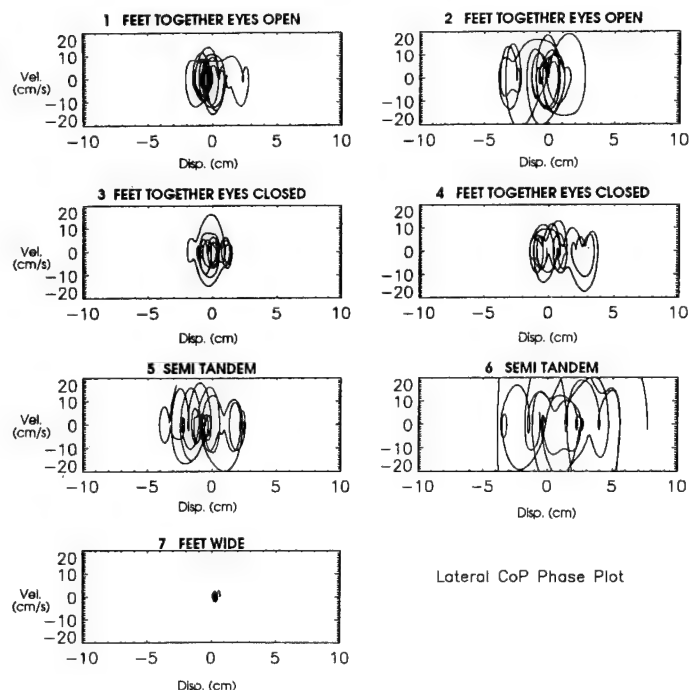
Figure 2b.
Lateral CoP Phase Plane Plots for two sets of seven standing posture control trials of the BVH subject in Figure 1b.

balance control: the subject was unable to stand quietly and had to take a small step to recover. Note that such trials were excluded from the statistical analysis described below.

Comparing the plots within a set provides an indication of the relative stability of the different conditions. The small pattern of the FW condition shows its relative stability. The larger patterns of the EO condition indicate the lesser stability of this condition, and the ST stance is less stable still. The effect of altering visual input may be accessed by comparing the EO and EC trials. Postural stability is somewhat less for EC than for the EO condition with the same base of support.

Figure 3 shows the AP CG phase plane plots for the data set of the subject whose lateral CG phase plane plots are shown in **Figure 1b**. Manipulating the base of support had a similar effect on the AP and the lateral phase plane plots for both CG and CoP. Similarly, removing vision affected both AP and lateral phase plane plots.

Stability Parameter Analyses

The Pearson correlations for the AP and lateral parameters are quite high. The correlation for AP

and lateral CG parameters was 0.8807 and the correlation for AP and lateral CoP parameters was 0.9316. The high correlation indicates that AP and lateral balance control are closely linked. The combined stability parameter σ_r, the root mean square of the AP and lateral stability parameters, was used for statistical comparison.

For each session, repeat trials were obtained for EO, EC, and ST conditions. The correlations between the first and second trial stability parameters σ_r are shown in **Table 2**. Except for CGAP, these values were reasonably well correlated for the healthy control subjects. For the BVH group, the stability parameters σ_r were poorly correlated. This is not a training effect, as the subjects practiced the stance before data were collected and the second trial was not consistently better than the first. In fact, there was a tendency for the BVH subjects to do worse on the second trial. For those conditions with repeat trials, the one with the best (lowest absolute value) stability parameter was used for statistical comparison as this represented the subject's best performance.

The mean and standard deviation of σ_r for each condition and group are shown in **Figures 4a** and **4b**. Both the CG and CoP parameters increase, indicating less stability, as the condition changes from FW to EO to EC to ST. The increase is more pronounced for the BVH group, as expected. The CoP and CG parameters are similar to each other for each of the different conditions and groups. The CoP values are slightly larger for each condition and group. This is consistent with our previous observation that the CG kinematics approximates a smoothed version of the CoP kinematics (17).

Between-Group Differences

The combined CG and CoP variables showed statistically significant differences between the BVH
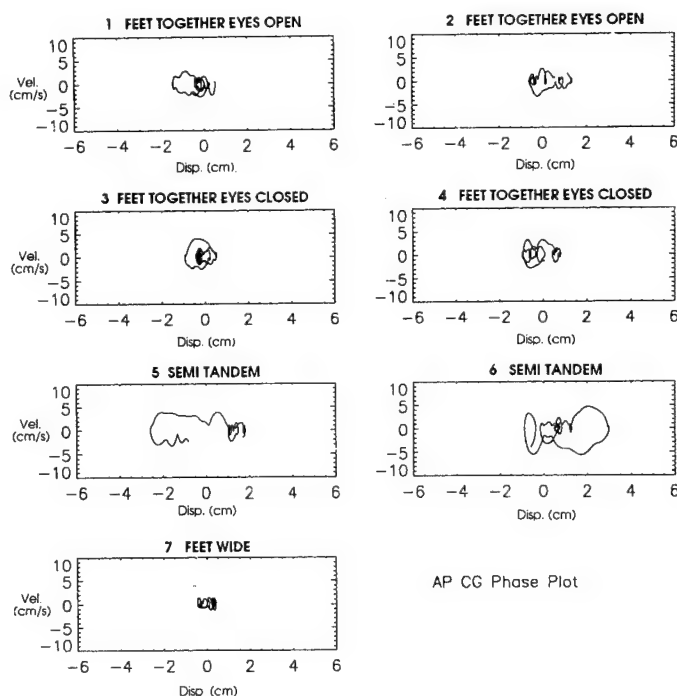
Figure 3.
AP CG Phase Plane Plots for the BVH subject, the same as shown in Figure 1b.

Table 2.
Pearson correlation coefficient: Trial 1 and Trial 2.

	CGL	CGAP	COPL	COPAP
BVH	0.4990	0.4234	0.3395	0.3926
Control	0.7459	0.5028	0.9134	0.7827

CGL = lateral center of gravity; COPL = lateral center of pressure; CGAP = anterior posterior center of gravity; COPAP = anterior posterior center of pressure; BVH = bilateral vestibular hypofunction.
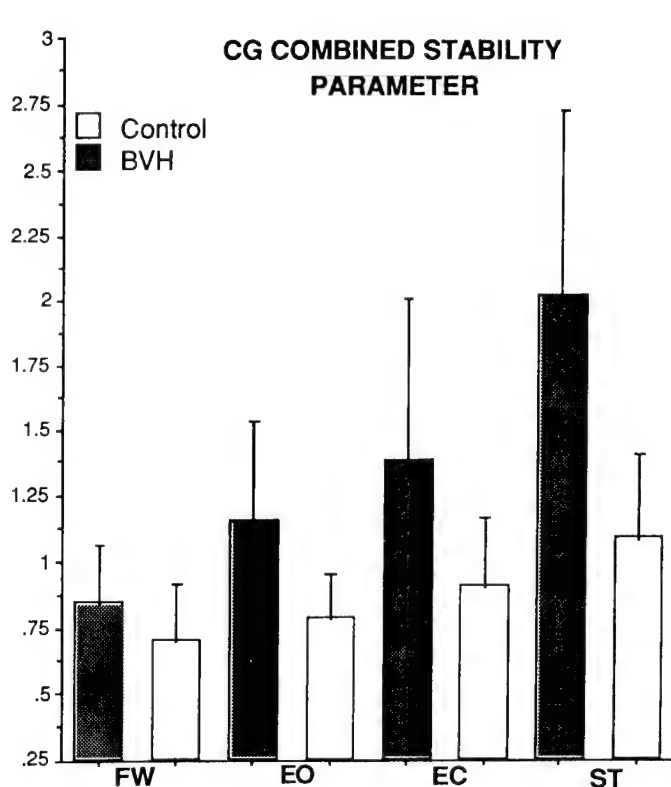
Figure 4a.
Mean and standard deviation of the CG stability parameter σ_r, the root mean square variance of Ap and lateral position and velocity, for all four test conditions for the control and BVH groups.
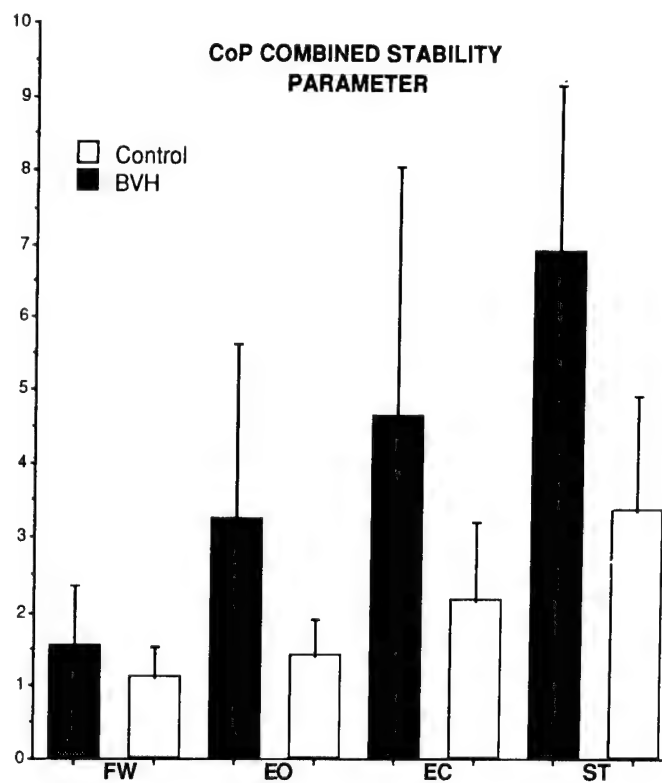
Figure 4b.
Mean and standard deviation of the CoP stability parameter σ_r, the root mean square variance of Ap and lateral position and velocity, for all four test conditions for the control and BVH groups.

and control groups **(Table 3)** over all conditions using a 2-factor repeated measures multivariate ANOVA. A repeated measures ANOVA was used to evaluate the group discriminating power of each test condition. The stable FW condition did not discriminate well between groups. The ST condition provided the best between-group discrimination. The EO and EC conditions also discriminated between groups, but the level of statistical significance was less.

We also examined the discriminating power of parameters based on displacement or velocity information alone. Stability parameters based on AP CoP displacement and velocity and lateral CoP velocity yielded statistically significant differences in between-group variances (p = 0.008, 0.048, and 0.0057, respectively). Stability parameters based on lateral CoP displacement, AP and lateral CG displacement, and velocity did not discriminate between groups at the p < 0.05 level.

Table 3.
Combined stability parameter (σ_r) for CG and CoP to compare between control and BVH group differences.

Condition	Significance (Pr > F) of Combined Parameter Between Group ANOVA CG	CoP
Combined	0.0007*°°	0.0042*°°
FW	0.1007	0.1141
EO	0.0052*°°	0.0211*
EC	0.0302*	0.0295*
ST	0.0007*°°	0.0003*°°

The p values for the ANOVA are shown. Statistically significant differences (p < 0.05) are identified by a *, p < 0.01 is identified by °°. FW = feet 30 cm apart; EO = feet together, eyes open; EC = feet together, eyes closed; ST = feet in semitandem position; CG = center of gravity; CoP = center of pressure.

Between-Condition Differences

The 2-factor repeated measures multivariate ANOVA showed that the variances of the combined

CG and CoP parameters were a significant function of the test condition for the combined control and BVH group data. Repeated measures ANOVA was used to determine which conditions produced significant differences in the variables; the results are summarized in **Table 4.** The control group showed a marginally significant difference between the EO and EC conditions for the CG parameter with a significant difference for the CoP parameter. The FW and EO conditions were not significantly different for the CG parameter and were marginally different for CoP parameter. For the control group, the other conditions were significantly different. The ST stance was significantly different from both the FW and EO stances.

The results for the BVH group were similar, but between-condition differences tended to be more significant. The BVH group showed a significant difference between the EO and EC conditions for both the CG and CoP parameters. In contrast to the controls, the FW and EO conditions were also significantly different for both the CoP and CG parameters. Again, ST stance differed from both the FW and EO conditions at very high levels of significance.

DISCUSSION

Most prior posturography studies focus on CG or CoP displacement, assuming those CG excursions near the perimeter of the base of support yield instability (19-26). Phase plane plots provide a pictorial and a quantitative measure of stability in quiet standing. These data suggest that the CG and CoP phase plane plots are useful in studying and quantifying relative postural stability. CoP phase plane plots, which are easier to obtain, are as informative as CG phase plane plots for these patients and conditions. The sensitivity of postural stability to base of support alterations is readily apparent.

One limitation of these plots is that relatively stable and unstable states both occupy the same phase space. In **Figure 2b,** for example, the subject is clearly less stable in ST stance than in FW stance. However, the phase plane plots for both conditions are centered at the same location in the two dimensional state space. As stability degrades, the bounds of the occupied space expand, but there is no sharply defined boundary between stability conditions. A state space mapping, in which different stability conditions occupied distinct regions is highly desirable. This state space may well be more than two dimensional.

When a simple parameter that combines AP and lateral position and velocity information is used, differences in lateral stability due to foot placement are apparent and can be easily quantified. The ST stance was significantly different from both the FW and feet together conditions for both groups, with this difference being more significant for the BVH group. ST stance provides the same lateral base of support width as feet together stance and provides a longer AP base of support than

Table 4.
Combined stability parameter (σ_r) for CG and CoP for the BVH and control subjects to compare the effect of activity conditions.

| | Significance (pr > F) of Between Conditions ANOVA | | | |
	CG-BVH	CG-Control	CoP-BVH	CoP-Control
Combined	0.0001*°°	0.0001*°°	0.0001*°°	0.0001*°°
FW-EO	0.0025*°°	0.0869	0.0036*°°	0.0435*
FW-ST	0.0004*°°	0.0009*°°	0.0001*°°	0.0002*°°
EO-EC	0.0374*	0.0474*	0.0277*	0.0043*°°
EO-ST	0.0011*°°	0.0024*°°	0.0001*°°	0.0003*°°

The p values for the ANOVA are shown. Statistically significant differences (p < 0.05) are identified by a *, p < 0.01 is identified by °°
FW = feet 30 cm apart; EO = feet together, eyes open; EC = feet together, eyes closed; ST = feet in semitandem position; CG = center of gravity; CoP = center of pressure.

either the FW or feet together conditions. Load bearing tends to be concentrated heavily on the hind leg and this may contribute to the instability of this position.

The effect of removing visual information is also measurable but less significant. The EO–EC difference was approximately the same for the BVH and control groups. The BVH group was expected to be especially dependent on visual information. The feet together condition did not stress balance control severely or induce severe dynamics. Hence, proprioceptive information may be adequate for balance control without either vestibular or visual information. It should be noted that one of the BVH subjects was not able to perform the EC task at all and several of the subjects were only successful for one trial out of two. The stability parameter σ_r was calculated based on successful trials only and may not completely reflect the difficulty that BVH subjects had with the EC condition.

The CG- and CoP-based phase plane plots provided very similar between-group discriminations. This suggests that phase plane studies using force plates only may be useful. For this particular analysis, estimation of the CG using whole body kinematics does not appear to add significantly to our knowledge. Velocity information alone and in combination with displacement information discriminated between groups more effectively than displacement information. CG or CoP position, which is often examined, did not discriminate between groups. Because the combined stability parameters measure both the displacement and velocity, they might be expected to be more robust measures over a range of pathologies.

We did not use mean sway path, mean sway area, or mean sway velocity to quantify CG or CoP movement. We did examine measures of the variability of CG and CoP positions during our trials. However, as our trials were only 7 seconds long, and the CoP variables are usually calculated for much longer data sets, the values would not be directly comparable. Technical modifications to our data acquisition and processing systems now permit us to obtain data sets of longer duration. In the future, we plan to determine if quiet standing for extended periods, 20 to 30 seconds, is really a stationary process. We will compare phase plane parameters for longer trials to those determined from 7-second trials. We will also explore the correlation between

phase plane based parameters and the more classic posturography parameters.

Further work is needed to determine if the analysis is useful for discriminating between balance impairment due to vestibular dysfunction and balance impairment due to other causes, such as Parkinson's disease. The ability to differentiate between different levels of vestibular dysfunction also needs to be determined. The patient population in this study was comparatively small.

The effect of age also needs to be addressed with comparisons of young and old normal subjects and comparisons of age-matched patient and control populations. This was not possible with our initial data, but we are currently expanding our database.

CONCLUSION

The usefulness of the phase plane analysis for quantifying balance impairment has been demonstrated. These data suggest that including combined displacement and velocity parameters in a phase plane analysis, clearly discriminates balance-impaired from non-impaired subjects. Whole body CG and CoP data discriminate equally well between normal controls and subjects with vestibular pathology. We conclude that combined displacement and velocity data are useful in studies of standing balance. The fact that the combined parameter and the velocity parameters were both highly discriminatory between balance-impaired and control subjects, while displacement-only parameters were not, supports our hypothesis that control of momentum is important even in such an apparently static activity as standing.

REFERENCES

1. Pentland B, Jones P, Roy C, et al. Head injury in the elderly. Age Aging 1986:15:193–202.
2. Baker SP, Harvey AH. Fall injuries in the elderly. Clin Geriatr Med 1985:1:501–12.
3. Gill-Body KM, Krebs DE, Parker SW, et al. Physical therapy management of peripheral vestibular dysfunction—two case reports. Phys Ther 1994:74(2):129–42.
4. Krebs DE, Gill-Body KM, Riley PO, et al. Double-blind, placebo-controlled trial of rehabilitation for bilateral vestibular hypofunction: preliminary report. Otolaryngol Head Neck Surg 1993:109(4):735–41.

5. Burl MM, Williams JG, Nayak USL. Effects of cervical collars on standing balance. Arch Phys Med Rehabil 1992:73:1181–5.

6. Enbom H, Magnusson M, Pyykko I. Postural compensation in children with congenital or early acquired bilateral vestibular loss. Ann Otol Rhinol Laryngol 1991:100(6):472–8.

7. Ishizaki H, Pyykko I, Aalto H, et al. Tullio phenomenon and postural stability: experimental study in normal subjects and patients with vertigo. Ann Otol Rhinol Laryngol 1991:100(12):976–83.

8. Ishizaki H, Pyykko I, Aalto H, et al. The Tullio phenomenon in patients with Meniere's disease as revealed with posturography. Acta Otolaryngol Suppl (Stockh) 1991:481:593–5.

9. Moller CG, Kimberling WJ, Davenport SL, et al. Usher syndrome: an otoneurologic study. Laryngoscope 1989:99(1):73–9.

10. Cybulski GR, Jaeger RL. Standing performance of persons with paraplegia. Arch Phys Med Rehabil 1986:67(2):103–8.

11. Kollegger H, Wober C, Baumgartner C, et al. Stabilizing and destabilizing effects of vision and foot position on body sway of healthy young subjects: a posturographic study. Eur Neurol 1989:29(5):241–5.

12. Schieppati M, Nardone A. Free and supported stance in Parkinson's disease: the effect of posture and postural set on leg muscle responses to perturbation, and its relation to the severity of the disease. Brain 1991:114:1227–44.

13. Bhattacharya A, Linz DH. Postural sway analysis of a teenager with childhood lead intoxication—a case study. Clin Pediatr (Phila) 1991:30(9):543–8.

14. Hamman RG, Mekjavic I, Mallinson AI, et al. Training effects during repeated therapy sessions of balance training using visual feedback. Arch Phys Med Rehabil 1992:73(8):738–44.

15. Shumway-Cook A, Anson D, Haller S. Postural sway biofeedback: its effect on reestablishing stance stability in hemiplegic patients. Arch Phys Med Rehabil 1988:69(6):395–400.

16. Barin K. Dynamic posturography: analysis of error in force plate measurement of postural sway. IEEE Eng Med Biol 1992:11:52–6.

17. Benda BJ, Riley PO, Krebs DE. Biomechanical relationship between center of gravity and center of pressure during standing. IEEE Trans Rehab Eng. In press.

18. Riley PO, Hodge WA, Mann RW. Modelling the biomechanics of posture and balance. J Biomech 1990:23:503–5.

19. Horak FB, Shupert CL, Mirka A. Components of postural dyscontrol in the elderly: a review. Neurobiol Aging 1989:10(6):727–38.

20. Horak FB, Jones-Rycewicz C, Black FO, et al. Effects of vestibular rehabilitation on dizziness and imbalance. Otolaryngol Head Neck Surg 1992:106(2):175–80.

21. Nashner LM. A model describing the vestibular detection of body sway motion. Acta Otolaryngologica (Stockh) 1971:72:429–36.

22. Nashner LM, Woollacott M. The organization of rapid postural adjustments of standing humans: an experimental-conceptual model. In: Talbott RE, Humphrey DR, eds. Posture and movement. NY: Raven Press. 1979:

23. Nashner LM, Shumway-Cook A, Marin O, et al. Stance postural control in selected groups of children with cerebral palsy: deficits in sensory organization and muscular coordination. Exp Brain Research 1983:49:393–409.

24. Nashner LM, McCollum G. The organization of human postural movements, a formal basis and experimental synthesis. Behav Brain Sci 1985:8:135–72.

25. Nashner LM, Shupert CL, Horak FB, et al. Organization of posture controls: an analysis of sensory and mechanical constraints. Prog Brain Res 1989:80:411–8.

26. Nashner LM, Peters JF. Dynamic posturography in the diagnosis and management of dizziness and balance disorders. Neurol Clin 1990:8(2):331–49.

Asymmetry in walking performance and postural sway in patients with chronic unilateral cerebral infarction

Ekaterina B. Titianova, MD, PhD and Ina M. Tarkka, PhD
Department of Neurology, Medical University, Sofia, Bulgaria; Division of Restorative Neurology and Human Neurobiology, Baylor College of Medicine, Houston, TX 77030

Abstract—The asymmetrical nature of hemiparetic gait is well known; however, the role of walking asymmetry for speed performance is unclear. The purpose of the present study was to determine whether the range of walking speeds in chronic hemiparetic patients is associated with their gait asymmetry and postural sway. Twenty ambulatory patients with chronic unilateral supratentorial infarction were studied. Foot-ground contact patterns during swing and stance phases at various self-selected walking speeds were analyzed. The magnitude and direction of asymmetry in durations of stride phases were evaluated and compared with healthy subjects. Posturographic studies were performed to estimate the postural sway during quiet standing. Hemiparetic patients walked slower, more asymmetrically, and swayed more laterally favoring their nonaffected leg than did healthy persons. Although there was variability in durations of stride phases when comparing the two sides, a prolonged swing on the affected side and a prolonged stance on the nonaffected side were observed in all patients. The magnitude of asymmetry in stride phases varied among the patients; however, it was significantly higher than in controls ($p < 0.03$). Increased mean lateral sway during quiet standing was indicative of restricted velocity performance during walking. Patients with higher swing asymmetry achieved their maximum speed performance at lower velocity levels. However, the ability of patients to ambulate with a number of self-selected speeds was not associated with the magnitude of their overall gait asymmetry. Patients with right hemisphere lesions appeared to have less ambulatory ability than patients with left hemisphere lesions.

Key words: *cadence, hemiplegia, posture, stroke, walking.*

INTRODUCTION

Impairments in posture, walking, and voluntary movements are common motor deficits in hemiparetic stroke patients. The degree of disequilibrium and the abnormalities of hemiparetic locomotion have been clinically evaluated and carefully described (1–6). A number of investigations using different approaches have shown the asymmetrical nature of hemiparetic standing and walking (7–12). Studies on standing balance in stroke patients have revealed a greater proportion of body weight distributed on the non-paretic than on the paretic limb (10,12). Stance duration during walking has been found to be relatively shorter for the affected than for the nonaffected leg along with a prolongation of the swing phase on the affected side (13–15). Furthermore, spatio-temporal parameters of gait have been shown to relate closely to the changes in walking velocity in both healthy subjects and stroke patients, suggesting that gait deficit can be classified on the basis of walking speed (16,17), although only some gait studies have used the walking speed as a parameter for evaluation of

hemiparetic ambulation (14,16,17). Walking asymmetry has been found to decrease when reaching the maximum walking speed (18). High correlation between postural stability, locomotor functions, and functional assessments using Fugl-Meyer Scale and Barthel Index has been established (19). However, the underlying mechanisms of restoration of ambulation after stroke and the relationship between the asymmetry in hemiparetic locomotion and the speed performance are unclear.

The purpose of the present study was to describe the ability of patients with chronic unilateral stroke to ambulate at different speeds and to examine the relationship between their postural sway and temporal parameters of gait. This was investigated evaluating the foot position patterns of various self-selected walking speeds, and the location of the center of gravity and the body sway during quiet standing. To understand the relationship between the variation of walking speed and the walking asymmetry, the direction and the magnitude of asymmetry in the durations of swing and stance phases were analyzed and correlated with walking velocity. The effects of age, degree of peroneal muscle paresis, localization of the brain lesion, and the time since the onset of stroke on hemiparetic ambulation were also evaluated.

METHODS

Subjects

Twenty patients (13 men and 7 women, mean age ± SD, 57.9 ± 12.9 years, range 33–77 years) with residual hemiparesis due to stroke were studied. The inclusion criteria were: an ambulatory patient; a unilateral stroke more than 6 months ago, medically stable; and no severe hearing, visual, cognitive, or communication problems. In our population, the time since the onset of stroke varied from 8 months to 12 years (mean ± SD, 42.9 ± 37.5 months). These patients had survived unilateral cerebral infarctions in the middle cerebral artery territory confirmed by computer tomography (CT) during the acute stage of the disease. There were 13 right-sided infarctions and 7 left-sided infarctions. Clinical assessment performed for each patient at the time of the investigation revealed a hemiparesis contralateral to the ischemic lesion, upper extremity being weaker than the lower extremity. Twelve of the patients had

primary motor and eight had combined motor and sensory deficits. The strength of peroneal muscle groups, known to be severely affected after stroke, was assessed by a modified Manual Muscle Test (MMT) using a 0–5 score system (20). At the time of the study, 12 of the patients were capable of independent standing although 4 of them used additional orthotic support during walking. The remaining 8 of the patients stood and walked with orthotic devices: an ankle foot orthosis and/or a cane.

Two control groups were used. Twenty right-handed healthy subjects (10 men and 10 women, mean age ± SD, 40 ± 9.4 years, range 29–67 years) were controls for posturography, and 12 right-handed healthy subjects (4 men and 8 women, mean age ± SD, 43.9 ± 10.5 years, range 30–70 years) were controls for the gait study. Seven healthy subjects were common to both investigations. The controls were free of medication and without any of the primary risk factors for cerebrovascular disease. All subjects and patients gave an informed consent prior to the studies. The Institutional Review Board for Human Research had approved the studies.

Recording methods

The posturographic study was performed on 12 stroke patients capable of independent standing (orthotic devices were removed prior to the study) and the control group. A Kistler piezoelectric force plate connected to a computer system (HP 2100) was used. All subjects were instructed to stand on the platform in a quiet, relaxed posture, with heels together and an angle of 30° between the medial aspects of the feet. The heels were 120 mm behind the center of the platform. To minimize variations in visual and vestibular input, subjects were instructed to look straight ahead at a target. The posturographic study consisted of six trials, three with eyes open (EO) and three with eyes closed (EC), each trial lasting 51.2 sec. The parameters of static posture and body sway were measured and calculated from the vertical forces exerted by the feet onto the platform. The forces were sampled at a rate of 40 Hz. The mean displacement of the center of force in sagittal and in lateral direction was determined as positive if the lateralization of the center of force was anterior (for controls and patients), or to the right side of the coordinate system (for controls). In stroke patients, a positive

lateral displacement of the center of force indicated lateralization to the nonaffected side (NS), and a negative value indicated lateralization to the affected side (AS). The body sway was estimated by measuring the mean sagittal (Msd) and the mean lateral (Mld) displacements. Both parameters were computed in mm from the center of the coordinate system. Individual and grand mean values from all trials with eyes open and eyes closed were determined.

The gait was analyzed in 20 stroke patients and in the control group. Foot switches were used to measure the timing of foot contacts with the ground during the stride. Conductive tape was fastened bilaterally under comfortable shoes on the heel, the ball, and the toes leaving a space of 1 cm from the tip of the toe and the heel (21). The encoded patterns of foot-ground contacts were connected to a recording system through a cable following the subject via a rail in the ceiling. The subjects were asked to walk along a 10 m special metal net walkway at five self-selected different speeds, which they considered as ordinary, faster, fastest, slower, and slowest. Speed was individually selected for each subject and was repeated twice. Most patients were able to repeat their walking speeds well. Three or four strides of each walking speed were analyzed and the individual and grand mean values of the following gait variables were determined: average velocity (m/s), range of velocity (m/s) between the slowest and the fastest walking, duration of stride phase and its components; swing (s), stance (s), and the total double support (the total time when both feet are in contact with the ground during one full stride cycle in s). The velocity was calculated from the time needed for traversing the whole walkway. The time was measured from the video records. The best speed performances for each subject were analyzed. Comparisons were made between the ordinary, the slowest, and the fastest speeds.

To obtain information about the symmetric nature of the walking pattern, the temporal variables of gait were evaluated separately for the right and the left leg, and for different speeds. The asymmetry was calculated as an asymmetry index (AI) according to the formula:

$$AI = \frac{(AS - NS)}{(AS + NS)/2} \times 100$$

where AS was stance, swing, or stride duration on the affected side, NS was the same parameters on the nonaffected side. The same parameters of the left and the right legs were used for controls. The sign of the AI indicated the direction of the asymmetry, while the magnitude of this ratio indicated the degree of asymmetry.

Patients and controls were compared with analysis of covariance and repeated measures analysis of covariance using age as a covariate in order to correct for the differences in ages. Paired t-tests were used to compare posturographic parameters in EO and EC conditions, and to compare gait variables between both sides. Spearman correlation was performed to examine the relationship between posturographic and gait parameters.

RESULTS

First, the ambulation of healthy persons and patients as one group was evaluated. With changing walking speed temporal variables of gait changed in both groups (Table 1). Hemiparetic patients walked slower than controls in all gait trials due to longer stride duration ($p < 0.05$). Patients' range of velocity of gait was significantly lower than controls ($p < 0.001$). In both groups, total double support time decreased with increasing velocity. Hemiparetic patients had different durations of swing and stance phases between AS and NS ($p < 0.001$). Their walking asymmetry is discussed in detail later.

In comparison to healthy persons, hemiparetic patients showed a tendency to increased mean lateral displacement toward the nonaffected side during quiet standing. Removal of visual input did not significantly influence posturographic parameters in either patient or in control group.

Second, the stroke patients were divided into subgroups according to (a) the side of the infarction and (b) the range of velocity between slowest and fastest walking (Table 2). Three patient subgroups were formed based on the velocity range: 1) ≥ 0.73 m/s; 2) 0.72–0.26 m/s; 3) ≤ 0.25 m/s. The first subgroup included patients who were able to produce velocity ranges similar to the control group. The remainder of the patients were subdivided based on their velocity range and the clinical evaluation of their walking performance. The subgroups were similar regarding their age, sex, side of infarction,

Table 1.
Mean (x) and standard deviation (SD) of temporal variables of gait and posturographic parameters in control group and in patient group.

Parameters	Trial	Control Group			Patients		
		n	Side	x ± SD	n	Side	x ± SD
Velocity (m/s)	Slowest	12		0.64 ± 0.20	20		0.40 ± 0.23
	Ordinary	12		1.18 ± 0.23	20		0.57 ± 0.34***
	Fastest	12		1.86 ± 0.36	20		0.89 ± 0.60***
	Range	12		1.22 ± 0.39	20		0.49 ± 0.41***
Swing phase (s)	Slowest	12	R	0.71 ± 0.16	20	AS	0.71 ± 0.26
		12	L	0.71 ± 0.13	20	NS	0.52 ± 0.15
		12	Al%	0.9 ± 11.1	20	Al%	29.9 ± 19.4***
	Ordinary	12	R	0.51 ± 0.05	20	AS	0.64 ± 0.22
		12	L	0.52 ± 0.05	20	NS	0.47 ± 0.12
		12	Al%	1.5 ± 3.8	20	Al%	29.2 ± 19.5***
	Fastest	12	R	0.43 ± 0.06	20	AS	0.54 ± 0.13
		12	L	0.44 ± 0.05	20	NS	0.42 ± 0.09
		12	Al%	1.1 ± 4.1	20	Al%	25.6 ± 15.9***
Stance phase (s)	Slowest	12	R	1.08 ± 0.27	20	AS	1.40 ± 0.71
		12	L	1.07 ± 0.24	20	NS	1.60 ± 0.73
		12	Al%	− 0.9 ± 4.8	20	Al%	− 13.9 ± 11.4**
	Ordinary	12	R	0.67 ± 0.13	20	AS	1.17 ± 0.71
		12	L	0.66 ± 0.11	20	NS	1.36 ± 0.73
		12	Al%	− 0.6 ± 2.2	20	Al%	− 16.2 ± 13.1***
	Fastest	12	R	0.48 ± 0.09	20	AS	0.97 ± 0.75
		12	L	0.48 ± 0.08	20	NS	1.09 ± 0.78
		12	Al%	− 0.7 ± 4.6	20	Al%	− 14.5 ± 8.8***
Total double support (s)	Slowest	12		0.37 ± 0.23	20		0.89 ± 0.75
	Ordinary	12		0.15 ± 0.12	20		0.72 ± 0.75
	Fastest	12		0.05 ± 0.07	20		0.55 ± 0.75
Mld (mm)	EO	20		− 4.4 ± 4.3	12		10.3 ± 12.9
	EC	20		− 3.9 ± 5.8	12		9.8 ± 14.3
Msd (mm)	EO	20		− 17.2 ± 17.9	12		− 14.1 ± 11.2
	EC	20		− 16.4 ± 17.8	12		− 14.7 ± 13.9

L, left; R, right; AS, affected side; NS, nonaffected side; Mld, mean lateral displacement; Msd, mean sagittal displacement; EO, eyes open; EC, eyes closed; ** $p < 0.01$, *** $p < 0.001$, significance between controls and patients (ANCOVA after adjustment for age).

and the time since the onset of stroke. The subgroup with lowest velocity range consisted of slightly older patients and significantly lower MMT score in comparison to the patients with highest velocity range. The pure motor deficit was predominant in patients with left-sided infarction (77.8 percent). The use of orthotic devices was more common among the patients with a small velocity range. Individual patients utilized their range of velocity differently. For example, some good walkers, patients with velocity ranges similar to normals (>0.73 ms/s), utilized only 18–38 percent of their range of velocity in achieving an ordinary walking speed,

preserving the rest of the velocity range for fast walking. This was also seen in the control group. The worst walkers from the group with smallest velocity range utilized almost all of their range of velocity to achieve their ordinary walking speed.

Comparing the two sides, a prolonged swing on the AS and a prolonged stance on the NS were observed in all subgroups although there was variability in the duration of the stride phases (**Figure 1**). During quiet standing, all patient subgroups were found to favor their nonaffected leg; however, some quantitative differences were observed among them (**Figure 2**). The changes in postural sway and gait

Table 2.
Characteristics of patient subgroups.

Subgroups	Total	Men	Women	Age	Months after stroke	Manual Muscle Test	Orthotic Devices	
	n	n	n	x ± SD	x ± SD	x ± SD	n	% [a]
Side of infarction								
Left	7	5	2	58.4 ± 10.5	49.7 ± 41.2	2.9 ± 1.8	4	57%
Right	13	8	5	57.6 ± 13.6	39.3 ± 34.8	2.5 ± 1.5	8	62%
Range of velocity								
≥ 0.73 m/s	4	4	0	53.5 ± 10.1	56.7 ± 49.5	4.0 ± 1.0	1	25%
0.72 – 0.26 m/s	10	6	4	55.6 ± 10.5	46.1 ± 37.9	3.1 ± 1.4	6	60%
≤ 0.25 m/s	6	3	3	64.6 ± 14.6	28.5 ± 17.4	1.8 ± 1.1 [b]	5	83%
Total	20	13	7	57.9 ± 12.6	42.9 ± 37.5	2.8 ± 1.5	12	60%

[a] The percentage of orthotic devices was calculated from the total number of patients of each group.
[b] $p < 0.05$, significance between the subgroups with highest and lowest range of velocity (ANOVA followed by multiple comparisons).

variables were more pronounced in the subgroup with right-sided infarction. The subgroup with lowest range of velocity showed a significantly longer stance duration during all speed trials in comparison to other subgroups.

The magnitude of asymmetry in duration of stride phases was analyzed comparing left and right sides in controls, and the AS and the NS in patients. Healthy persons had nearly symmetrical swing and stance durations, which contrasted with marked asymmetries in the patient group ($p < 0.03$). This difference between controls and patients was not associated with age. When the swing AI increased, the stance AI also increased but toward the other side (**Figure 3**). The sign in **Figure 3** indicates the direction of asymmetry; for instance, if swing and stance AI both were negative, the patient would lean continuously to one side during walking.

The asymmetries were remarkably present in all patient subgroups regardless of the speed trial. The patients with right-sided infarction had somewhat higher AI in stride phases than the subgroup with left-sided infarction (**Figure 4**). The asymmetries persisted also in patients who were able to produce a range of velocity similar to that of the controls.

In healthy persons, no relationship between velocity and asymmetry indices were found. Hemiparetic patients with high swing AI produced low ordinary ($r = -0.57$, $p < 0.01$) and fastest ($r = -0.46$, $p < 0.05$) velocities. However, the ability

of patients to produce a range of velocities was not associated with the range of asymmetry indices calculated from their speed trials (**Figure 5**).

To understand the relationship between postural sway and ambulation in chronic stroke, we searched for correlations between posturographic and gait parameters. No significant relationship was found between gait and posture in the control group. In hemiparetic patients, the increase in the mean lateral displacement was associated with lower fastest velocity ($r = -0.68$, $p < 0.05$). The larger mean sagittal displacement was associated with increasing stance AI during slowest walking ($r = 0.77$, $p < 0.01$). These relationships were present in both EO and EC conditions.

We analyzed the impact of other factors on the ambulation parameters in our patients and found that the site of the lesion and the time after the onset of stroke were insignificant.

DISCUSSION

The present study reveals that patients with residual hemiparesis due to chronic unilateral supratentorial ischemic infarction walk slower, more asymmetrically, and sway more laterally favoring their nonaffected leg, than healthy persons. Similar patterns of standing and locomotion were observed previously in hemiparetic patients, some of them
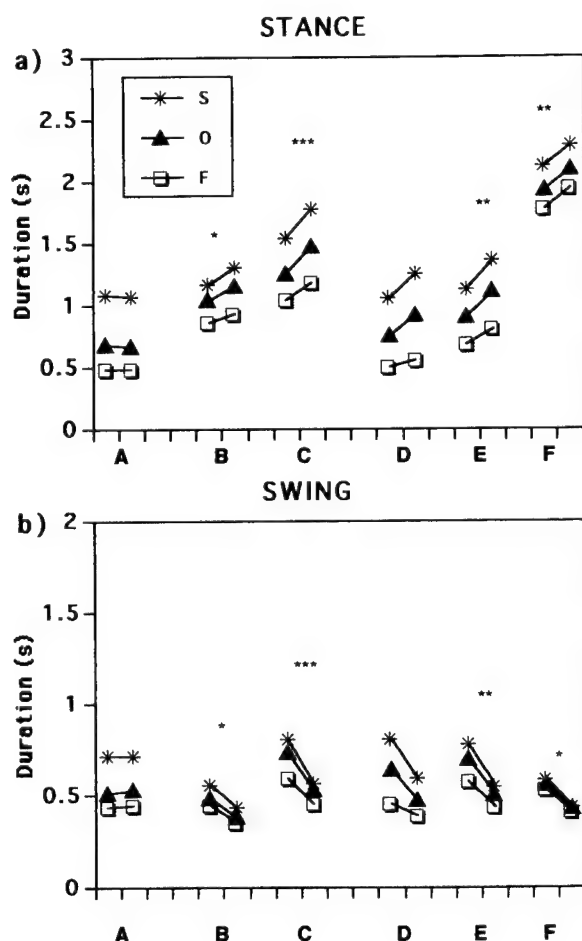
Figure 1.
Mean durations of stance (a) and swing (b) phases of gait obtained during slowest (s), ordinary (o), and fastest (f) speeds in control group (A) and patient subgroups with left-sided infarction (B), right-sided infarction (C), and different ranges of walking velocity: ≥ 0.73 m/s (D), 0.72–0.26 m/s (E), and ≤ 0.26 m/s (F). The data from different speeds are shown above each other in the respective order. Horizontal lines connect right and left leg values in controls, and the values of affected (AS) and nonaffected (NS) sides in patients. Significant differences were found between AS and NS, * $p < 0.05$, ** $p < 0.01$, *** $p < 0.001$.

Figure 2.
Mean $\pm$ SD of the mean lateral (Mld) and the mean sagittal (Msd) displacement in control group (A, $n = 12$), and patient subgroups with left-sided infarction (B, $n = 5$), right-sided infarction (C, $n = 7$), and in the subgroups according to the range of walking velocity obtained by patients: ≥ 0.73 m/s (D, $n = 2$); 0.72–0.26 m/s (E, $n = 6$); and ≤ 0.26 m/s (F, $n = 4$). EO refers to eyes open condition and EC refers to eyes closed condition.

with different types and locations of stroke (10,12,19). The balance disturbances and the alterations of gait varied among the patients: they were associated with the degree of peroneal muscle paresis (evaluated by MMT) and were more pronounced in the subgroup with right-sided infarction and those with a small range of walking velocity. The differences among the patients were found quantitative rather than qualitative in nature. The foot-ground contact patterns of the hemiparetic gait

changed in a stereotyped manner, resulting in a prolonged swing duration on the AS and a prolonged stance duration on the NS. Changes in the walking speed were indicative of changes in stance, swing and total double support time confirming previous findings (16,17).

The major emphasis of this study was the walking asymmetry and its impact in speed performance. Previously, asymmetries in durations of swing and stance phases were expressed as a simple ratio between affected and nonaffected sides or as a percentage of each phase from the duration of the whole stride (7,8,11). In addition, Wall and Turnbull (10) evaluated the pattern of gait in patients with residual hemiplegia using an asymmetry ratio between the single support time of AS and NS. However, all these studies did not evaluate the
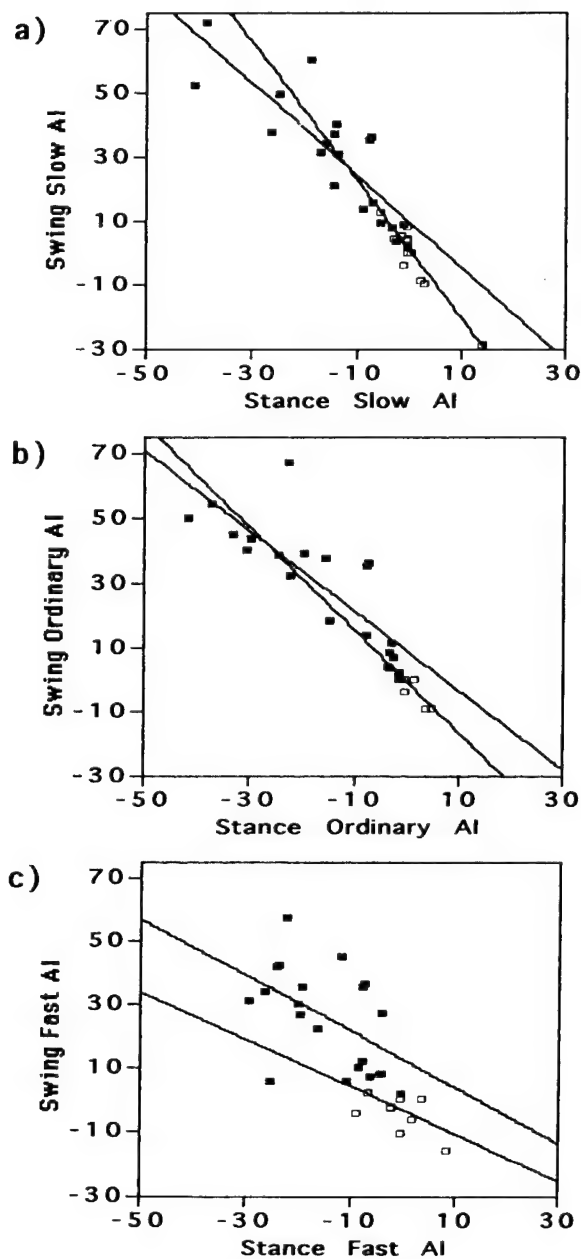
Figure 3.

Relationship between swing and stance asymmetry indices at slowest (a), ordinary (b), and fastest (c) speeds in control subjects (empty squares) and all patients (filled squares).

Figure 4.

Asymmetry index (AI, mean ± SD) of durations of swing and stance phases in patient subgroups with left-sided and right-sided infarction (a), and patient subgroups with different ranges of walking velocity (b). The positive values of Y-axis indicate a direction of AI toward the affected side; the negative values indicate the direction of AI toward the nonaffected side; s = slowest walking speed; o = ordinary walking speed; f = fastest walking speed.

magnitude of asymmetry and the question if asymmetry is related to speed performance. The present study indicates that the asymmetries in stride phases were present in all patient subgroups regardless of their speed performance. Also, the magnitude of asymmetry in hemiparetic ambulation was significantly higher than in controls. Large swing asymmetry indicated slower overall walking velocity. How-

ever, the ability of patients with stroke to ambulate using various self-selected walking speeds was not related to the highest number of walking asymmetry. This was demonstrated by patients who had a large swing asymmetry but were able to ambulate with a number of speeds using lower velocities. Increased postural stability, increased muscle strength of the paretic limb, and increased symmetry of walking contributed for shifting the velocity performance to higher velocity level, although the range of velocity may remain unaltered.

A more symmetrical weightbearing in hemiplegia is known to be related to greater ambulatory independence (22,23). Our study demonstrates that the hemiparetic postural sway during quiet standing, even in those patients who had a walking
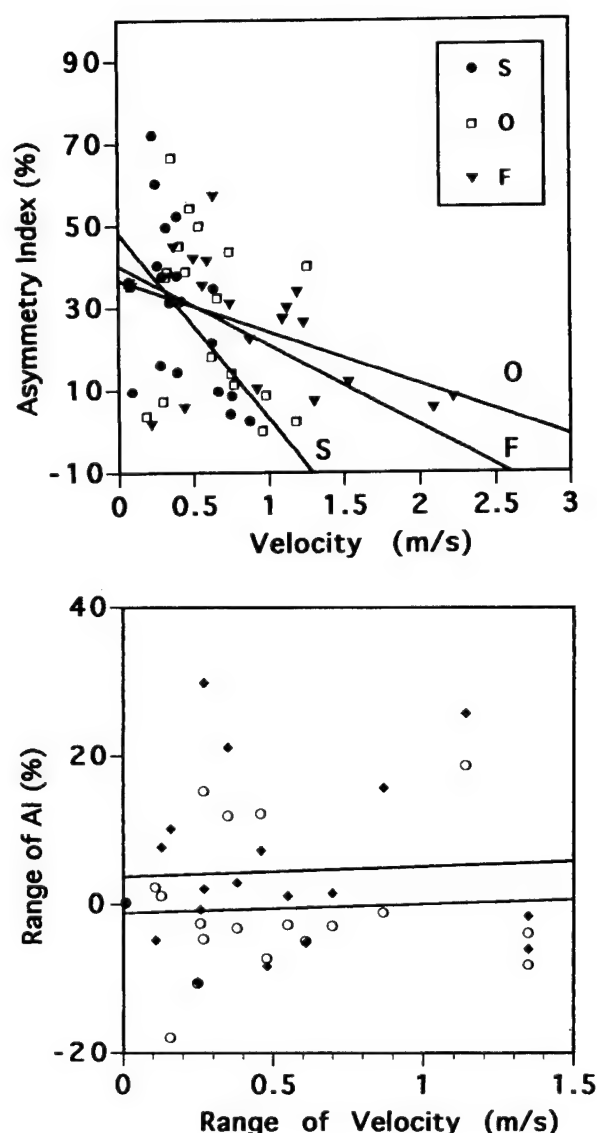
Figure 5.
The relationship between swing asymmetry index and walking velocity of the hemiparetic patients in slowest (s), ordinary (o) and fastest (f) speeds at the top. The relationship between the range of asymmetry indices and the range of velocities of each patient at the bottom.

velocity range close to that in healthy persons, was reflected in interlimb coordination and in the symmetry of limb movements during walking. The larger mean lateral sway toward the NS was related to slower fastest walking speed, while the larger sagittal backward sway was related to increased stance phase asymmetry during slowest walking. Control subjects showed nearly symmetrical patterns of walking during all speeds and no association between posturographic and gait param-

eters. These findings suggest a strong affiliation between postural sway and hemiparetic ambulation and the increase in mean lateral sway during quiet standing of hemiparetic patients may be an indication for the restricted velocity performance during walking.

The effect of lesion site on the postural stability and gait after stroke is difficult to judge in our relatively small patient group. However, a tendency to increased postural sway and gait abnormalities in the subgroup with right-sided infarction was found compared to the left-sided infarction group. Although 62 percent of the right-sided infarction group used additional support of orthotic devices, known to improve walking performance (24-26), these patients tended to have higher postural sway, and walk more slowly and more asymmetrically than did the patients with left-sided infarction. Previous studies on the effects of lateralized cerebral damage have shown that right hemisphere lesions are associated with greater sensorimotor deficits than left hemisphere lesions (27).

The neurobiological basis of spontaneous recovery after stroke, and particularly the restoration of the ambulatory function, are not completely understood (28). The greater part of walking recovery after a stroke occurs within the first 3-6 months (29), although recovery can continue over a period of years in some patients (30). The present study shows that the hemiparetic postural stability and gait changes occur in a stereotyped manner. One explanation for this behavior may be related to the preserved central pattern generators in the spinal cord (31) which may operate in a stereotyped manner under the residual descending supraspinal influence. The ability of hemiparetic patients to ambulate with different walking speeds is a complex phenomenon that results from the relationships between motor functions, morphological lesions, and structural and functional reorganization of the brain, and is associated with the recovery after stroke (32,33).

ACKNOWLEDGMENTS

REFERENCES

1. Bobath B. Adult hemiplegia: evaluation and treatment. London: Heinemann Medical Books, 1978.
2. Brunnstrom S. Recording gait pattern of adult hemiplegic patients. J Am Phys Ther Assoc 1964:44:11-8.
3. Dimitrijevic MR, Faganel J, Sherwood AM, McKay BW. Activation of paralysed leg flexor and extensors during gait in patients after stroke. Scand J Rehabil Med 1981:13:109-15.
4. Marks M, Hirschberg G. Analysis of the hemiparetic gait. Ann NY Acad Sci 1958:74:59-77.
5. Perry J. The mechanics of walking in hemiplegia. Clin Orthop 1969:63:23-31.
6. Twitchell TE. The restoration of motor function following hemiplegia in man. Brain 1951:54:443-81.
7. Brandstater ME, deBruin H, Gowland C, Clark BM. Hemiplegic gait: analysis of temporal variables. Arch Phys Med Rehabil 1983:64:583-7.
8. Dewar ME, Judge G. Temporal asymmetry as gait quality indicator. Med Biol Eng Comput 1980:18:689-93.
9. Sackley CM. Falls, sway, and asymmetry of weight-bearing after stroke. Int Disab Studies 1991:13:1-4.
10. Wall JC, Turnbull GI. Gait asymmetries in residual hemiplegia. Arch Phys Med Rehabil 1986:67:550-3.
11. Wall J, Ashburn A. Assessment of gait disability in hemiplegics. Scand J Rehabil Med 1979:11:95-103.
12. Winstein CJ, Gardner MS, McNeal DR, Barto PS, Nicholson DE. Standing balance training: effect on balance and locomotion in hemiparetic adults. Arch Phys Med Rehabil 1989:70:755-62.
13. Bohannon RW, Larkin PA. Lower extremity bearing under various standing conditions in independently ambulatory patients with hemiparesis. Phys Ther 1985:65:1323-5.
14. Drillis R. Quantitative recording and biomechanics of pathological gait. Ann NY Acad Sci 1958 1981:74:86-109.
15. Seliktar R, Susak Z, Najenson T, Solzi P. Dynamic features of standing and their correlation with neurological disorders. Scand J Rehabil Med 1978:10:59-64.
16. Andriacchi TP, Ogle JA, Galante JO. Walking speed as a basis for normal and abnormal gait measurements. J Biomech 1977:10:261-8.
17. Wagenaar RC, Beek WJ. Hemiplegic gait: a kinematic analysis using walking speed as a basis. J Biomech 1992:25:1007-15.
18. Wagenaar RC. Functional recovery after stroke. Amsterdam: University Press, 1990.
19. Dettmann MA, Linder MT, Sepic SB. Relationships among walking performance, postural stability, and functional assessments of the hemiplegic patients. Am J Phys Med 1987:66:77-90.
20. Mendell JR, Florence J. Manual muscle testing. Muscle Nerve 1990:13:S16-S20.
21. Norlin R. Corrective surgery and gait analysis in cerebral-palsied children. Linköping University Medical Dissertations, Linköping, Sweden, 1984:187.
22. Caldwell C, MacDonnald D, MacNiel K, McFarland K, Turnbull G, Wall F. Symmetry of weight distribution in normals and stroke patients using digital weight scale. Physiother Pract 1986:2:109-16.
23. Gruendel TM. Relationship between weight-bearing characteristics in standing and ambulatory independence in hemiplegics. Physiother Can 1992:44:16-7.
24. Lehmann JF. Biomechanics of ankle-foot orthosis. Prescription and design. Arch Phys Med Rehabil 1979:60:200-7.
25. Lehmann JF, Conton SM, Price R, deLateur BJ. Gait abnormalities in hemiplegia: their correction by ankle-foot orthosis. Arch Phys Med Rehabil 1987:68:763-71.
26. Nakamura R. Recovery of gait in hemiparetic stroke patients with reference to training program. In: Shimamura M, ed. Neurobiological basis of human locomotion. Tokyo: Japan Scientific Societies Press, 1991:425-35.
27. Hom J, Reitan RM. Effect of lateralized cerebral damage upon contralateral and ipsilateral sensorimotor performances. J Clin Neuropsychol 1982:4:249-68.
28. Goldstein LB, Davis JN. Restorative neurology. Drugs and recovery following stroke. Stroke 1990:25:19-24.
29. Skilback CE, Wade DT, Hewer RL, Wood VA. Recovery after stroke. J Neurol Neurosurg Psychiatry 1983:46:5-8.
30. Bach-y-Rita P. Central neuron system lesions: sprouting and unmasking in rehabilitation. Arch Phys Med Rehabil 1981:62:413-7.
31. Brooks VB. Locomotion. In: The neuronal basis of motor control. New York: Oxford University Press, 1986:181-201.
32. Chollet F, DiPiero V, Wise RJS, Brooks DJ, Dolan RJ, Frackowiak RSJ. The functional anatomy of motor recovery after stroke in humans: a study with positron emission tomography. Ann Neurol 1991:29:63-71.
33. Weiller C, Chollet F, Friston KJ, Wise RJS, Frackowiak RSJ. Functional reorganization of the brain in recovery from striatocapsular infarction in man. Ann Neurol 1992:31:463-72.

Strain-based fatigue analysis of wheelchairs on a double roller fatigue machine

J. David Baldwin, PhD and **John G. Thacker, PhD**

*School of Aerospace and Mechanical Engineering, University of Oklahoma, Norman, OK 73019;
Department of Mechanical, Aerospace, and Nuclear Engineering, University of Virginia,
Charlottesville, VA 22903*

Abstract—Results are presented from an experimental program that recorded the outputs of strain gages mounted on two wheelchair frames (one manual, one power) as the wheelchairs were run on a double roller fatigue machine. Rectangular strain gage rosettes were attached to the frames near the cross tube center pin and on the side frame behind a front caster. Thirty data sets were recorded from each rosette on each wheelchair frame. The fatigue test machine and test protocol were in substantial conformance with the recently published ANSI/RESNA Standard for wheelchair fatigue testing.

Two analyses have been performed on the recorded strain data. The von Mises stress histories were computed from the strain data and show that peak stresses are frequently twice the mean value. Also, estimates of the number of fatigue machine cycles to failure have been made using a strain-based fatigue analysis. These data will provide wheelchair designers with useful data to incorporate into their design process.

Key words: *double roller fatigue machine, fatigue, strain, wheelchair.*

INTRODUCTION

Any load bearing metal structure subjected to variable loads is a candidate for fatigue failure. The widely studied phenomenon of metal fatigue has long been known to be a principal failure mode of components carrying dynamic loads even though the stresses are significantly below the material's yield strength. Because failures can occur at loads lower than those considered for static failure, the designer of such dynamically loaded structures must consider sufficient fatigue life as a primary design constraint.

Metal fatigue analysis is complicated by two factors. First, fatigue failures can be thought of as the culmination of two processes: fatigue crack initiation and crack propagation to failure. In the ideal case, the designer will have full knowledge of the time-varying loads imposed on the structure and will have a fatigue theory available that can accurately predict the failure of the critical sections of the structure. In reality, the loading is not often known with complete accuracy and our crack initiation models are simplified curve fits based on experimental observations. Similarly, crack propagation models, such as the Paris relation

$$\frac{da}{dN} = C\,(\Delta K)^n$$

are also based on empirical formulations. In Equation 1, a is the crack length, N is the number of

loading cycles, ΔK is the stress intensity at the crack tip and C and n are curve fit parameters for a given material.

The second issue that complicates a fatigue analysis (and one that is usually ignored) is the fact that the fatigue lives of highly polished specimens tested under nominally identical situations can fail at lives that vary by over one order of magnitude (1,2). Efforts at incorporating this fundamental, material-based, life scatter have been mainly of theoretical interest up to this point.

Given the uncertainties associated with the analysis and design of a dynamically loaded structure, the designer is often left with no alternative other than to perform fatigue tests on prototypes to assess the adequacy of the structure. In fact, the fatigue test may be imposed on the manufacturer by contract or regulatory requirements.

The purpose of this paper is to present recorded strain data taken from two wheelchairs as they were driven on a double roller fatigue machine and to illustrate a strain-based fatigue analysis that may be useful in estimating the fatigue life based on the response data. Stress histories computed from the strains are also presented. The stress versus time histories illustrated here could be useful to a wheelchair designer in the preliminary stress analysis design phase. Our data establish order of magnitude values for some stress measures used in design and show the stress variability experienced on a double roller fatigue machine. Although our machine was built before the circulation of the latest wheelchair fatigue test standard, *ANSI/RESNA WC/08: RESNA Standard: Wheelchairs - Static, Impact and Fatigue Strength Tests* (3,4), it is in substantial conformance with that standard. It should be emphasized, however, that the wheelchairs used in this investigation were not tested to failure. They were being used concurrently in other projects and could not be sacrificed for this one. As a result, the fatigue life predictions illustrated here have not been verified by actual test data.

The results reported here are strictly applicable to the two wheelchairs tested. These data will be useful, however, in guiding wheelchair designers as they prepare their structures for an ANSI/RESNA Standard fatigue test. The fatigue life analysis may also be useful in stimulating discussion among designers about the long-term survivability of their designs.

METHODS

Current Test Program

The testing program described in this paper was part of a larger effort to record dynamic strain histories from wheelchair frames as they traversed different terrains. Experimentally measured strain histories were to be used as the input data for a fatigue reliability analysis of wheelchair structural elements; the structural reliability model was to be incorporated into an integrated electro-mechanical wheelchair system reliability analysis.

Two wheelchairs were used in the testing: an Invacare Rolls IV (manual) and an Invacare Rolls Arrow (power). Both wheelchairs were of the folding type with two steel cross tubes pinned together at the center. The tube carbon steel alloy was assumed to be 1010-1020 grade commonly used in steel wheelchair frames; no metallurgical analysis was done to verify this assumption. The manual wheelchair had solid front and rear tires and chrome plated frame tubes. Front tire dimensions on this wheelchair were 20 cm (7.9 in) diameter by 1.9 cm (0.75 in) radial thickness. The manual wheelchair's solid rear tires were 50.8 cm (20 in) diameter by 5.4 cm (2.125 in) radial thickness. The power wheelchair had solid front tires and pneumatic rear tires and painted frame tubes. On this chair, the front tires had an outside diameter of about 19 cm (7.5 in) and a radial thickness of about 3.8 cm (1.5 in); dimensions of the rear tires were 61.0 cm (24 in) outside diameter by 1.3 cm (0.5 in) radial thickness. Seventy pounds of steel plates were substituted for batteries on the power chair.

As described below, strain gages were attached to the wheelchair frames and connected to a data acquisition system. The strain gage installations were identical on both wheelchair frames. Test results and analysis of the stress histories for the wheelchairs rolling over bumps on a treadmill and falling off an elevated platform were reported previously (5).

Instrumentation

Three rectangular strain gage rosettes were attached in approximately the same locations to each wheelchair frame. Two rosettes were located on the front cross tube, one directly below the center connecting bolt on the bottom of the tube, and the other on the front of the tube next to the bolt. These

gages were designated "XG1" and "XG2." The third rosette was mounted on the horizontal tube directly behind the right front caster and was designated "CG1" **(Figure 1).** The cross tube gage locations were chosen because this area of the frame has been shown to be subjected to high stresses under static loading (6). The caster location was chosen to measure the tube response to front caster impacts, such as those experienced on the double-roller fatigue machine. Each strain sensing element of the rosette was connected to a Wheatstone bridge in a quarter bridge pattern. The bridge output voltage was amplified by a strain gage conditioner, filtered by a low pass filter and sampled by a computer-mounted data acquisition board. The assumption has been made that each strain gage element is in a field of essentially uniform strain (i.e., small strain gradients) and that the strains at nearby geometric discontinuities can be computed, by an appropriate strain concentration factor, from the recorded strains. The strain gage installations and data acquisition system used in this study were the same as those reported in Baldwin and Thacker (5), to which the reader is referred for details.

Test Regime

The wheelchairs were tested on the double roller fatigue machine developed in 1986 at the University of Virginia (4). Any variances from the ANSI/RESNA test standard procedure (3), the "test standard," will be noted.

The double roller fatigue machine consisted of two 91.4 cm (36 in) long by 27.3 cm (10.75 in) diameter aluminum rollers mounted on a steel channel frame. Each roller had two rectangular slats, 30.5 cm (12 in) long by 1.3 cm (0.5 in) high by 3.8

Figure 1.
Rosette CG1 installation site.

cm (1.5 in) wide attached to the surface. On either roller, the slats were oriented 180° apart (i.e., the slat on the left end of the roller was located 180° around the circumference of the roller from the slat on the right end). The slats provided "texture" to the rolling surface. The rollers were positioned so that no two tires were in contact with their respective slat simultaneously during the rotation. These dimensions are within the ranges given in the test standard.

A 560 W (¾ HP) electric motor drove the back roller through a right angle gear head; a toothed belt running over pulleys transmitted torque from the back roller to the front roller. The motor turned the back roller at approximately 60 revolutions per minute (RPM) which translates into a roller surface speed of approximately 0.86 m/s. The test standard specifies a surface speed of 1.0 ± 0.1 m/s.

For this investigation, the pulleys were the same diameter; thus, the front roller turned at the same RPM as the rear. The test standard specifies that the speed of the roller under the wheels that are not being driven (in this case, the front wheels) are 2–7 percent faster than the other drum. The front roller was mounted so that the roller's axis made an angle of 5° with its axis of rotation; the front axis of rotation was horizontal and parallel with the rear roller's axis. Making the axes offset caused a reversed torque to be applied to the frame through the front casters on each revolution. The test standard specifies that the roller axes are horizontal. The difference in the test data due to these two variances from the test standard is not known. It is felt, however, that the cyclic loading on the frame caused by off-axis rollers is more severe than that due to a speed differential between the rollers and that the test data reported here reflects a harsher test than the test standard.

Surrounding the fatigue machine bed frame was a set of support bars that attached to the rear axles of the wheelchair under test to maintain these wheels in the correct position with respect to the rear roller. Note that the rear wheels were only restrained from side to side (i.e., along the axis of the roller) and from front to back. The wheelchair was free to move vertically. The front casters were free to bounce.

Once the wheelchair was positioned on the rollers and its rear axles attached to the support bars, one of its strain gages was connected into the instrumentation system. The test protocol specified
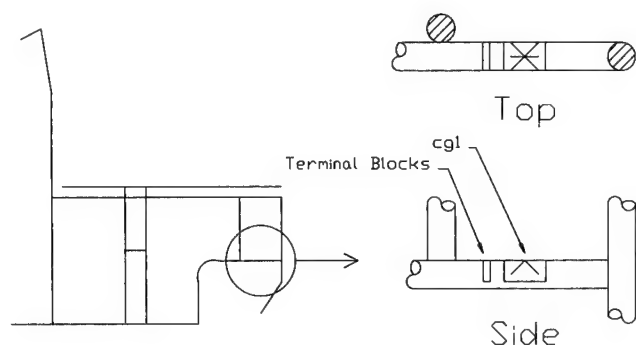
that any strain gage under test was to have been continuously energized for 24 hours before the beginning of the test. This period was sufficient for the gages to warm up and for any thermal transients to die out. With the wheelchair unloaded and resting on a temporary flat platform above the rollers, the strain gage circuit was balanced to show zero strain output. The platform was removed, the wheelchair was lowered onto the rollers, and the chair was then loaded with 100 kg of weight in the seat and 10 kg on the footrests. The ISO standard 100 kg load dummy (4,7) was secured with straps to the wheelchair seat and back. The dummy was loosely tethered from an overhead gantry that would support the weight in case of failure of the wheelchair frame.

Strain Data Preparation

A data collection run consisted of recording the output of one strain gage rosette for 4 sec as the wheelchair was run on the double roller fatigue machine. The data was sampled at a rate of 512 samples/sec/gage element; thus, the strain signal consisted of 2048 data points recorded from each of the three rosette arms. The analog voltage data was digitized and stored on disk in terms of integers in the interval -2047 through $+2048$. The quantity of data that could be recorded in a test was limited by the memory capacity of the data acquisition computer. Four sec of data corresponded to approximately four complete revolutions of the fatigue machine rollers.

The first step in preparing the digital strain data was to convert them back into engineering strain values. In this calculation, the strain gage outputs were corrected for gage transverse sensitivity and nonlinearity. Then, using the strain transformation rule, the three elements of rosette strain could be expressed as the strain existing at any specified angle from the rosette. Specifically, if the strains recorded from rosette arms 1, 2, and 3 are labeled ϵ_0, ϵ_{45}, and ϵ_{90}, respectively, the strain existing at any angle ϕ is given by

$$\epsilon_\phi = \frac{\epsilon_0 + \epsilon_{90}}{2} + \frac{\epsilon_0 - \epsilon_{90}}{2} \cos 2\phi$$

$$+ \frac{2\epsilon_{45} - (\epsilon_0 + \epsilon_{90})}{2} \sin 2\phi \qquad [2]$$

For the data presented and discussed here, the strains at 45° from rosette arm 1 were used in the fatigue analysis. These strains were collinear with rosette arm 2 that was always aligned along the axis of the frame tube; in this case, Equation 2 reduces to $\epsilon_\phi = g_{45}$. In principle, however, the strains at any angle could have been used.

Beyond using the strain gage outputs in fatigue calculations, we also used them to compute the von Mises stress histories at the gage locations. The von Mises stress can be calculated from rectangular strain gage rosette outputs by first computing the principal normal strains. At any sampling instant, the principal normal strains, ϵ_1 and ϵ_2, can be expressed in terms of the instantaneous rosette arm output strains using the relationship

$$\epsilon_{1,2} = \frac{\epsilon_0 + \epsilon_{90}}{2} \pm \frac{\sqrt{(\epsilon_0 - \epsilon_{90})^2 + [2\epsilon_{45} - (\epsilon_0 + \epsilon_{90})]^2}}{2} \qquad [3]$$

and the instantaneous principal stresses, σ_1 and σ_2, are given by,

$$\sigma_1 = \frac{E}{1 - \nu^2} (\epsilon_1 + \nu\epsilon_2)$$

$$\sigma_2 = \frac{E}{1 - \nu^2} (\epsilon_2 + \nu\epsilon_1) \qquad [4]$$

where ν is the tube material Poisson ratio. In terms of the principal stresses, the instantaneous von Mises stress is given by

$$\sigma_e = \sqrt{\sigma_1^2 + \sigma_2^2 - \sigma_1\sigma_2} \qquad [5]$$

Fatigue Life Model

Using the histories recorded from the strain gages, an estimate was made of the fatigue life of each gage location. The life estimate was made using a strain-based fatigue analysis. The primary assumption involved in the strain-based fatigue model is that the appearance of a crack in a component can be related to the fracture of a small specimen in a fatigue test. This method has been shown (8) to be reasonably accurate in predicting cracking in test specimens subjected to complex load histories. The strain-based analysis carried out in this investigation was explained in more detail in references 9–11.

When a metal specimen is loaded such that the possibility of plastic deformation exists, we must use a constitutive relationship that reflects this fact.

Even moderate stresses can be magnified by the presence of a geometric discontinuity (stress concentration) to the point where localized plasticity occurs. The linear elastic stress-strain relationship, $\sigma = E\epsilon$, is inadequate in the situation where plastic strains are present. In contrast to a monotonic stress-strain relationship, a cyclic stress-strain expression is necessary when examining the inelastic response due to fatigue loading.

The cyclic stress-strain curve is given by Landgraf, et al. (12)

$$\epsilon = \frac{\sigma}{E} + \left(\frac{\sigma}{K'} \right)^{\frac{1}{n'}} \qquad [6]$$

The first and second terms of Equation 6 represent the elastic and plastic contributions to the total strain, respectively. The parameters K' and n', called the cyclic strain hardening coefficient and the cyclic strain hardening exponent, respectively, are material properties derived from laboratory tests. In the strain-based fatigue method, Equation 6 is used to model the material response to the first load application.

After the first load application, especially if there is inelastic strain, the material will exhibit hysteresis. This means that upon unloading the stress-strain does not follow the loading curve. We model the behavior of the material as it follows the *hysteresis stress-strain curve*, which is given by

$$\Delta\epsilon = \frac{\Delta\sigma}{E} + 2\left(\frac{\Delta\sigma}{2K'} \right)^{\frac{1}{n'}} \qquad [7]$$

Equations 6 and 7 represent the fundamental material response (stress-strain) to cyclic loading.

While the average strain in the smooth areas of a structural member can be measured with a strain gage, the strain near a notch or other discontinuity is not so easily measured. Neuber (13) found that for an edge notch geometry, the theoretical stress concentration factor, K_t, is related to the stress concentration factor, K_σ, and the strain concentration factor, K_ϵ by the equation

$$K_t^2 = K_\sigma K_\epsilon \qquad [8]$$

The nominal stress s and the nominal strain e are measured outside the notch strain gradient. If the measured (remote) strain remains elastic, that is, $s = Ee$, *Neuber's rule becomes*

$$\sigma \epsilon = (K_t\, e)^2\, E \qquad [9]$$

Note that Equation 9 is valid only for the first load cycle, where the σ–ϵ curve is the constitutive relation. In a manner similar to the cyclic stress-strain curve, Neuber's rule is modified to handle all strain reversals after the first. The "hysteresis Neuber's rule" corresponding to the hysteresis stress-strain curve is

$$\Delta\sigma\, \Delta\epsilon = (K_t\, \Delta e)^2\, E \qquad [10]$$

The (possibly inelastic) strains and stresses appearing in Equations 9 and 10 are related through the cyclic stress-strain and hysteresis stress-strain constitutive relationships (Equations 6 and 7). Because the cyclic stress-strain equations and Neuber's rule provide unique relationships between stress and strain, the two equations must be solved simultaneously at each strain reversal. This is called a *notch strain analysis*. Of course, if a more accurate finite element or experimentally determined notch strain calibration is available, it should be used for the Neuber analysis. Globally convergent iterative solutions for the Neuber notch strain analysis can be obtained using Newton's method (9).

Using the cyclic stress strain curves, (Equations 6 and 7), and Neuber's model for the notch strains in way of a geometric discontinuity, (Equations 9 and 10), we can convert a strain history recorded away from the stress riser to a strain history at the root of the notch. For a highly variable history, the strain cycles (which will be used to estimate the number of cycles to failure) are not readily apparent. In such a case, we choose a technique known as "rainflow cycle counting" (14) to identify the closed stress-strain loops from the history. The rainflow cycle counting procedure given by Downing and Socie (15) has been implemented to convert the computed notch strain history to a series of constant amplitude strain cycles for comparison with the strain-life curve.

The elastic-plastic strain life (ϵ–N) relationship, given by

$$\frac{\Delta\epsilon}{2} = \frac{\sigma'_f}{E}\, (2N_f)^b + \epsilon'_f\, (2N_f)^c \qquad [11]$$

has been used to model the failure of smooth laboratory specimens subjected to cyclic elastic and plastic strain. In Equation 11, the quantity $2N_f$ is the number of strain cycles to failure at strain range $\Delta\epsilon$;

parameters E, σ_f', b, ϵ_f', and c are the modulus of elasticity, fatigue strength coefficient, fatigue strength exponent, fatigue ductility coefficient and fatigue ductility exponent, respectively. The strain range $\Delta\epsilon$ is that for each closed stress-strain hysteresis loop identified by the rainflow cycle counting procedure. The number of strain cycles to failure at a given strain range can be computed iteratively from Equation 11 using Newton's method. This iteration can also be shown to be globally convergent.

Equation 11 implies that for arbitrarily small strain ranges, the number of cycles to failure can become very large. Because computers cannot represent arbitrarily large and small numbers without loss of precision, some limit is placed on how large a value of N_f can be accurately computed. Also, large values of N_f begin to lose their significance when it is realized that such a large number of cycles could not be realized in a device's anticipated life. For these reasons, if a given strain range resulted in $N_f \geq 10^{10}$ cycles in Equation 11, the reported number of cycles to failure was set to 10^{10}. In practice, this upper limit could be set to any value deemed reasonable.

Miner's linear cumulative damage rule

$$D = \sum_i D_i = \sum_i \frac{n_i\,(\Delta\epsilon)}{N_f\,(\Delta\epsilon)} \qquad [12]$$

is used to compute the damage D for a block of strain loading. In Miner's rule, $n_i(\Delta\epsilon)$ is the number of strain cycles of range $\Delta\epsilon$ as found by the rainflow cycle counting procedure, $N_f(\Delta\epsilon)$ is the number of strain cycles to failure at range $\Delta\epsilon$ as given by the strain-life curve, Equation 11, and the index i runs over the collection of strain cycles. Failure is assumed to occur when the damage sum is equal to 1.0. In the strain-based analysis, failure is assumed to occur at the appearance of a small crack, typically 2.5 mm, or 0.1 in (8). If the damage sum for a given strain history is less than 1.0, failure is predicted after the occurrence of more than one block of that history. In such a case, the number of blocks to failure is given by

$$blocks = \frac{1.0}{\sum_i D_i} \qquad [13]$$

For purposes of fatigue analysis, the wheelchair frames were assumed to be made of cold-drawn 1010 carbon steel, or equivalent. The relevant fatigue properties were as listed below (16):

σ_f'	= 538 MPa (78,000 psi)	b	= -0.073
ϵ_f'	= 0.110	c	= -0.410
K'	= 490 MPa (71,000 psi)	n'	= 0.110
E	= 200 GPa (29,000,000 psi)	ν	= 0.30

RESULTS

Each wheelchair was tested on the fatigue machine while each of its three strain gages was monitored in turn. A test series consisted of recording the output of one strain gage for a total of 30 intervals of 4 sec each. Therefore, there was a total of 180 strain records; each was 4 sec long and consisted of the output of the three arms of a single strain gage rosette. We believe this data set represents the most comprehensive ever recorded from a double roller fatigue machine.

Because it would be impractical to present full details of these data sets here, two key aspects of the data will be examined. First, the nature of the von Mises stresses for the six strain gage installations will be illustrated. The von Mises stress is a commonly used measure of the potential for inelastic deformation in steels. These data will be presented in condensed form by showing von Mises stress versus time histories form one selected data set from each test series. Second, the computed number of 4-sec blocks to failure will be summarized for each test series. The failure estimates were computed using the strain-based fatigue analysis.

Recorded Stress Peaks

For each of the six test series, the von Mises stress history of one of the data sets will be discussed. Specifically, the last data set of the test series will be used in this illustration. The last data set was chosen because, by the time it was recorded, the wheelchair had stabilized on the fatigue machine and was running smoothly. For each chosen data set, the von Mises stress at each time increment was calculated using Equations 2–5; the maximum, mean, and minimum values are given in **Table 1**. Note that no stress concentration factors were incorporated into the stress computations; the stresses are as measured at the strain gages, not near geometric discontinuities. The "Data Set Number"

column contains the data set index number ("DRF xxx") and the wheelchair and rosette under test ("y-zzz").

Computed Lives and Statistical Analysis

Each of the 180 strain gage rosette data sets was analyzed using the fatigue life estimating procedures outlined above. The estimated number of 4-sec strain blocks to failure for each data set was computed using the strain life curve (Equation 11). **Table 2** summarizes the maximum, mean, minimum, and the standard deviation of the number of blocks to failure for each data set. The stress concentrations factors, K_t, used in the notch strain calculations were computed from empirical correlations given in reference 17 ($K_t = 4.77$ for rosette XG1) and reference 18 ($K_t = 2.94$ for rosette CG1). Because an earlier analysis (5) showed that the cross tube loading was predominantly bending and axial compression with very little cyclic torsion, the bending stress concentration factor has been used for XG1. Because it was not installed in way of a geometric discontinuity, the rosette XG2 strains had a stress concentration value of $K_t = 1.0$ (i.e., no stress increase).

It is important to note here that the value of the stress concentration factor for the cross tube center pin holes used here is based on a plain hole through the tube (17). In reality, these connections have smaller tubes inserted into the transverse holes that provide stiffening and reinforcement to the holes. The added reinforcement would be reflected in a value of K_t less than the value used here. At this time, there are no published values for the stress concentration factor for a tube with a stiffened transverse hole.

DISCUSSION

The von Mises stress histories for the six sample data sets are illustrated in **Figures 2–4**. The stress histories clearly show the periodic nature of the fatigue machine loading. Whereas the XG1 and XG2 responses show distinct differences between the manual and power wheelchairs, the CG1 data for the two chairs are essentially identical. **Figures 2–4** and **Table 1** show that the largest maximum and mean stresses and the largest stress ranges (maximum-minimum) occurred in the cross tubes of both wheelchairs. The stress levels and ranges behind the

Table 1.
Summary of von Mises stresses.

Data Set Number	Maximum, MPa (psi)	Mean, MPa (psi)	Minimum, MPa (psi)
DRF 180 (M-CG1)	72.1 (10,451)	19.3 (2795)	2.4 (348)
DRF 90 (P-CG1)	79.9 (11,585)	17.2 (2491)	1.0 (148)
DRF 120 (M-XG1)	116.3 (16,869)	43.5 (6311)	6.4 (935)
DRF 30 (P-XG1)	157.9 (22,904)	89.6 (12,989)	0.7 (102)
DRF 240 (M-XG2)	270.4 (39,219)	193.7 (28,092)	126.7 (18,373)
DRF 210 (P-XG2)	259.5 (37,643)	138.0 (20,018)	16.8 (2432)

Table 2.
Summary of computed blocks to failure.

Test Series	Maximum	Mean	Minimum	Standard Dev.
M-CG1 (N = 30)	10,000,000,000	7,002,437,799	1,381,758,002	2,879,933,312
P-CG1 (N = 30)	640,921,000	177,755,227	9,367,898	174,946,994
M-XG1 (N = 30)	47,414	29,395	22,674	5921
P-XG1 (N = 30)	652	254	140	117
M-XG2 (N = 30)	10,000,000,000	8,711,326,648	293,108,482	3,341,680,157
P-XG2 (N = 30)	10,000,000,000	10,000,000,000	10,000,000,000	0

One block = 4 seconds.

a.

b.
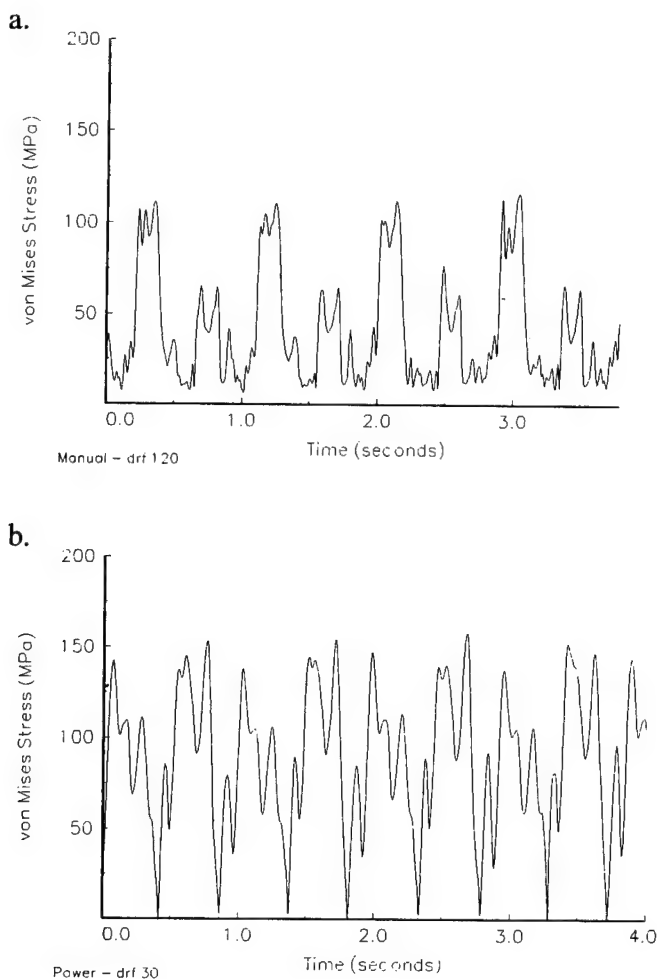
Figure 2.
von Mises stress histories for rosette XG1.

a.

b.

Figure 3.
von Mises stress histories for rosette XG2.

front casters were the lowest of those measured. It can also be seen that, for all three rosette locations, the power wheelchair experienced larger stress ranges than the manual wheelchair. Presumably, this result is due to the added loading on the power chair due to the batteries and drive apparatus.

It is interesting to note, however, that the maximum stresses recorded in the power wheelchair are not a great deal higher than in the manual wheelchair (and in the case of rosette XG2, are actually lower). It is felt that the comparable maximum stress levels can be attributed to the fact that, even though the tubes in the two chairs had the same outside diameter and wall thickness, the power wheelchair was slightly smaller than the manual chair, making it stiffer. The power chair's stiffer structure was able to carry its added load by developing relatively low stresses.

Table 2 summarizes the number of blocks to failure computed by the fatigue model described above. Recall that each block referred to in **Table 2** is a 4-sec history; therefore, the estimated total time to failure (in seconds) is four times the numbers given in the table. A standard wheelchair fatigue test at the University of Virginia requires a chair to survive for 100,000 cycles (roller revolutions) on the fatigue machine. This test duration corresponds to 25,000 4-sec blocks in the data presented here. It can be seen from **Table 2** that the estimated mean life for the manual wheelchair rosette XG1 is about 100,000 cycles and that the estimated mean life for the same rosette on the power wheelchair is roughly 1,000 cycles. It is felt that the low life estimates for the power wheelchair reflect the uncertainty in the value of the stress concentration factor for the cross tube center hole. If we assume that this chair is

Figure 4.
von Mises stress histories for rosette CG1.

smoothly. It seems that a single recorded strain history of 4 sec is not sufficient to fully capture the wheelchair dynamics; perhaps longer contiguous strain samples would lead to less scatter in the fatigue life estimates. Recall that the total sampling time was limited by computer storage.

While considering the estimated fatigue lives of the wheelchair frames, the reader should bear in mind that these chairs were not tested to failure. The lives quoted here are based on a mathematical model of fatigue and have not been verified by destructive tests; as mentioned earlier, the wheelchairs were being used concurrently in other projects and were not available for a fatigue test to destruction. One should remember that the fatigue life estimates are sensitive to the value of K_t and that the values used here are approximate. We do, however, feel that the life estimates are useful in identifying locations in the frames that may be susceptible to fatigue.

CONCLUSIONS

Using strain histories recorded from two wheelchairs on a double roller fatigue machine, the von Mises stress histories and the estimated number of strain cycles to failure for three frame locations have been presented. The stress histories showed that, of the three frame locations monitored, the most highly stressed point in both wheelchairs was on the cross tube below the cro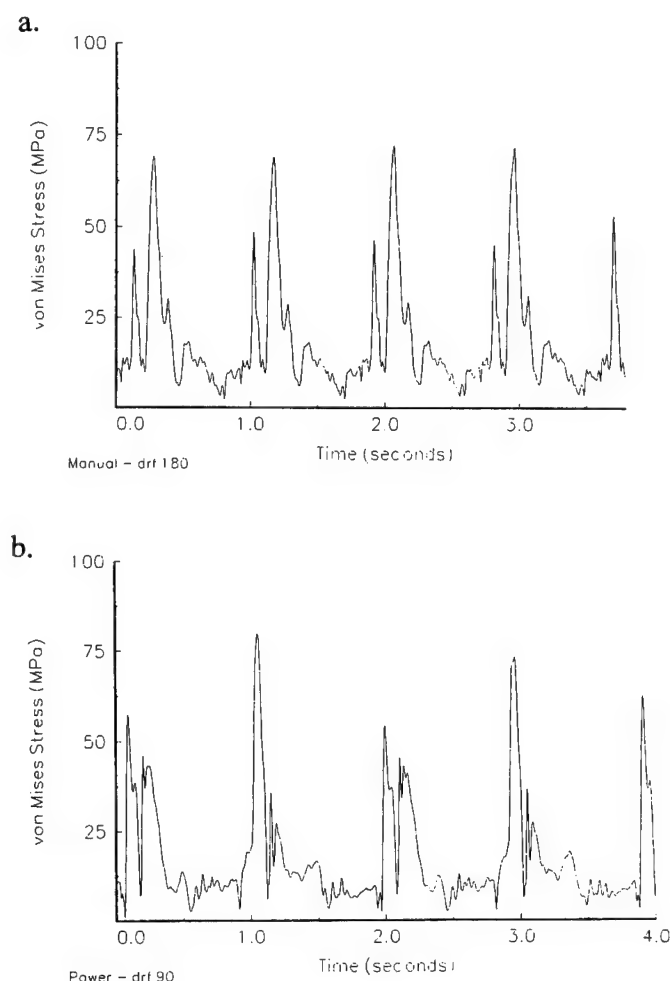ssing pin at rosette XG2. The mean stress in the manual frame was about 40 percent higher than in the power frame; the manual frame peak stress was only about 4 percent larger. At rosette XG1, the power wheelchair frame experienced higher mean (106 percent higher) and maximum (36 percent higher) stresses than the manual frame. The peak stresses at XG1 for both wheelchairs were typically about 100–150 MPa lower than at XG2. It was also shown that the stresses behind the front casters at rosette CG1 were very similar between the two wheelchairs in peak magnitude and waveform. These peak stresses were approximately 200 MPa lower than those recorded at rosette XG2. The von Mises stress data could provide wheelchair builders with additional information to use in their frame strength calculations.

In contrast to the von Mises stress results where the highest stresses were recorded at rosette XG2, the fatigue calculations predicted that failure was

capable of surviving 100,000 cycles on the double roller fatigue machine, K_t must have a value smaller than 4.77 used here. At this time, there is no published data for the stress concentration factor for a stiffened diametral hole in a tube. The life estimates for the other rosettes on the chairs are significantly more than 100,000 cycles.

Perhaps the most striking result to be taken from this analysis is the degree of variability in the fatigue life estimates. **Table 2** shows that the standard deviations of blocks to failure are quite large, ranging from 20 percent to 98 percent of the mean. This is surprising, because one would expect the nominally identical dynamic strain histories recorded in these tests to result in life estimates of considerably less scatter. As noted earlier, the data records were initiated after the wheelchairs had stabilized on the fatigue machine and were running

most likely on the side of the cross tube at the pin hole at rosette XG1. At this location, the mean life (as computed from the 30 test data sets) for the power wheelchair was about 1,000 cycles on the fatigue machine; the mean life for the manual chair was over 100,000 cycles. It is noted that the fatigue life estimate for the XG1 location is complicated by the uncertainty in the value of the stress concentration factor at that point. The mean estimated fatigue lives for the other rosette locations suggest that both wheelchairs would survive the 100,000 cycle fatigue test. The fatigue life estimates for rosette CG1 are only for the tubular joint behind the casters. This result, however, makes no statement about the strength of the caster connections to the frame tubes. It was surprising to note that the fatigue life estimates for a given frame location showed large variability for the nominally identical test data series.

Readers interested in obtaining copies of the strain histories used here may contact the lead author.

ACKNOWLEDGMENTS

REFERENCES

1. Freudenthal AM. Planning and interpretation of fatigue tests. Symposium on statistical aspects of fatigue, ASTM STP-121. Philadelphia: American Society for Testing and Materials, 1952:3–22.
2. Sinclair GM, Dolan TJ. Effect of stress amplitude on statistical variability in fatigue life on 75S-T2 aluminum alloy. In: Proceedings of the American Society of Mechanical Engineers 1953:75:867–72.
3. ANSI/RESNA WC/08 1991: RESNA standard: Wheelchairs - static, impact and fatigue strength tests.
4. Duffey TM, McLaurin CA, Thacker JG. Construction and operation of the ISO double roller fatigue tester, University of Virginia Rehabilitation Engineering Center Report Number UVAREC-107-86, 1986.
5. Baldwin JD, Thacker JG. Characterization of the dynamic stress response of manual and powered wheelchair frames. J Rehabil Res Dev 1993:30:224–32.
6. Thacker JG, Todd BA, Disher TD. Stress analysis of wheelchair frames. In: Proceedings of the 8th Annual RESNA Conference, Memphis, TN. Washington, DC: RESNA Press 1985:84–6.
7. ANSI/RESNA WC/11 1991: RESNA standard: test dummies.
8. Wetzel RM, ed. Fatigue under complex loading. Warrendale PA: Society of Automotive Engineers, 1977.
9. Baldwin JD. Dynamic structural testing and strain-based fatigue reliability analysis of wheelchair frames (Dissertation). University of Virginia, 1993.
10. Baldwin JD, Thacker JG. A strain-based fatigue reliability analysis method. J Mech Des 1995:117:(A):229-34.
11. Bannantine JA, Comer JJ, Handrock JL. Fundamentals of metal fatigue analysis. Englewood Cliffs, NJ: Prentice Hall, 1990.
12. Landgraf RW, Morrow J, Endo T. Determination of the cyclic stress-strain curve. J Mater 1969:4:176–88.
13. Neuber H. Theory of stress concentration for shear-strained prismatical bodies with arbitrary nonlinear stress-strain laws. J Appl Mech 1961:E28:544–50.
14. Dowling NE. Fatigue failure predictions for complicated stress-strain histories. J Mater 1972:7:71–87.
15. Downing SD, Socie DF. Simple rainflow counting algorithms. Int J Fatigue 1982:31–40.
16. Technical report on fatigue properties - SAE J1099. SAE Handbook. Warrendale, PA: Society of Automotive Engineers.
17. Young WC. Roark's formulas for stress and strain, 6th ed. New York: McGraw-Hill, 1989.
18. Gurney TR. Fatigue of welded structures, 2nd ed. Cambridge, UK: Cambridge University Press, 1979.

Power wheelchair range testing and energy consumption during fatigue testing

Rory A. Cooper, PhD; David P. VanSickle, MS; Steven J. Albright, BS; Ken J. Stewart, BS; Margaret Flannery, BS; Rick N. Robertson, PhD

Human Engineering Research Laboratories, Highland Drive VA Medical Center, Pittsburgh, PA 15206; Departments of Rehabilitation Science and Technology, Mechanical Engineering, Medicine and Bioengineering Program, School of Health and Rehabilitation Sciences, University of Pittsburgh, Pittsburgh, PA 15261; Department of Biomedical Engineering, School of Engineering and Computer Science, California State University, Sacramento, CA 95819-6019

Abstract—The range of a power wheelchair depends on many factors including: battery type, battery state, wheelchair/rider weight, terrain, the efficiency of the drive train, and driving behavior. The purpose of this study was to evaluate the feasibility of three methods of estimating power wheelchair range. Another significant purpose was to compare the current draw on pavement to current draw on an International Standards Organization (ISO) Double Drum tester at one m/sec. Tests were performed on seven different power wheelchairs unloaded, and loaded with an ISO 100 kg test dummy. Each chair was configured according to the manufacturer's specifications, and tires were properly inflated. Experienced test technicians were used for the tennis court tests, and treadmill tests. An ISO 100 kg test dummy was used for the ISO Double Drum test. Energy consumption was measured over a distance of 1500 m for each of the three test conditions. The rolling surface was level in all cases. Repeated measure analysis of variance (ANOVA) revealed a significant difference (p = 0.0001) between the predicted range at maximum speed for the three tests. Post hoc analysis demonstrated a significant difference ($p < 0.01$) in estimated range at maximum speed between the Double Drum test and the treadmill test, as well as between the Double Drum test and the tennis court test. Our results indicate no significant difference ($p > 0.05$) between the predicted range at maximal speed between the treadmill and tennis court tests. A simple relationship does not exist between the results of range testing with the Double Drum tester and the tennis court. An alternative would be to permit the use of a treadmill for range testing as simple relationships between all pertinent treadmill and tennis court range data were found. For the Double Drum tester used, the current demand is higher than under normal usage. This presents a problem as current is related to load torque in a power wheelchair. Hence, the Double Drum tester friction must be reduced. The predicted range for the tennis court test at maximum speed ranges from a low of 23.6 km to a high of 57.7 km. The range of the power wheelchair can be improved by the use of wet lead acid batteries in place of gel lead acid batteries.

Key words: *batteries, fatigue testing, range, standards, wheelchair.*

INTRODUCTION

The range of a power wheelchair depends on many factors including: battery type, battery state, wheelchair/rider weight, terrain, the efficiency of

the drive train, and the driving behavior of the user (1–6). Various wheelchairs have different ranges. This variation in range may be related to the intended purpose of the power wheelchair or the settings selected by the user (7). Batteries are rated in ampere hours (amp-hrs). The amp-hr rating and the current drawn by the power wheelchair will, to a large extent, determine the range. Range is an important metric in power wheelchair selection and design.

The range of a power wheelchair provides an estimate of the total distance that the wheelchair can be driven on a new, fully charged, set of batteries. This estimate may vary depending upon terrain and driving/maintenance habits (8). Determination of energy consumption for electric wheelchair standards that require use of large external areas (e.g., parking lots, tennis courts) may be prohibitive for some test laboratories that do not have access to tennis courts due to expense, parking lots because of space limitations, and/or weather that precludes working outdoors (WG1/620).

Kauzlarich et al. (8), examined battery performance of electric wheelchairs during indoor and outdoor conditions. Driving cycles were used to bench test various types of batteries. A single instrumented wheelchair was used for all tests. The indoor test consisted of a 0.241 km test track including numerous obstacles and floor surfaces. The wheelchair was driven continuously over the course for 11.1 km (3.85 hrs) until the battery was depleted. The outdoor test route covered 2.75 km per lap which included grades up to 4°. A paved footpath and parking lot were used for this test. The wheelchair was driven for 15.6 km (2.74 hrs) when the battery became depleted.

Fatigue testing is an important component of wheelchair standards testing. The ISO Double Drum tester plays a pivotal role in fatigue testing of power wheelchairs. During Double Drum testing, the power wheelchair can drive the rollers or the rollers can be used to drive the power wheelchair while in neutral. Many power wheelchairs are designed to be driven only short distances (i.e., a few hundred meters) while in neutral. This has lead to some power wheelchair drive and disengagement mechanisms being destroyed during Double Drum testing. This type of failure does not commonly occur in field use. Some test laboratories have interpreted the standard to imply that the wheelchair was to drive

the rollers with the joystick set for one m/sec. However, not all Double Drum testers are alike. The friction of one Double Drum tester may vary significantly from another. It is also likely that the friction seen by the wheelchair while driving the Double Drum tester will be different from that when driving over a common cement walkway. In order for tests of power wheelchairs to be comparable, the current draw while driving the rollers of a Double Drum tester must be similar to that of a common driving surface (i.e., a cement walkway).

In response to concerns regarding range test and Double Drum test methods, we developed a set of experiments to determine if relationships exist between energy consumption at maximal speed on an ISO Double Drum tester, a motor driven treadmill, and while circumventing a tennis court (as proposed in the current ISO draft range test standard). The current draw at one m/sec was also recorded for each of the three test apparatus. Comparisons between results from the different methods were made using regression and ANOVA with repeated measures.

METHODS

Tests were performed on seven different power wheelchairs unloaded, and loaded with an ISO 100-kg test dummy. A specially designed circuit was used to measure battery voltage and load current (**Figure 1**), which was interfaced to Motorola MC6811-based analog-to-digital computer interface attached to the serial port of a computer. Data were collected at 20 Hz per channel on a DOS compatible 486 computer for the Double Drum and treadmill tests. A DOS compatible 8088-based laptop computer was used for the tennis court tests. Current and voltage were monitored at the battery terminals. Each wheelchair was tested on a Double Drum tester, treadmill, and tennis court. The slats were removed from the Double Drum tester prior to the experiment. New batteries were installed in each power wheelchair prior to testing, and all batteries were fully charged (as determined from open circuit voltage and charging current) before each experiment.

The state of charge for a new battery is somewhat subjective. Typically new batteries do not reach their full capacity until 30/40 charge/discharge
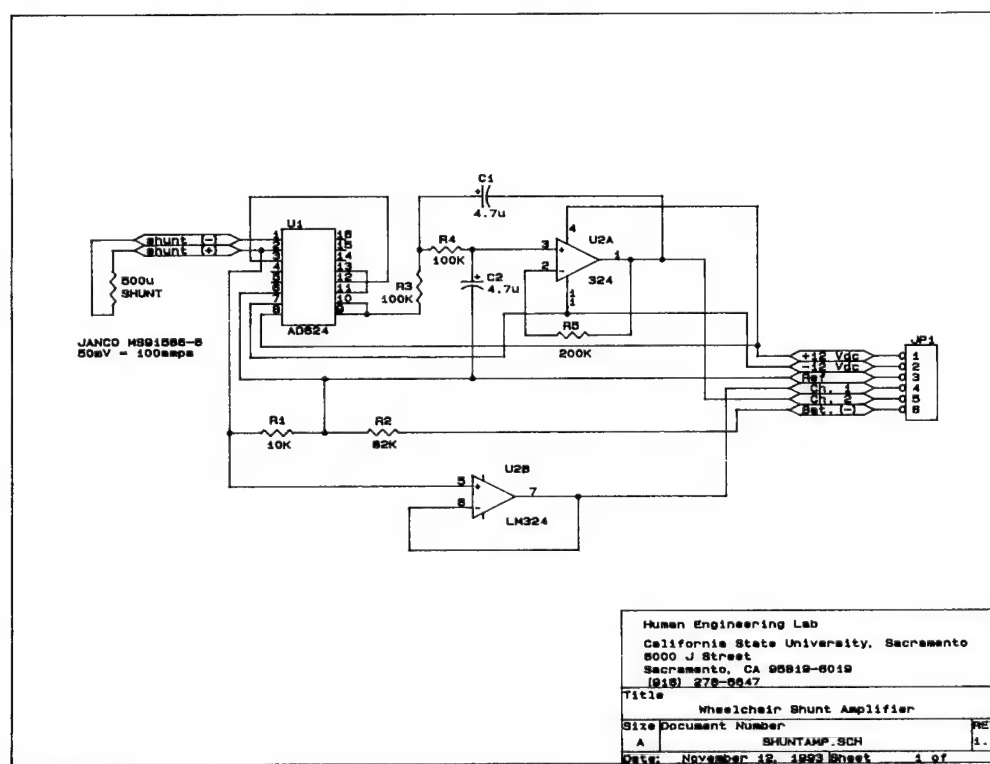
Figure 1.
Energy consumption computer interface circuit.

cycles. This can add variability in range when driving to discharge. However, each wheelchair was driven only 2250 m per test, which is well within the capacity of the battery. Thus, variations in state of charge will have minimal effect on the range estimates. In actual driving situations, range will be less than the idealized estimates of range determined with these methods. These methods are valuable for comparison purposes. The capacity (amp-hr) rating for batteries of the same size may vary considerably. For the purposes of these experiments and the draft ISO Range Test Standard (ISO-7176-04), the capacity reported by the battery manufacturer is used. Each wheelchair had its own batteries for this study. The short distance actually driven should minimize the variability. Furthermore, ISO and ANSI/ RESNA range tests will be conducted in test laboratories around the world with various wheelchairs and batteries. One of the ISO and ANSI/ RESNA objectives is to have tests of similar wheelchairs yield consistent results at each laboratory.

Each chair was configured according to the manufacturer's specifications, and tires were prop-

erly inflated (9–14). Experienced test pilots (technicians) were used for the tennis court tests and treadmill tests. An ISO 100-kg test dummy was used for the ISO Double Drum test **(Figure 2)**. Each power wheelchair was used to drive front and rear drums with the Double Drum tester motor disconnected. The front roller is driven through a tooth belt drive. The dummy was seated properly in the chair as per ISO 7176-07. The types of chairs and their battery type are given in **Table 1** (15,16). All of the power wheelchairs tested used either inductive or resistive joysticks and switching servo-amplifiers with power MOSFET bridges.

Energy consumption was measured over a distance of 1500 m for each of the three test conditions **(Figure 1)**. The rolling surface was level in all cases. The direction of motion remained constant on the Double Drum tester; whereas, with the proposed ISO standard tennis court range test, direction of rotation (i.e., direction was changed from clockwise to counter clockwise) was changed at 750 m. Wheelchairs were always driven in the forward direction. Each wheelchair was warmed up

Figure 2.
Experimental set-up for Double Drum testing.

for 750 m at or near maximal speed prior to data collection to minimize the variation in current associated with heating electrical and electromechanical components. Hence, each wheelchair was driven a distance of 2250 m for each load case. Care was taken during treadmill testing to gradually increase the speed of the wheelchair and treadmill in synchrony. Each chair p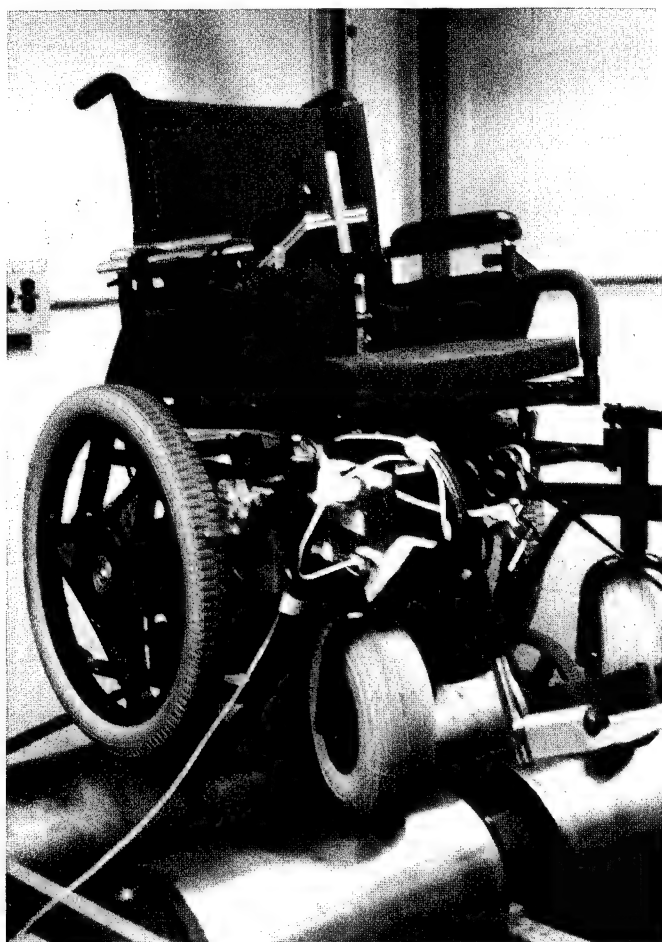erformed a no-load 1500-m range test, and a 100-kg load range test. A test technician walked/jogged alongside each chair providing guidance during the no-load tests for the tennis court. For the treadmill and Double Drum tester, a simple aluminum bracket was made to hold the joystick in the proper position, and a technician insured proper operation of the chair. The time required to complete the 1500 m was recorded and later used to calculate maximum speed of each wheelchair while performing each experiment. Distance was measured to the nearest revolution on the

Double Drum tester by using both an optical encoder interfaced to a DOS compatible 8088-based computer and a mechanical counter which counted each revolution of the driven drum. Distance was measured on the treadmill using a mechanical counter which measured the distance traveled by the treadmill's belt in feet. For the tennis court test, a course was laid out around the perimeter of the tennis court, and the distance measured with a steel tape. The pilot was instructed to follow the course as closely as possible.

The 1 m/sec current draw was measured using the same methods as for the range tests. Three wheelchairs were tested on the Double Drum tester; whereas, seven were tested using a treadmill and a tennis court. Speed was adjusted by turning the speed potentiometer to a 1 m/sec maximum speed as measured over a known distance. For wheelchairs without a speed adjusting potentiometer, an experienced technician drove the wheelchair while carefully controlling the joystick position. In each case, the wheelchair was timed over a distance of 25 m. Several trials were made until the speed was consistently within ± 5 percent of 1 m/sec. Once the desired speed was achieved, current data were collected for 10 secs using the circuit described in **Figure 1**. All data were collected using a 100 kg load.

ANALYSIS

The raw data were converted to voltages (V) and amperes (amp), as appropriate. A program was written in Matlab which used 20 point smoothing prior to calculating current, voltage, and power. Power was calculated as the instantaneous product of current and voltage. This is valid as the current and power were measured in phase. Using the same program, energy was calculated by integrating power (using Simpson's Rule) from the time the test was started until the power wheelchair completed 1500 m. Range was estimated to be the product of the nominal battery capacity and the speed traveled, divided by the amps consumed (Equation 1).

$$range = \frac{nominal\ battery\ capacity \times speed\ traveled}{amperes\ consumed} \quad [1]$$

Correlation analysis was used to determine the existence of linear relationships between current,

Table 1.
Description of power wheelchairs tested.

Make & Model	Battery Size	Battery Type	Amp•hour rating	System voltage
E&J Premier with 21st Century power components	Group 24	Wet Cell* Gel Cell	85 amp • hour 70 amp • hour	24 volts dc
E&J Tempest	Group U1	Wet Cell* Gel Cell	48 amp • hour 32 amp • hour	24 volts dc
E&J Marathon	Group 24	Wet Cell* Gel Cell	85 amp • hour 70 amp • hour	24 volts dc
Quickie P100	Group 22NF	Wet Cell Gel Cell*	55 amp • hour 48 amp • hour	24 volts dc
Quickie P110	Group 22NF	Wet Cell Gel Cell*	55 amp • hour 48 amp • hour	24 volts dc
Quickie P300	Group 24	Wet Cell* Gel Cell	85 amp • hour 70 amp • hour	24 volts dc
E&J Scooter Premier 3-Wheeler	Group U1	Wet Cell Gel Cell*	48 amp • hour 32 amp • hour	24 volts dc

All wheelchairs used deep cycle lead acid batteries, * indicates type of battery used during testing.

voltage, power, energy, and range for the three test conditions. ANOVA with repeated measures was used to examine differences between test methods (i.e., Double Drum, treadmill, and tennis court).

RESULTS

The data obtained from range testing on a Double Drum tester, treadmill, and tennis court with and without load are presented in **Table 2**. The mean current and power for the wheelchairs when loaded (I = 13.3 amps, P = 325 Watts) were higher than those when unloaded (I = 10.3 amps, P = 261 Watts). The results indicate that there is an increase in current (p = 0.447) and power (p = 0.543) with the 100 kg load added; however, they were not statistically significant. This apparent insensitivity to loading is likely a result of the variability in current and power among the different wheelchairs and their components (e.g., motors, drive-trains, tires, wheel types/sizes, total mass, and controllers), which creates a large standard deviation requiring higher

differences between the means (loaded and unloaded) to attain significance. Repeated measures ANOVA showed that there were no significant differences between voltage (p = 0.725), current (p = 0.725), and power (p = 0.628) for the three experimental conditions. There were significant differences between the maximum speed (p = 0.0008) and energy (p = 0.0109) among the three experimental conditions. Post hoc tests showed the energy consumption for the Double Drum tests were significantly different (p ≤ 0.05) from the energy consumption for the treadmill and tennis court tests. There were no statistically significant differences between energy consumption among the treadmill and tennis court tests. Post hoc tests also revealed a statistically significant difference (p ≤ 0.05) between the maximum speed for the Double Drum and treadmill, as well as between the treadmill and tennis court.

Correlation analysis revealed a statistically significant linear relationship between treadmill and tennis court current (r = 0.802, p = 0.0006), power (r = 0.896, p = 0.0001), and energy (r = 0.831,

Table 2.
Range test mean values of each test for the three experiments.

	Double Drum				Treadmill				Tennis Court			
	amps	watts	kJ	m/s	amps	watts	kJ	m/s	amps	watts	kJ	m/s
No Load												
Ch.1	10.3	255	195	2.7	30.9	761	355	3.2	33.3	824	446	2.8
Ch.2	9.2	230	223	1.7	10.7	267	212	1.9	2.4	57	45	1.7
Ch.3	9.9	233	233	1.8	6.2	144	101	2.1	5.7	138	111	1.9
Ch.4	10.0	249	220	1.7	4.4	109	90	1.8	4.8	118	97	1.8
Ch.5	11.2	278	278	2.3	12.8	500	254	2.9	10.5	260	136	3.0
Ch.6	14.5	349	227	2.4	6.7	162	91	2.7	7.1	179	108	2.6
Ch.7					4.3	106	75	2.1	0.3	8	7.5	2.2
100 kg												
Ch.1	12.6	307	307	2.4	27.6	692	345	3.0	19.1	466	304	2.3
Ch.2	12.7	288	288	1.5	8.9	222	187	1.8	6.6	155	139	1.7
Ch.3	12.8	297	297	1.7	8.3	195	144	2.0	8.8	198	126	1.8
Ch.4	13.3	310	284	1.6	8.8	195	185	1.6	8.4	205	184	1.7
Ch.5	22.6	553	552	1.6	22.5	607	332	2.7	19.8	545	327	2.5
Ch.6	16.3	390	253	2.4	10.7	252	143	2.6	12.2	301	200	2.3
Ch.7					7.3	175	137	1.9	6.0	146	101	2.0

amps = current in amperes, watts = power in watts, kJ = energy in kilojoules,
m/s = average speed in meters per second.

p = 0.0002) at maximum speed (Equation 2). The person-product correlation is given by 'r,' and the probability that the linear relation is due to chance is given by 'p.' Treadmill speed and tennis court speed were also significantly correlated with one another (r = 0.908, p = 0.0001).

$$I_{TC} = 0.78\,I_{TM} + 2.62 \qquad amperes$$
$$P_{TC} = 1.08 P_{TM} + 81.42 \qquad watts \qquad [2]$$
$$E_{TC} = 1.01 E_{TM} - 24748 \qquad joules$$
$$v_{TC} = 0.75 v_{TM} + 0.42 \qquad m\,/\,s$$

The maximum speed on the Double Drum tester was statistically significantly correlated with treadmill (r = 0.839, p = 0.0006) and tennis court (r = 0.779, p = 0.0029) maximum speed. This is probably a manifestation of the digital speed control used by most of the power wheelchairs in this test group.

Current was measured for each power wheelchair while traveling at or near 1 m/sec (**Table 3**). This speed is representative of a brisk walking pace. ISO and ANSI fatigue tests on the Double Drum test machine are performed at 1 m/sec. For power wheelchairs, this machine can be used to test the robustness of the electrical system as well as the durability of the frame and components. Typically, the drums of the test machine are driven by the power wheelchair. If the load current of the power wheelchair varies significantly from that of normal use, the electrical system may fail prematurely. Our results indicate that the current required to drive the rollers of the Double Drum tester is statistically significantly higher (p < 0.05) than it is to drive the wheelchair on a treadmill or around a tennis court. Correlation analysis revealed that the 1 m/sec current for the Double Drum (r = 0.789, p = 0.4213), and treadmill (r = 0.71, p = 0.0737) were not significantly related to the tennis court current. The 1 m/sec current for the Double Drum tester and treadmill were significantly correlated (r = 0.999, p = 0.0108).

The range of each chair was estimated using the measured data and Equation 1. The 1 m/sec range data are susceptible to greater variability because data were collected for only 10 seconds during steady-state (**Table 4**). Wet cell batteries provide longer range of operation than gel cell batteries in every instance. This is because the amp-hr rating of a wet cell battery is consistently higher than that of a gel cell battery of the same size (16,17,18).

Table 3.
One meter per second test data.

	Double-Drum		Treadmill		Tennis Court	
	Speed	**Current**	**Speed**	**Current**	**Speed**	**Current**
Chair 1	1.02	11.25	1.00	28.0	0.93	5.45
Chair 2	1.02	9.4	1.00	7.3	0.98	2.21
Chair 3	1.02	9.4	1.00	7.7	1.00	4.22
Chair 4			1.00	6.3	0.98	3.63
Chair 5			1.00	19.7	1.03	3.77
Chair 6			1.00	3.1	1.12	3.75
Chair 7			1.00	1.0	1.00	2.85

All tests were conducted with 100 kilogram load, speed is in m/s, and current in amperes.

Table 4.
Estimated range with 100 kilogram load at maximum speed and at approximately one meter per second. (Units are in kilometers)

	Double-Drum		Treadmill		Tennis Court	
	1 m/s	**Full Speed**	**1 m/s**	**Full Speed**	**1 m/s**	**Full Speed**
Gel Cells						
Chair 1	22.8	30.3	9.0	27.4	43.0	30.3
Chair 2	18.8	20.4	23.7	34.9	76.6	44.5
Chair 3	12.5	15.3	15.0	27.8	27.3	23.6
Chair 4		20.8	27.6	31.4	46.7	35.0
Chair 5		17.8	12.8	30.2	68.8	31.8
Chair 6		37.1	80.5	61.2	75.3	47.5
Chair 7			11.5	30.0	40.4	38.4
Wet Cells						
Chair 1	27.7	36.8	10.9	33.3	52.2	36.8
Chair 2	21.5	23.4	27.2	40.0	87.8	51.0
Chair 3	18.8	23.0	22.5	41.7	41.0	35.4
Chair 4		23.8	31.6	36.0	53.5	40.1
Chair 5		21.6	15.5	36.7	83.5	38.6
Chair 6		45.1	97.8	74.3	91.4	57.7
Chair 7			17.3	45.0	60.6	57.6

$$R_{TCmax} = 0.57R_{TMmax} + 18.32 \quad kilometers \qquad [3]$$
$$R_{TCMmax} = 0.65R_{DDmax} + 22.41 \quad kilometers$$
$$R_{TC1m/s} = 0.40R_{TM1m/s} + 48.94 \quad kilometers$$

Repeated measure ANOVA revealed a significant difference (p = 0.0001) between the predicted range at maximum speed for the three tests. Post hoc analysis demonstrated a significant difference (p < 0.01) in estimated range at maximum speed between the Double Drum test and the treadmill test, as well as between the Double Drum test and the tennis court test. Our results indicate no significant difference (p ≥ 0.05) between the predicted range at maximal speed between the treadmill and tennis court tests.

Regression analysis revealed a significant correlation between the predicted maximal range between the treadmill (r = 0.756, p = 0.0018) and tennis court tests, as well as between the Double Drum (r = 0.614, p = 0.0336) and tennis court tests. The predicted range at 1 m/sec were also significantly correlated between the treadmill and tennis court tests (r = 0.536, p = 0.0481).

Repeated measure ANOVA showed a significant difference (p = 0.0029) between the predicted range at 1 m/sec for the three tests. Post hoc

analysis revealed that both the results of the Double Drum and treadmill tests were significantly different ($p < 0.05$) from the tennis court test. The analysis also showed no significant difference between the predicted range at 1 m/sec for the Double Drum and treadmill tests.

DISCUSSION

The range testing of power wheelchairs is a very important component of the ISO and ANSI/RESNA wheelchair standards. However, the use of a tennis court presents some problems for test facilities. Indoor tennis courts are often operated by private clubs or organizations who do not care to have their tennis courts used to test power wheelchairs. Some test laboratories are located in regions that frequently have inclement weather during some months of the year, which prohibits testing outdoors. Other facilities, such as parking garages, or sports gymnasiums, also may be suitable for testing. However, in most cases, these facilities are not associated with the test center. In addition, testing outside the laboratory requires specialized portable equipment which may not be readily available for the use of the test center.

All complete wheelchair laboratories are required to have a Double Drum tester for fatigue-testing manual and powered wheelchairs. This would be a convenient tool for range testing as well, but our results indicate that a simple relationship does not exist between the results of range testing with the Double Drum tester and tennis court testing. An alternative to the current ISO draft standard and ANSI/RESNA Standard, would be to permit the use of a treadmill for range testing as simple relationships between all pertinent treadmill and tennis court range data were found. The equations presented in this paper represent a possible means to relate treadmill and tennis court range tests. Some power wheelchairs will likely vary from these results, and this presents a potential problem when comparing results from different laboratories using varying test methods. At maximum speed, this should not present too great a problem as analysis of variance showed no significant difference.

Fatigue testing is also a very important component of power wheelchair testing. Unlike manual wheelchairs, whose wheels are driven by an external

motor while being tested on a Double Drum tester, power wheelchairs must drive the drums with their internal motors. This permits the Double Drum tester to be used to evaluate the durability of the frame and components, as well as to assess the robustness of the electrical system. A persistent problem has been that the current used by the power wheelchair while turning the drums of the Double Drum tester may be substantially different from the current seen by the power wheelchair under normal circumstances. Our results indicate that, for the Double Drum tester used, the current demand is higher than under normal usage. This presents a problem as current is related to load torque in a power wheelchair. Therefore, the load torque must be reduced. This may be accomplished by increasing the diameter of the drums, effectively reducing rolling friction, reducing the friction of the bearings, and improving the efficiency of the coupling between the front and rear drums. Another method would be to leave the Double Drum motor coupled to the test apparatus, and use it to reduce the torque required by the power wheelchair. This last method requires the use of a closed-loop feedback control system to achieve reliable results.

The results in **Tables 2** and **3** show variability among wheelchairs and between tests. This is to be expected, since the wheelchairs include a variety of drive components (e.g., motors, drive-trains, tires, wheel types/sizes, total mass, and controllers). Some of the wheelchairs used open-loop control, whereas others used closed-loop speed control. Closed-loop speed controllers are designed to maintain constant speed regardless of surface friction or slope and can produce higher torque than open-loop controllers. The wheelchairs in the study used direct helical gear trains, worm-gear drives, or belts and pulleys. These drive trains have different efficiencies, and in the case of the treadmill, some can receive energy from the treadmill, whereas others can not. These factors all contribute to the results of this study, and to the wheelchair's actual driving behavior. The predicted range for the tennis court test at maximum speed ranges from a low of 23.6 km to a high of 57.7 km. The range of the power wheelchair can be improved by the use of wet lead acid batteries in place of gel lead acid batteries. However, wet batteries often require greater maintenance, and care during transport. No alternative batteries were tested (19,20). All of the manufacturers specified lead acid batteries for

their wheelchairs. The range at 1 m/sec was typically greater than it was at maximum speed. This information may be useful to consumers; a low battery warning could extend their range by reducing the speed. Current draw on an incline will be greater than the values indicated in this paper. Some wheelchairs incorporate regenerative braking which allows some of the energy expended while going up an incline to be regained through charging the batteries while driving down an incline. Range will also vary with driving habits. An interesting result of this study is the finding that the tennis court test has an excess of 40 turns which require the pilot to slow the chair and than accelerate out of the turn. Yet all values recorded during the treadmill test, which is always straight at constant speed, were correlated with the tennis court results.

REFERENCES

1. Aylor JH, Thieme A, Johnson BW. A battery state-of-charge indicator. IEEE Trans Ind Elect 1992:39(5):398–409.
2. Ford MR, Kauzlarich JJ, Thacker JG. Powered wheelchair gearbox lubrication. In: Proceedings of RESNA International '92; 1992 June 6–11; Toronto, ON. Washington, DC: RESNA Press: 316–18.
3. Ford MR, Thacker JG, Kauzlarich JJ. Improved wheelchair gearbox efficiency. In: Proceedings of the 14th Annual RESNA Conference, Kansas City, MO. Washington, DC: RESNA Press, 1991:146–7.
4. Junkman BC, Aylor JH, Kauzlarich JJ. Estimation of battery state-of-charge during charging using the charge recovery process. In: Proceedings of the 11th Annual RESNA Conference, Montreal, QC. Washington, DC: RESNA Press, 1988:280–1.
5. Kauzlarich JJ. Wheelchair batteries 11: capacity, sizing, and life. J Rehabil Res Dev 1990:27(2):163–70.
6. Kauzlarich JJ, Thacker JG, Ford MR. Electric wheelchair drive train efficiency. In: Proceedings of the 16th Annual RESNA Conference, Las Vegas, NV. Washington, DC: RESNA PRess 1993:310–2.
7. Stout G. Some aspects of high performance indoor/outdoor wheelchairs. Bull Prosthet Res 1979:10(32):330–2.
8. Kauzlarich JJ, Ulrich V, Bresler M, Bruning T. Wheelchair batteries: driving cycles and testing. J Rehabil Res Dev 1983:20(l):31–43.
9. Tempest Owner's Manual, Everest & Jennings, Earth City, MO 63045, 1993.
10. Marathon Owner's Manual, Everest & Jennings, Earth City, MO 63045, 1990.
11. Premier Scooter Owner's Manual, Everest & Jennings, Earth City, MO 63045, 1990.
12. Quickie P100 Owner's Manual, Quickie Designs, Fresno, CA 93727, 1993.
13. Quickie P110 Owner's Manual, Quickie Designs, Fresno, CA 93727, 1993.
14. Quickie P300 Owner's Manual, Quickie Designs, Fresno, CA 93727, 1993.
15. Bode H. Lead-Acid Batteries. New York: John Wiley & Sons, 1977.
16. Fisher WE, Garrett RE, Seeger BR. Testing of gel-electrolyte batteries for wheelchairs. J Rehabil Res Dev 1988:25(2):27–32.
17. Lavanchy C. Comparative evaluation of major brands of lead-acid batteries. In: Proceedings of the 15th Annual RESNA Conference, Toronto, ON. Washington, DC: RESNA Press, 1990:541–3.
18. Ulrich V, Bresier M, Kauzlarich JJ. Wheelchair battery testing. In: Proceedings of the 3rd Annual RESNA Conference, Washington, DC: RESNA Press, 1980:132–3.
19. Kauzlarich JJ, Dwyer MA. Test of nickel-zinc battery for wheelchairs. In: Proceedings of the 5th Annual RESNA Conference, Houston, TX. Washington, DC: RESNA Press 1982:110.
20. Ulerich PL, Demcyzk BG, Buzzelli ES. Battery-in-vehicle analysis of the iron-air battery system. Technical Report#: 81-9j22-EVMOT-Pl, Pittsburgh, PA: Westinghouse R&D Center.

An augmented computer vision approach for enhanced image understanding

Malek Adjouadi, PhD; John Riley, ME; Frank Candocia, ME; Jean Andrian, PhD; Habibie Sumargo, ME
Center for Advanced Technology and Education, Department of Electrical and Computer Engineering, Florida International University, University Park, Miami, FL, 33199

Abstract—This paper addresses the design concept of a spatially and spectrally augmented computer vision approach toward enhanced image analysis and understanding. The concept of spatially augmented computer vision refers to the inclusion of the stereo disparity measure (½-D) along with the two-dimensional (2-D) spatial coordinates of the images, together yielding the augmented (2½-D) representation. The concept of spectrally augmented computer vision refers to the implementation of the multiresolution concept of the wavelet theory to analyze and assess in detail the local properties of the 2-D images. The principal objective in applying this augmented, and more revealing, computer vision approach is to provide the added dimension in spatial and spectral resolutions for the enhanced understanding of images. To this end, imaging techniques are developed to exploit, in an optimal fashion, the information acquired by the camera system to yield useful descriptions of the viewed scenes. Experimental results are provided in support of this research direction.

Key words: *augmented image representation, feature extraction, scene analysis, stereo vision.*

INTRODUCTION

The important steps considered for the augmented computer vision approach include: 1) the extraction of image features for the construction of disparity maps; 2) the understanding and exploitation of the mapping principles between the augmented (2½-D) representation and the 3-D real world to yield enhanced image interpretation; and 3) the development of appropriate image analysis and interpretation techniques based on this spatially and spectrally augmented image representation. It is clear that this research endeavor calls for significant theoretical and practical reflections. In an earlier publication (1), an assessment was given on earlier studies based on the applications of sonic and electromagnetic technologies for the provision of obstacle detection cues, and the tactile-based systems for object identification and recognition. Considering the progress made in the field of computer vision, along with our enhanced understanding of biological vision, more efforts should be invested in this research direction to enhance the prospects of scene analysis and understanding under the augmented representation. In taking up such a challenge, and for the formidable task of implementing such a vision-based system as a possible guidance aid for the blind individual, however, we remain conscientious to the fact that "...they who are blind tend to doubt the information gathered by other sources" (2). Such doubts are legitimate. Therefore, a change in attitude, to at least accept the explora-

tion of computer vision-based mobility techniques, becomes another necessity which can be addressed only through a strong commitment to the development of a sound theoretical framework followed by feasible and reliable practical implementations.

METHODS

A Dimensionally Augmented Vision Approach

The functional structure of the integrated vision system is illustrated in **Figure 1.** In this approach, the main thrust of the research efforts is placed on taking the new direction of incorporating the stereo disparity measure along with the pixels gray-level information to enhance the interpretation of images and to seek effective results for 1) enhanced image analysis and interpretation based on the augmented image representation, while establishing the 3-D spatial relationships of the user within the context of the viewed scene; and 2) automated guidance, providing reliable guidance cues with the possibilities for obstacle detection and avoidance and the identification of objects deemed important in the guidance process.

In view of this design, the feature extraction process is introduced first, using (*a*) the Laplacian of a Gaussian operator, (*b*) the multiscale edge detection of the wavelet transform, and (*c*) the principles of the simple cells of the hypercolumn theory. Using these features, a stereo vision algorithm is described for the extraction of the stereo disparity measure

Figure 1.
Design of an augmented vision system.

that is used to construct the augmented representation. Key visual algorithms are then introduced to illustrate the potential for enhanced image interpretation.

Fundamentals of Image Feature Extraction
The Feature Extraction Process

The process of feature extraction remains an essential step for: (*a*) the implementation of stereo vision for the disparity extraction, (*b*) object recognition, and (*c*) automated guidance. The inherent problem of this step of feature extraction relates directly to the decision to be made about what intensity differential is significant enough such as to distinguish a potential feature point from a potential noise point. Such a decision is often subjective in nature and is based on empirical observations. Some degree of tolerance in this type of decision making is usually achieved through the use of preprocessing steps to eliminate such things as isolated potential noise points, and to correct those feature points whose disparities take on values that are considered inconsistent in the context of neighboring disparities. It will be shown here that the concept of multiscale edge detection of the wavelet theory and the functional principles of the hypercolumn theory of the visual cortex based on the notion of simple cells (depicted here as different edge operators with varying resolutions) show great promise in the resolution of the feature versus noise dilemma in the extraction process of features. The Laplacian of the Gaussian is perhaps the best known operator that can be considered for the extraction of image features (3). The choice between the direct use of derivative-based operators versus the use of the Laplacian of the Gaussian is solely based on the compromise between accuracy in localizing image features and the attenuation of noise in the feature maps which comes from the choice of the standard deviation (σ) of the Gaussian function.

In a recent study (4), for example, we have shown that the first and second order 1-D Walsh operators can be used to approximate the first and second order derivative operators. The dimension n of these (*nxn*) operators relates to the standard deviation of the Gaussian function, in that a larger n results in an attenuation of the effect of noise, but at the expense of accuracy in locating the feature and determining its true contribution in terms of amplitude. Another recent recourse to the problem
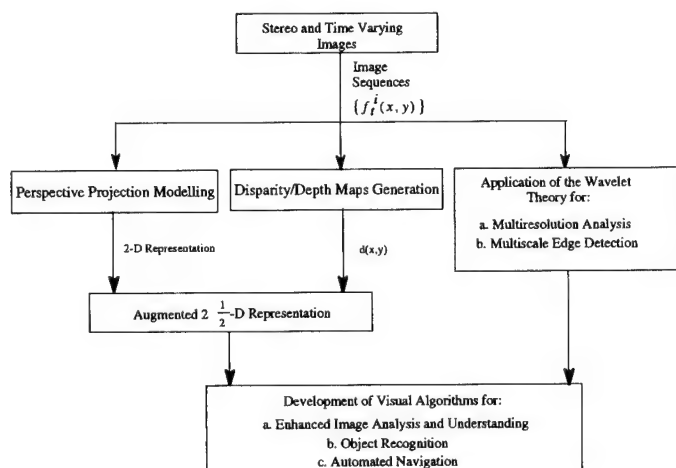
of feature extraction involves the application of the wavelet theory (5–8). With respect to the application of the wavelet transform, there are two evolving concepts that are deemed of great importance for enhanced applications of computer vision: 1) the concept of multiscale edge detection; and 2) the concept of multiresolution which, through dilations and translations of the mother wavelet, allows for "zooming-in" in any part of the signal, seeking in an optimal way the desired information, with the potential to filter out unwanted fluctuations (noise). Illustrative examples shown in this study clearly demonstrate the important reason why the wavelet is referred to as the "mathematical microscope."

The Laplacian of the Gaussian Approach

In the 1960s, Hubel, Weisel, Campbell, and Robson introduced certain notions about how information is processed in the visual cortex (9,10). In the past two decades, it has been shown that visual information is processed in parallel by innumerable spatial-frequency-tuned channels in the brain (11–14). This implies that the visual system analyzes the scene at different resolutions. Psychological experiments have been found to be consistent with this notion.

An appropriate filter for detecting separately, and at different scales, intensity changes in images, was found to be the second derivative of the Gaussian filter (15). In general, this filter is not orientation dependent as are a majority of the other known operators. Thus, intensity changes at a given scale are best detected by locating the zero-crossings of the convolution $\nabla^2 G(x,y)*f(x,y)$ where ∇^2 is the Laplacian operator, $G(x,y)$ is a 2-D Gaussian distribution and $f(x,y)$ is a 2-D image. A 2-D Gaussian distribution, with the mean value of the distribution located at zero, is given by

$$G(x,y) = \frac{1}{2\pi\sigma^2} e^{-\frac{1}{2}\frac{x^2+y^2}{\sigma^2}} \qquad [1]$$

where σ is the standard deviation of the distribution or the scale of the filter. With the Laplacian operator defined as: $\nabla^2 = (\frac{\partial^2}{\partial x^2} + \frac{\partial^2}{\partial x^2})$, the Laplacian of the Gaussian distribution yields:

$$\nabla^2 G(x,y) = \frac{1}{2\pi\sigma^4} \left(\frac{x^2+y^2-2\sigma^2}{\sigma^2} \right) e^{-\frac{1}{2}\frac{x^2+y^2}{\sigma^2}} \qquad [2]$$

The convolution $\nabla^2 G(x,y)*f(x,y)$ is best performed in the Fourier (F) domain as the inverse Fourier transform of a product given by: $\mathbf{F}^{-1}\{F\{f(x,y)\} \cdot F\{\nabla^2 G(x,y)\}\}$. The Gaussian filter has been proven to be the only filter, in any dimension, that does not create generic zero-crossings as the scale factor of the filter increases (16). This filter has applications, not only in the extraction of image features, but in the important role of attenuating noise effects present in images.

Applications of the Wavelet Theory

A more objective assessment of the feature extraction process should involve both the time/spatial and frequency/scale domains. This means that a feature is now identified both in its time/spatial domain in terms of its locality and its frequency/scale domain in terms of its harmonic content. The wavelet transform provides the answer to this issue and allows for the study of 1) the time-frequency representations of the wavelet for multiscale edge detection, and 2) the multiresolution property for the analysis of the local properties of a given signal under different scales. Wavelet transforms, unlike the traditional Fourier transforms, are thus suitable to analyze a given signal containing localized variations. Moreover, these localized variations can be analyzed at different scales. Thus, if the wavelet transform is applied successively on the details of the signal, it allows for an in-depth look at the nature of the fluctuations and will allow for the separation of the trend from fluctuations, with potential to trap unwanted fluctuations (a possible effect of noise) in a well-defined frequency band and have them filtered out. All these characteristics and attributes make the wavelet transform a very attractive tool in any automated vision or object recognition problem.

Time-Frequency Representations and
Multiscale Edge Detection

Wavelet analysis allows, in the most optimal manner, for the extraction of image features. This is a direct result of the zooming effect which can be achieved through dilations of the analyzing wavelet.

It is through such wavelet dilations that features can be represented simultaneously in both time and frequency domains. With conventional Fourier analysis, this is not possible, since the basis function for Fourier is not well localized in time. This implies that there are consequences for even the most minute change in frequency over the entire time spectrum. Wavelets, however, sacrifice some localization in frequency for localization in time. The yielded result allows for a more enhanced analysis and understanding of the signal through a more complete representation. A wavelet can thus be adjusted by dilations (compression) and translations (convolution) to localize particular feature points in both spatial coordinates and harmonic content. Thus, by considering each row of a 2-D image as a spatially/time varying signal, we can isolate image characteristics both in time and frequency. The analogy of time-frequency representation in the 2-D case relates to the property of multiscale edge detection. Through this last property, there is a potential application for data compression by storing only the information pertinent to edges, as it is possible to reconstruct images through projections of these wavelet transformations.

It is this exact theme that is adopted here in the application of several operators at various resolutions to provide some insight on how the brain may interpret images projected onto the striate cortex, based on the functional principles of the simple cells of the hypercolumn theory of the visual cortex (12).

Results of the Feature Extraction Process

Results illustrating the process of feature extraction through the application of (*a*) the Laplacian of the Gaussian operator, (*b*) the wavelet Transform, and (*c*) the principles of the simple cells of the hypercolumn theory are given in **Figure 2.** From these results, the next logical step is to assess the 3-D information of these features to begin the process of enhanced image analysis and interpretation under the augmented representation.

Extraction of the Depth Information

If somehow we were to assume a flat ground plane such as indoor walkways, it would be easy to determine the geometrical mappings relating real-world points to their image projections. Thus, an image area delimited by the image coordinates x_i, x_j,

y_i, y_j , as shown in **Figure 3,** can be related to the real-world width (W) and range (R) using triangulation:

with R $(y_j, y_i) = y_j - y_i$, we find that:

$$R(y) = \frac{(f + y \tan\alpha)\, h \tan(\beta + \alpha) - fh \tan\alpha}{f + (f \tan\alpha - y) \tan(\beta + \alpha)} \qquad [3]$$

and,

$$W(x_j, x_i) = \frac{f + R(y_i, y_o)}{f}(x_j - x_i) \qquad [4]$$

where h is the camera height. The term R (y_j, y_o) is evaluated as $y_j - y_o$ with $y_o = 0$. Note, for example, if the position of the image plane is such that $\alpha = 0$, then Equation 3 takes the simple form:

$$R(y_j, y_i) = \frac{fhL^2}{(fh - y_j L)(fh - y_i L)}(y_j - y_i) \qquad [5]$$

With respect to the idea of having the image analysis focused on a specific region of the environment, let us treat an example where it is desired to process the environment that is within a range $R(y_k)$ from the observer, where $(R(y_k) = L + R(y_o, y_k))$. This problem reduces to finding the image coordinate y_k corresponding to the range $R(y_k)$. From Equation 3, y_k is derived as

$$y_k = \frac{f[R(y_k) + h \tan\alpha] + f[R(y_k)\tan\alpha - h]\tan(\beta + \alpha)}{[R(y_k) + h \tan\alpha]\tan(\beta + \alpha)} \qquad [6]$$

and if we let $\alpha = 0$, Equation 6 takes the following simple form:

$$Y_k = \frac{fh[R(y_k) - L]}{LR(y_k)} \qquad [7]$$

Such an approach to image versus real-world mapping will be limited at best to known indoor environments. To take on a more general approach, we need to use stereo and/or motion vision with the objective to recover the third dimension. The next section will focus on an application of stereo vision to provide a solution to this problem.

An Application to Stereo Vision

Success in stereo matching is inherently linked to the problem of identifying corresponding feature
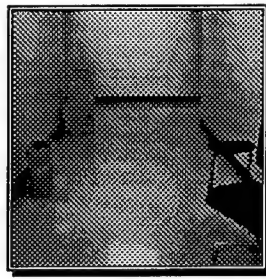
(a1) Input Image
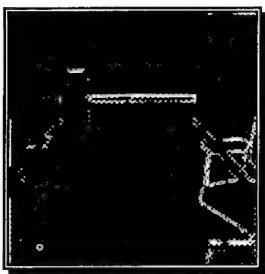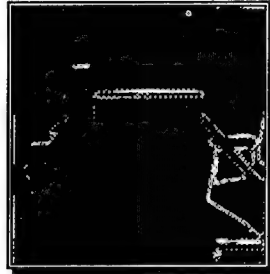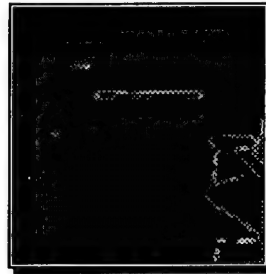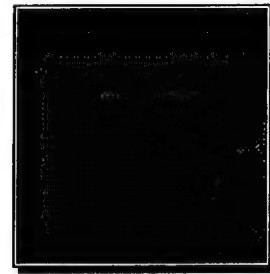
σ=0.65   σ=0.70   σ=1.0   σ=1.5

(a2) Feature Extraction using Laplacian of the Gaussian operator with various standard deviations
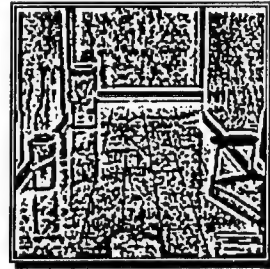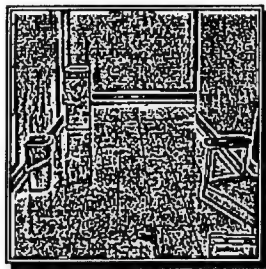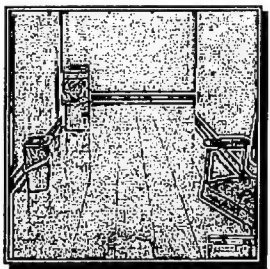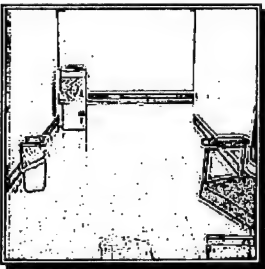
(a3) Binary Images of the Results Obtained in Part (a2)
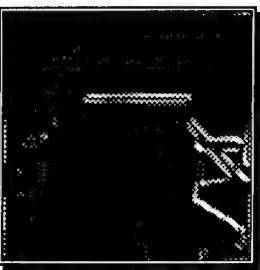
(b1) Wavelet 1st Order   (b2)Binary Image of (b1)   (b3) Wavelet 2nd Order   (b4) Binary Image of (b3)
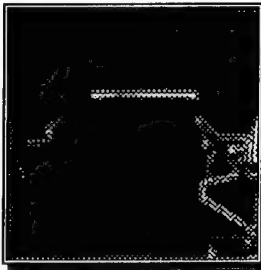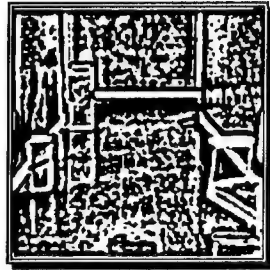
Figure 2a and b.
a. Image feature extraction using the Laplacian of the Gaussian operator. b. Image feature extraction using the Wavelet Transform.
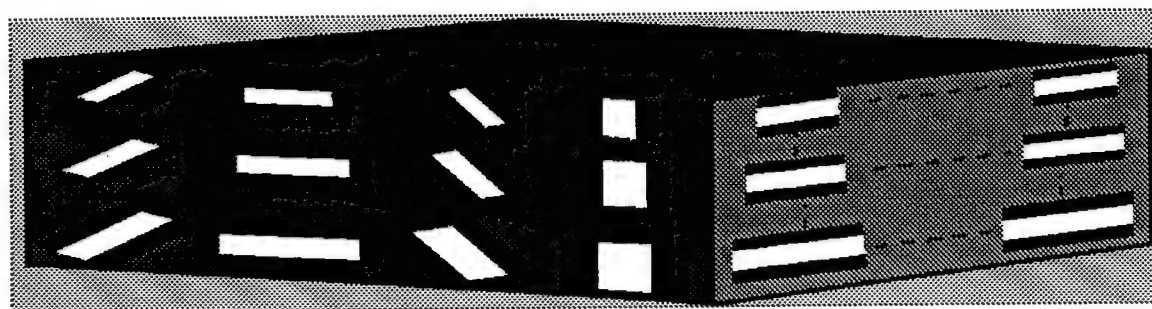
(c1) Detectors used for Feature Extraction

(c2-1) detector size 4x4   (c2-2) detector size 8x8   (c2-3) detector size 16x16 (c2-4)detector size 32x32

(c2) Summed Activity with Positive Response
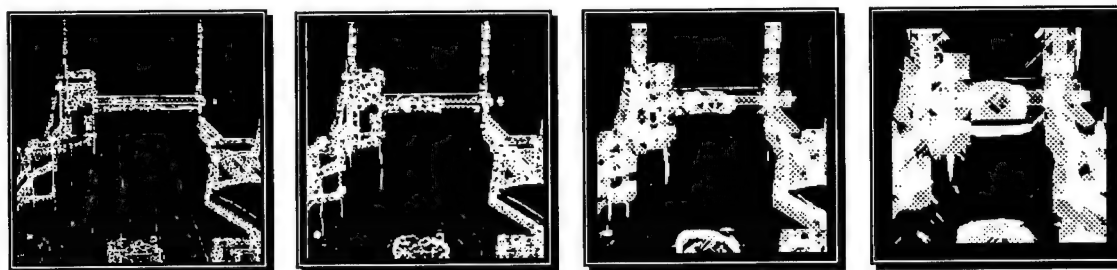
(c3-1) detector size 4x4   (c3-2) detector size 8x8   (c3-3) detector size 16x16 (c3-4)detector size 32x32

(c3) Summed Activity with Negative Response

Figure 2c.
Image feature extraction using the principles of the simple cells of the Hypercolumn Theory of the Visual Cortex.

locations based on the nature of the characteristics of the features extracted and their neighborhood information. The key objective is thus to establish a matching strategy that is sensitive, reliable, and effective in evaluating a match, and with the capability to confirm such a match with a high degree of certainty (17). The key developments introduced here are:

1. The establishment of a new and very effective similarity measure designed in a generalized form to reflect accurately not only the positioning of the feature(s) but the contribution of any attribute or combination of attributes that may be associated with the feature(s). These attributes can be gathered from any contextual information surrounding a given feature point
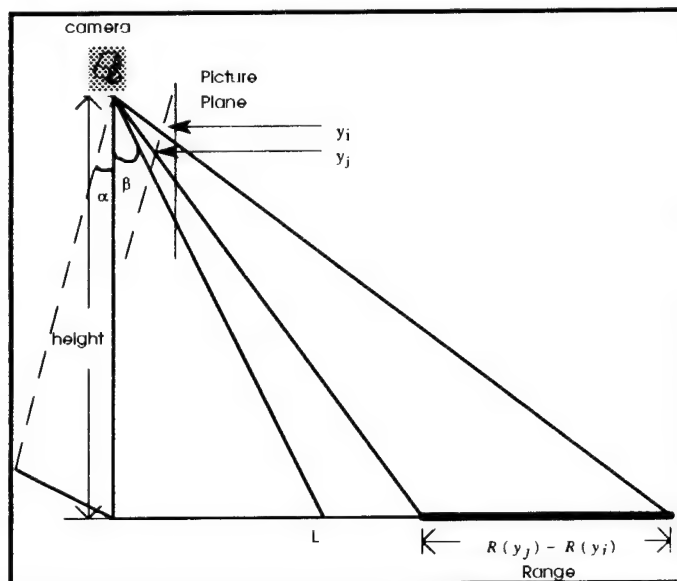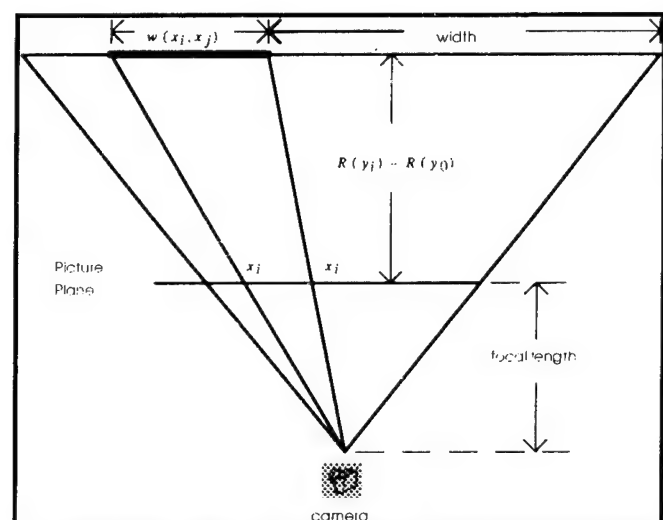
Figure 3.
Simplified 2-D mapping principles.

or from the elementary information, such as neighboring gray-level information and directional gradients.

2. The development of a new matching strategy based on the application of a global analysis on similarity measures which yielded the highest values under confined search spaces, and which have passed a consistency check such as to comply with the uniqueness constraint. This global analysis, the objective of which is to assess results obtained from localized searches for potential matches, stems from the idea that

a search for a match should begin with those features that show the closest resemblance; thus allowing for the validation of potential matches as correct matches with the highest possible degree of certainty. The characteristic of "closest resemblance" is reflected here by the yielding of a highest similarity measure from the global analysis view point. The challenge here lies in answering to the complex issues of matching primitives and matching rules that effectively address the problem of stereo matching, while preserving the computational requirements at a realistic level (18–21).

The Similarity Measure

Given two windows that contain feature patterns, a similarity measure is established here to numerically describe the likeness of the patterns in the two windows. The window under consideration in one image of the stereo pair is referred to here as the reference window. A window in the confined search space of the other image of the stereo pair that is being compared is the non-reference window.

The formulation of the similarity measure between a window A in one image to a window B in the other image of the stereo pair is denoted by $\Psi(A \rightarrow B)$. In this notation, the set pointed to by the arrow is considered the reference set (or window). The similarity measure is obtained as a function of the locality of features within the window and any other attributes associated with these features. That is, $\forall \ [f_{ij}]_{\in \mathcal{T}} \subset A$ and $[f_{kl}]_{\in \mathcal{T}} \subset B$, where $[f_{ij}]_{\in \mathcal{T}} \subset A$ means feature points at locations i,j within window A, and given that the window size is mxn, with $i,k = [0,1,...,m-1]$ and $j,l = [0,1,...,n-1]$, we obtain:

$$\Psi(A \rightarrow B) = \sum_{q=1}^{h} \frac{P}{(D_q + 1)} \cdot \left[\prod_{s=1}^{t} \left(1 - \frac{|\Delta V_s|_q}{\eta_s} \right) \right] \quad [8]$$

where, $\Delta V_s = v_{sr} - v_{sl}$ is the noted variation of the sth attribute in the two windows under comparison with $0 \leq |\Delta V_s| \leq \eta_s$, t denotes the number of attributes considered, and η_s is a normalization factor for the sth attribute such that the following condition holds for any attribute considered. Parameter $P = 1/N_B$ is the weight associated to the matching of a feature. This weight is a function of the total number of features contained in the reference window B de-

noted by N_B. Parameter $h = \min(N_A, N_B)$ is the minimum number of total feature points found in either window A or B, and D_q is the minimum distance between the qth feature point in the reference window and its closest feature in the non-reference window. Note that in finding D_q, the distance of all features in A to those in B are computed.

The two features, one in A and one in B, which corresponded to the minimum distance, are the two considered when $q = 1$. After their contribution to the similarity measure for the window pair considered is assessed, they are removed and the contribution from the next two closest features is calculated. This continues until the contribution of all h features is assessed. It is noted here that the use of contributory similarity, in which case excess features in A are ignored, is a more feasible approach in dealing with such situations often complicated by the presence of noise, occlusion, light reflections, and so forth. Thus, rather than penalize the similarity measure for the excess feature information, the interest should rather be focused in finding a similar feature pattern regardless of feature variations surrounding the pattern of interest.

The Matching Strategy

The foundation of the matching strategy proposed here is a generalized similarity measure which accurately reflects the positioning of features (sensitivity to feature locality), and is stable enough to allow for feature variations and distortions due to the common problems associated to noise, photometric and geometric distortions, discontinuities, and occlusion. The generality in the similarity measure is depicted through a formulation which reveals the ease of integrating any matching primitive or attribute to be used in assessing a potential match. A consistency check supports this matching strategy such as to enforce the uniqueness constraint. This matching strategy is further reinforced through a unique approach which performs a global assessment of results found through a localized search to exploit the view that matching should begin with those features which have the closest resemblance.

A left image window W_{x_l, y_l}^L, positioned at x_l, y_l, is compared to all of those windows in the right image that are contained within a specified search space. All window displacements within the search space are in one pixel increments. When the window in the right image yielding the highest similarity measure is found, its location is marked as x_r^*, y_r^*. This window is then compared with those windows in the left within the same predetermined search space. The location of the left window yielding the highest similarity measure is now marked as x_l^*, y_l^*. A consistency check is said to be satisfied if the windows under comparison from a left to right search and from a right to left search are found to correspond.

The following formulation reflects this consistency check satisfying a left to right search and a right to left search:

$$x_r^*, y_r^* \Leftarrow \max\left\{\Psi\left(W_{x_l, y_l}^L \rightarrow W_{x_r, y_r}^R\right)\right\};$$
$$x_r = x_l \pm k_1, \; y_r = y_l \pm k_2 \qquad\qquad [9]$$
$$x_l^*, y_l^* \Leftarrow \max\left\{\Psi\left(W_{x_r^*, y_r^*}^R \rightarrow W_{x_l, y_l}^L\right)\right\};$$
$$x_l = x_r^* \pm k_1, \; y_l = y_r^* \pm k_2$$

The variables k_1 and k_2 represent the extent of space to be searched in number of rows and columns, respectively, from the position of the window under consideration. With the relations established in relations Equation 9 above, correspondence is said to be satisfied if the conditions that $x_l^* = x_l$ and $y_l^* = y_l$ hold.

The features within the windows that have been found to consistently correspond locally under the confined search space are now to be matched under the global view. The matching procedure begins with the windows that have the highest similarity measure. This is done because there is more probability that the windows with the highest similarity measure are indeed truly corresponding windows than those with smaller similarity measures. In this global matching strategy, it is possible that a feature that has already been matched is matched again with another feature at a later stage of the matching process, but such outcomes are ignored. This is done in compliance with the uniqueness constraint and in support of the match achieved with a higher degree of certainty (a match through a higher similarity measure).

Results of the Stereo Matching Approach

Stereo scenes were tested and illustrative examples are shown and assessed below. In the assessment of these results, it is revealed that the proposed stereo matching technique performed extremely well,

yielding 80 percent or better of the features matched. It should be noted that these percentages do not reflect the fact that among the totality of features considered in the left or the right image, a number (a small percentage) of these features is actually missing in the left and in the right due to the stereo displacement. The execution time of this matching technique implemented on the Silicon Graphics R4400-based computer varied between a few seconds to 3 to 4 hours for the examples considered. This execution time is a function of the complexity of the scene which is reflected by the total number of features extracted. The authors foresee potential for the application of the similarity measure to various pattern matching and pattern recognition algorithms. In an earlier study (4), we have shown the results where the approach attempts to limit the execution time to within a few seconds even for complex scenes but at the expense of fewer features matched, while still maintaining the objective of finding practical results.

It is important to point out that another avenue to the recovery of the depth information is the exploitation of the motion vision principle. Simply stated, the basis of motion vision is the functional relationship that exists between the motion of the observer (the user) and the induced spatial and temporal information changes in a sequence of images. These information changes are functions of both the observer's motion and the depth map of the scene. Under certain fairly broad conditions, both the observer's motion and the depth map of the scene can be determined (22). Researchers in the field of computer vision tend to agree that a more effective approach to a solution of depth perception may come with an integration of stereo vision and motion vision.

RESULTS

Image Analysis and Interpretation Under The Augmented 2½-D Representation

A stereo pair of 2-D images has been used to establish the disparity measure of corresponding feature points in these images. At these corresponding points, once the disparity is extracted, depth can be derived using simple triangulation. If we assume the lens center defined at point $(x,y,z) = (0,0,-f)$ as

the reference point, the relation between disparity $d(x,y)$ in the 2-D images and depth Z in the real world is established as follows:

$$d(x,y) = \frac{f \cdot B}{f + Z} \qquad [10]$$

where B is the baseline distance between the two cameras, and f is the cameras' focal length (assumed equal in the two cameras). Furthermore, a perspective effect is mathematically derived so as to establish a relationship between the 2-D image plane and the 3-D real world. With this knowledge, an initial step for understanding the relationship between the augmented (2½-D) representation (which includes the disparity measure) with the 3-D real world is presented. Methods of analysis and interpretation can then be explored to stress and emphasize the importance of this augmented representation.

Perspective Projection

An analysis of the projection of a 3-D point in space onto a 2-D point in the image plane is expressed mathematically as: $(x,y,z) \rightarrow (x^*,y^*,z^*)$, or

$$[x^* \quad y^* \quad z^* \quad 1] = \left[\frac{xf}{f+z} \quad \frac{xf}{f+z} \quad 0 \quad 1 \right] \qquad [11]$$

The coordinate $z^* = 0$ implies a 2-D image point representing the projection of a 3-D point. To establish the desired geometrical relationships, simple triangulation can be used in reference to **Figure 4.** Projection (P) of a segment of length (r) between a point at range R_n and another point at range R_{n+1}, as shown in **Figure 4a,** is given by the following relationship:

$$P(n, R_n, R_{n+1}) = \frac{fh(R_{n+1} - R_n) \cos \alpha}{(R_n \cos \alpha + h \sin \alpha) \cdot (R_{n+1} \cos \alpha + h \sin \alpha)} \qquad [12]$$

where $R_n = L + nr$ and $n = 0, 1, \ldots, k$ is a positional index of the range points considered. Parameters f, h, and α denote the camera's focal length, height from ground plane, and tilt angle, respectively. Note that in the case where the tilt angle $\alpha = 0$, that is, when the camera image plane is perpendicular to the ground plane, which is assumed flat, Equation 12 above takes the simple form:

$$P(n, R_n, R_{n+1}) = \frac{fhr}{R_n \cdot R_{n+1}} \qquad [13]$$
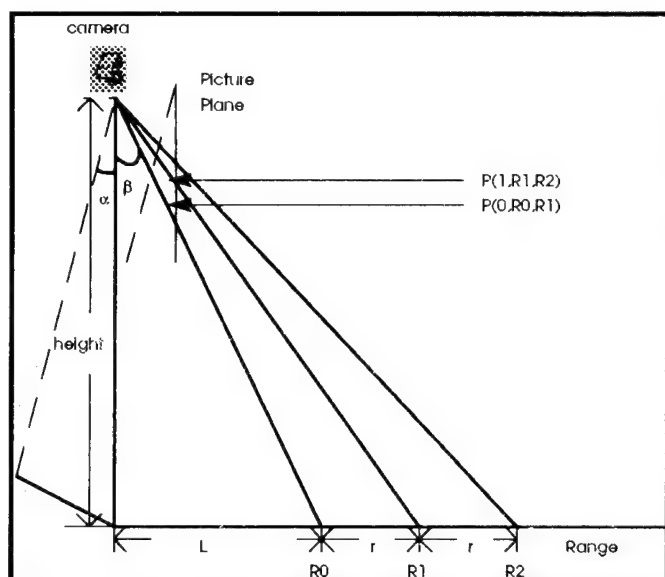
(a) Mapping of the Range Measure
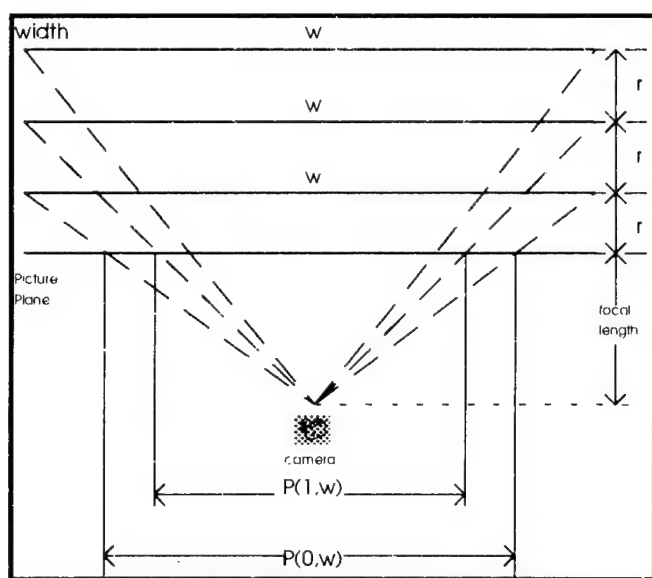
(b) Mapping of the Width Measure

Figure 4.
Mapping principles of the perspective effect.

Similarly, referring to **Figure 4b,** we find that the projection (P) of any segment of width (w) is given by the following relationship:

$$P(n,w) = \frac{fw}{L + nr} \qquad [14]$$

Given the camera viewing position and the camera parameters, using the above projection relation-

ships, the perspective effect is easily established. This actual perspective effect is then implemented as an added tool for the enhanced interpretation of images under the augmented representation.

A camera need not be in any particular orientation for this information to be obtained. The transformation matrices corresponding to rotation, translation, and scaling about any of the principal axes can be accounted for, as illustrated in **Figure 5.**

This perspective effect, as will be shown later, provides support to the analysis of images under the augmented (2½-D) representation. For known camera parameters, this task reduces to finding the geometrical relationships between the real-world measurements of range and width with their respective projections onto the picture plane. The advantages in the analysis provided by integration of the perspective effect into account are (*a*) the image analysis conforms to the real-world representation, (*b*) processing time and results of the walking straight ahead analysis are enhanced since only the desired vicinity of the blind is considered at any given level of the virtually partitioned image, (*c*) if an object is detected within the path of travel, its size can be estimated.

Scene Analysis Based on the 2½-D

Representation

Illustrative examples can now be explored for possible cases of enhanced scene analysis and interpretation. Consider **Figure 6**, which illustrates a stereo pair of a hallway scene containing select objects, cast shadows, and a reflected light spot from a light fixture on the ceiling of the hallway. Now, each depth region in the superimposed perspective map is set to correspond to approximately 1 meter. The object projection closest to the camera is that of the chair, both in the perspectively mapped image and in the disparity map. Looking solely at the perspective map, the contours describing the chair seem to fall on four depth regions in the perspective map. Information from the disparity map though, yields roughly uniform disparity measures for all features encompassing this object. These uniform disparities must correspond to a single depth region in space. The conclusion is that the object must be upright. Similar conclusions can be drawn for the case of the trash can. The paper recycling receptacle yields some interesting results.
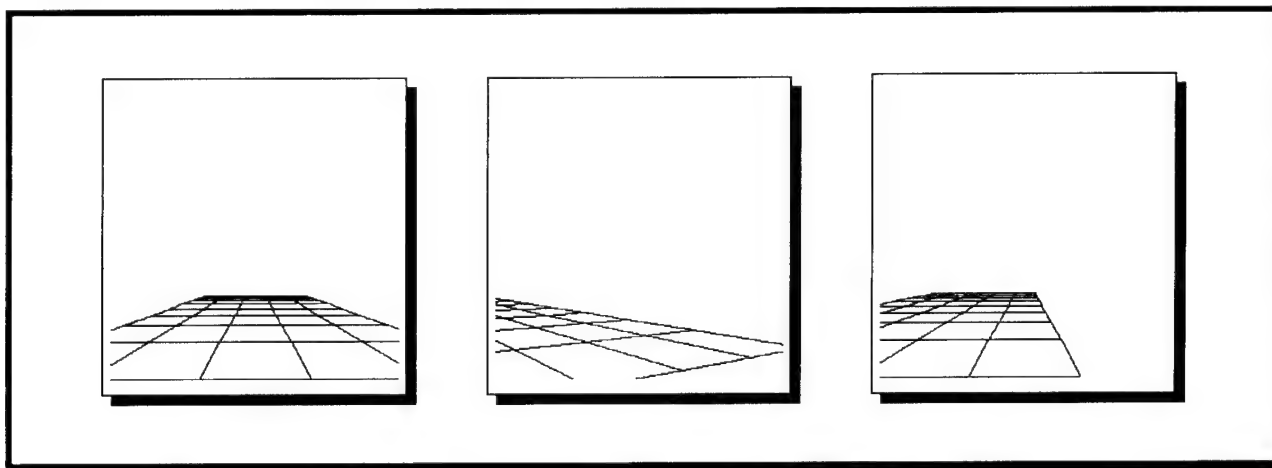
Figure 5.
Illustration of perspective projection examples.

Note that connected contours that encompass this object extend from the second perspective map depth region all the way past the last one shown. From the perspective view point, this particular object must be several meters in length. From the disparity information, the object should be contained in the fifth depth region of the perspective map. A conclusion that can be drawn is that a cast shadow (or a reflection) of an object may exist from the second to the fifth depth region in the perspective map.

The reflected light spot at the bottom of the image reveals another interesting case of interpretation. Now note that in the mapped region of furthest disparity, the vertical edges corresponding to the reflected light appear in the first perspective map depth region. From the extracted disparity measure, the reflected light must appear beyond the fourth depth region of the perspective map. There is a conflict between the extracted disparity and the information from the perspective projection. This virtual object can only be a reflection of a true object situated as the extracted disparity measure indicates. In fact, the floor of the hallway is actually mirroring a light fixture on the ceiling. The second example shown in **Figure 7,** (which illustrates a stereo pair of images) which included a mirror in the scene, was used to confirm that objects seen through a mirror will in fact have disparities that are equivalent to their real-world disparities.

The third example, shown in **Figure 8,** is the stereo pair of a photograph of a house. Using the perspective and disparity information, the conclusion can be drawn that this house scene is a flat surface or a photograph. Analysis of the stereo pair yields approximately equivalent disparity information throughout the entire image. This in itself results in all contours detected in this stereo pair to be at the same depth in 3-D space. These contours must therefore correspond to that of a flat surface.

A 2½-D world can become a new possibility with a fast implementation of the proposed stereo matching algorithm. The ramifications of this 2½-D world are of great potential for: (*a*) Scene segmentation, (*b*) object identification, and (*c*) enhanced automated guidance (23,24).

An Interpretation Example of a Staircase in

Contrast to a Crosswalk

The staircase is an interesting problem because, in general, shading is what distinguishes the rise, the upright step, from the tread, the flat step (25,26). The staircase is a succession of rises and treads, while a crosswalk a succession of painted and unpainted stripes. It is shown here that beyond standard measurements such as $(r(s,k) \cdot t(s,k) / r(s,k) + t(s,k))$ where $r(s,k)$ denotes the rise/painted stripe and $t(s,k)$ denotes the tread/non-painted stripe which can may be used to discriminate such

(a) Left Image + Perspective   (b) Right Image + Perspective   (c) Disparity Map + Perspective

(d) Closest Region   (e) Middle Region   (f) Furthest Region
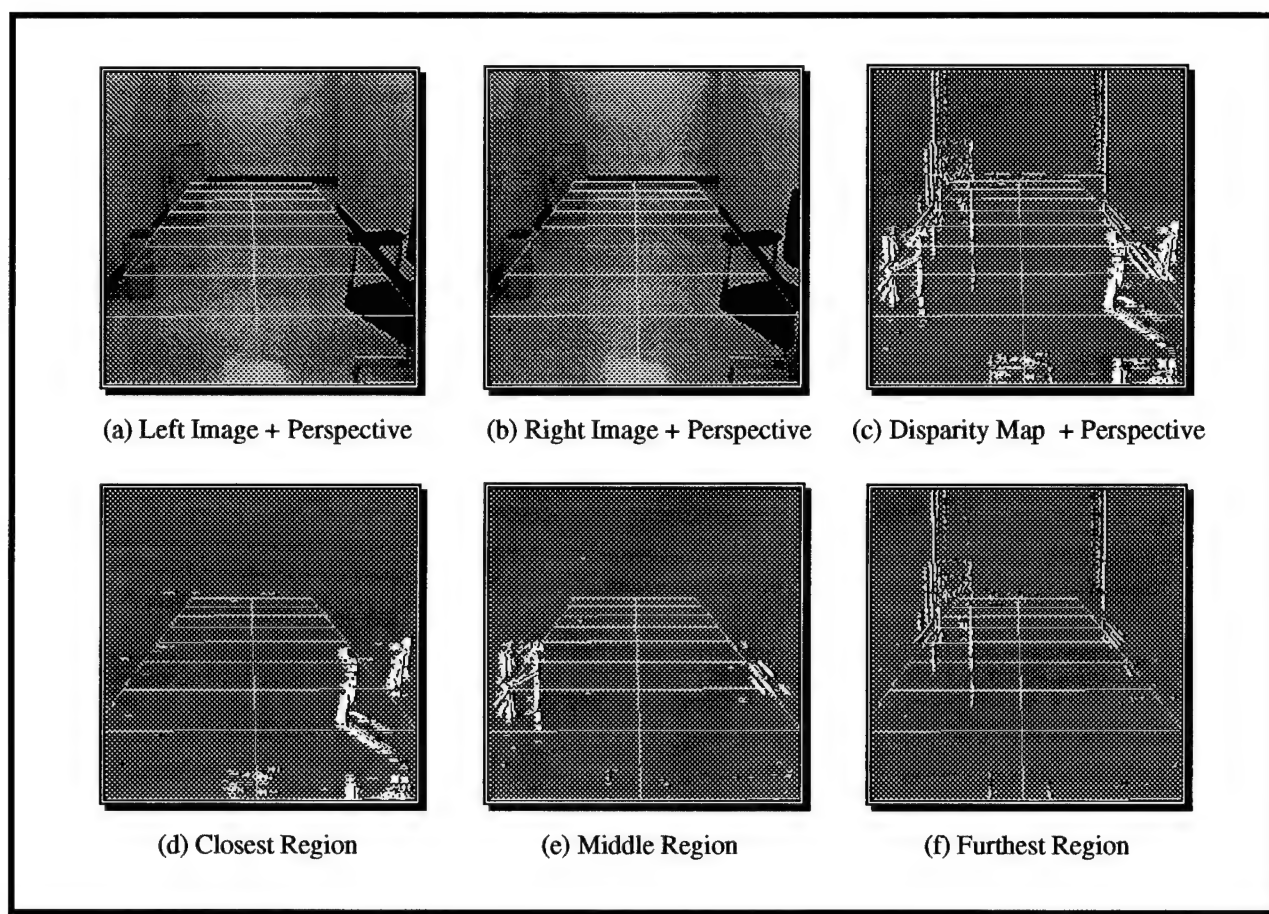
Figure 6.
Disparity map of a hallway scene superimposed with a perspective projection.

Left Image   Right Image   Left Image Features   Right Image Features

Complete Disparity Map   13-14 Pixel Disparity   10-12 Pixel Disparity   0-9 Pixel Disparity
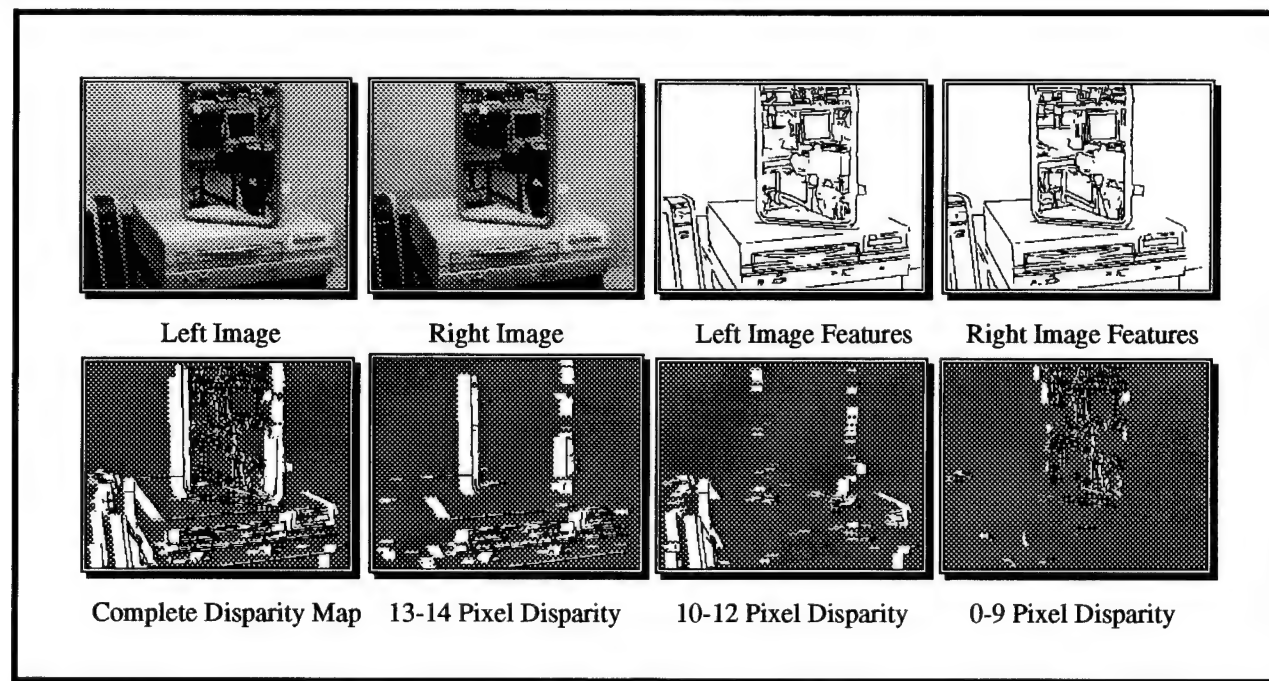
Figure 7.
Example of mirrored objects in a real-world scene.

(a) Left Image + Perspective   (b) Right Image + Perspective   (c) Disparity Map + Perspective
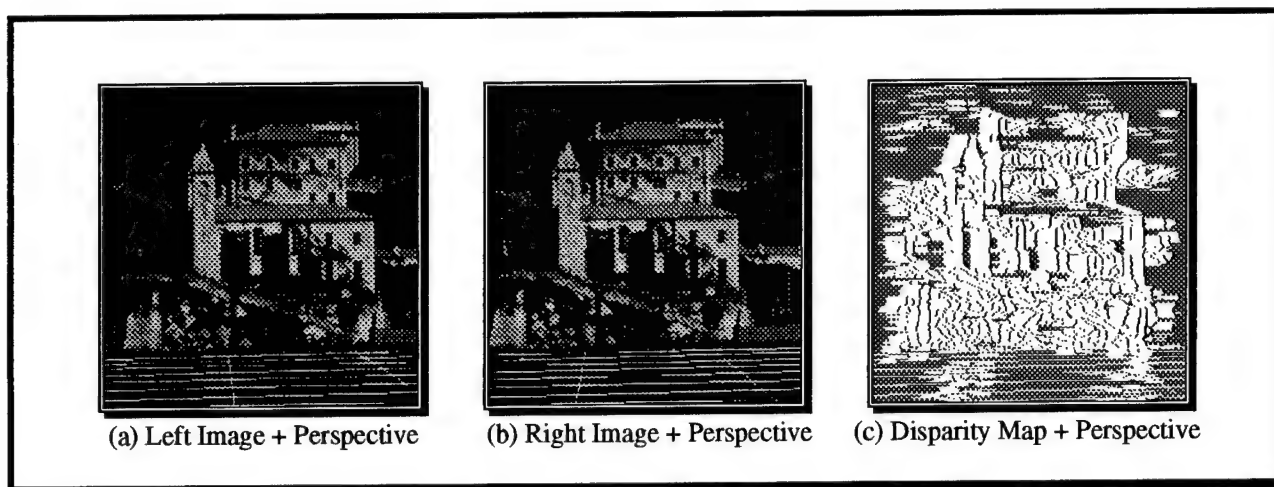
Figure 8.
Surface level perspective maps superimposed on stereo-image projections.

cases (27), the disparity measure in the augmented representation constitutes the most important feature to reach any conclusive assessment of the two cases. The results for this comparison are illustrated in **Figure 9.**

An Analysis of the Problem of Shadows under the Augmented Representation

The characterization of the effect of shadow is based on the fact that shadows cast on any surface would not change the surface physical characteristics and would only introduce a uniform gray level shift on those pixels under the shadow. But unlike mirrored objects, which display a disparity conforming to their real-world disparity with respect to the observer, cast shadows reveal a disparity which relates directly to the spatial position of the shadow itself rather than the object that casts it. The augmented representation in its essence would not help enhance the identification process of shadows unless overall context in the scene is used to exploit information such as "shadows are not free-standing," and that they always extend toward the object which cast them, ignoring flying objects.

Scene Analysis for the Detection of Depressions

Many visual cues, such as stereopsis, occlusion cues, context in the scene, and change in textural properties, can all be part of the recognition process of depressions. A computer implementation exploit-

ing any one of the above cues is a complex information processing problem. The concern in the detection of depressions or drop-offs is to extract the presence of any occluded information. In the 2-D case, one might consider context in the scene, or to look into a set of dynamic (time-varying) images and seek to extract any new information revealed through new peaks in the image intensity profiles (28). In the augmented (2½-D) representation, we can look for discontinuities in the disparities of the newly revealed information.

Scene Analysis of Upright Objects Versus Flat Objects

Upright objects, unlike flat objects, are not affected by the perspective effect. On the other hand, flat objects project on the 2-D image plane proportionally to their actual length (in the direction of travel) in terms of size of the object. Upright objects project on the 2-D image plane proportionally to the extent (in length) of the area they occlude or the extent of information in the scene that is occluded. This observation confirms the results obtained in the staircase versus crosswalk comparison.

A Possible Man-Machine Interface

These 2½-D representation results can be conveyed to the blind individual as tactile maps of disparities as illustrated in **Figure 6,** where edge

(a) Left Image   (a1) Right Image   (a2) Average Perspective Projection

(a4) Complete Disparity Map   (a5) 18-20 Pixel Disparity   (a6) 16-17 Pixel Disparity

(a7) 14-15 Pixel Disparity   (a8) 12-13 Pixel Disparity   (a9) 10-11 Pixel Disparity

(a) Disparities Conforming to the Perspective Projection of a Simulated Crosswalk

(b1) Right Image   (b2) Left Image   (b3) Right Image Features   (b4) Left Image Features

(b4) Complete Disparity Map   (b5) 28-29 Pixel Disparity   (b6) 24 Pixel Disparity   (b7) 21 Pixel Disparity

(b) Disparities Conforming to the Staircase Example

Figure 9.
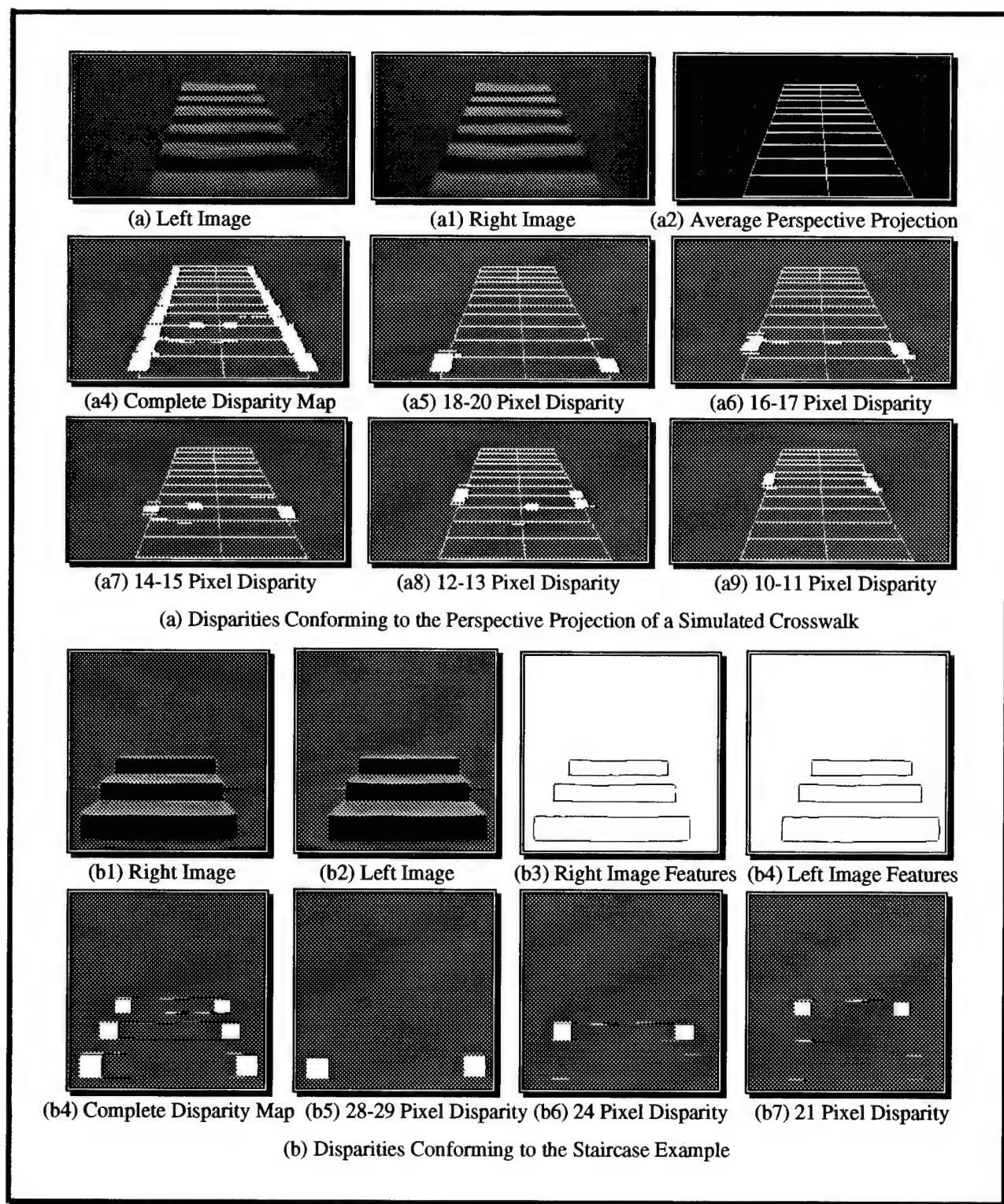Example contrasting a staircase and a crosswalk in the augmented representation.

information will help in determining the contours of objects and possibly their eventual identification if need arises, especially for cases such as a crosswalk, a staircase, a curb, and so forth, and where the horizontal thickness of these edges shown in white is directly proportional to their stereo disparity and, therefore, their real-world depth. The overall disparity map can also be a segmented function of the disparity measure such as to display (a) the disparity map of closer objects, (b) the disparity map of mid-range objects, (c) the disparity map of far away objects, and (d) any other map of objects within any disparity range desired. An example showing this kind of display is also shown in **Figure 6.** Furthermore, safety paths provided for automated guidance, and which are generated as simple markers showing the direction of safe travel, can also be displayed in tactile form. Simple audio cues can be also given in the form of "path clear straight ahead for X steps or Y meters," "you may turn left/right after X_1 steps or Y_1 meters," or "straight ahead leads to a dead end."

These types of results are given and discussed in Adjouadi, 1992 (1). There are, however, concerns for these types of audio displays, since images are dynamic in nature, and the time processing required to make sense of the changing information is computationally taxing. Also, it is extremely difficult to synchronize the audio output with the changes experienced in the image. This constitutes another interesting research avenue.

CONCLUSION

This study addressed the design of a dimensionally and spectrally augmented vision system based on enhanced spatial representations and an effective stereo paradigm. The central objective is based on the fact that by using this augmented vision system, enhanced image understanding will result. Such a system will find practical use in many automated robotics applications, including the automated guidance of robots, telerobotics, industrial tasks with hand-eye coordinated systems, and other man-machine interfaces with emphasis placed in the use of such a vision-based system as a possible guidance aid for the blind individual. For this last mentioned application, we remain conscious of the many extremely important ramifications and implications,

theoretical and practical, such a vision-based guidance system entails. The impetus in this endeavor draws from the properties of the wavelet transform as well as from the functional principles of the hypercolumn theory of the human visual cortex. Preliminary results in the application of the hypercolumn theory applied to image features understanding reveal tremendous potential for the development of algorithms which can provide credence to the principles of size constancy and orientation independence. Implementation of constituents of the hypercolumn theory will undoubtedly constitute a milestone in the field of computer vision. The development of algorithms based on the multiresolution and multiscale principles of the wavelet reveal a zoom-in characteristic which is significant for feature extraction and object recognition. Efforts remain to be extended toward real-time implementation of the proposed image techniques in an integrated fashion. At this juncture, the computational extensive tasks involve the application of stereo vision and the application of the multiresolution of the wavelet transform. Parallel processing should be a criterion to be considered at all levels, from the development of the image techniques to the building of the structure which integrates them.

REFERENCES

1. Adjouadi M. A man-machine vision interface for sensing the environment. J Rehabil Res Dev 1992:29(2):57–76.
2. Freedman S. Vision prosthesis and aids readiness or appropriateness. Report: Board of Education and Services for the Blind, Wethersfield, CT, 1989.
3. Marr D, Hildreth E. Theory of edge detection. In: Proceedings of the Royal Society of London B 1980:207:187–217.
4. Adjouadi M, Candocia F. A stereo matching paradigm based on the Walsh transformation. IEEE Trans Pattern Anal Mach Intel 1994:16(12):1212–8.
5. Daubechies I. Orthonormal bases of compactly supported wavelets. In: Communications on pure and applied mathematics. Vol. XLI. New York: John Wiley & Sons, Inc., 1988:909–96.
6. Meyer Y. Les ondelettes: algorithmes et applications. Paris: Armand Collin, 1992.
7. Rioul O, Vetterli M. Wavelets and signal processing. IEEE Signal Process Mag 1991:8(4):14–38.
8. Chui CK, ed. Wavelets: a tutorial in theory and applications. Vols. 1 and 2. San Diego, CA: Academic Press, Inc., Harcourt Brace Jovanovitch, 1992.

9.   Campbell FW, Robson J. Application of Fourier analysis to the visibility of gratings. J Physiol (Lond) 1968:197:551–66.

10. Hubel DH, Wiesel TN. Receptive fields and functional architecture of monkey striate cortex. J Physiol (Lond) 1968:195:215–43.

11. Hubel DH. Eye, brain, and vision. New York: Scientific American Library, 1988.

12. Frisby JP. Seeing: illusion, brain, and mind. Oxford: Oxford University Press, 1978.

13. Marr D. Vision. San Francisco: Freeman Publishing Co., 1982.

14. Rose D, Dobson VG, eds. Models of the visual cortex. New York: John Wiley & Sons, 1985.

15. Marr D, Poggio T. A computational theory of human stereo vision. In: Proceedings of the Royal Society of London B 1979:204:301–28.

16. Yuille AL, Poggio T. Scaling theorems for zero crossings. IEEE Trans Pattern Anal Mach Intel 1986:8(1):15–25.

17. Candocia F, Adjouadi M. Stereo feature matching using a new similarity measure. IEEE Trans Pattern Anal Mach Intel. In press.

18. Drumheller M, Poggio T. On parallel stereo. Proceedings of the IEEE, Robotics and Automation, 1986.

19. Dhond UR, Aggarwal JK. Structure from stereo: a review. IEEE Trans Syst Man Cybern 1989:19(6): 1489–510.

20. Ohta Y, Kanade T. Stereo by intra- and inter-scanline search using dynamic programming. IEEE Trans Pattern Anal Mach Intel 1985:7:2:139–54.

21. Cochran SD, Medioni G. 3-D surface description from binocular stereo. IEEE Trans Pattern Anal Mach Intel 1992:14(10):981–94.

22. Horn BKP, Weldon EJ, Jr. Robust direct methods for recovering motion. Int J Comput Vis 1988:2:51–76.

23. Iyengar SS, Elfes A, eds. Autonomous mobile robots: perception, mapping and navigation. Vol. 1. Los Alamitos, CA: IEEE Computer Society Press, 1991.

24. Thorpe C, Herbert M, Kanade T, Shafer SA. Vision and navigation for the Carnegie-Mellon Navlab. IEEE Trans Pattern Anal Mach Intel 1988:10(3):362–73.

25. Horn BKP, Brooks MJ. Shape from shading. Cambridge, MA: MIT Press, 1989.

26. Tou JT, Adjouadi M. Shadow analysis in scene interpretation. In: Proceedings of the 4th Scandinavian Conference on Image Analysis, Trondheim, Norway, June 1985.

27. Sakamoto L, Mehr EB. A new method of stair markings for visually impaired people. J Visual Impairm Blindn 1988:82(1):24–7.

28. Adjouadi M. Image techniques for the detection of depressions in autonomous guidance. Vision Interface '86, Vancouver, BC, Canada, May 1986.

**Department of
Veterans Affairs**

CLINICAL REPORT

Ultrasonic Head Controller for Powered Wheelchairs

Prepared by James M. Ford, BS, MA, KT, Health Science Specialist and Saleem J. Sheredos, BEE,
MHCA, Rehabilitation Engineer, Program Manager, Technology Transfer Section, Rehabilitation Research
and Development Service, Department of Veterans Affairs, Baltimore, MD 21202-4051

Abstract—This report describes an evaluation by the
Department of Veterans Affairs, Rehabilitation Research
and Development Service, Technology Transfer Section
(TTS). The Ultrasonic Head Controller Unit (UHCU) is
the result of research and development conducted by the
Palo Alto VA Rehabilitation Research and Development
Center, under sponsorship of the Paralyzed Veterans of
America and the VA Rehabilitation Research and Devel-
opment Service. The UHCU provides an alternative to
currently available human/machine interfaces for severely
disabled individuals. Unlike switches or proportional
joysticks, the UHCU operates without physical contact
between the unit and the user. The UHCU produces
analog signals in direct response to changes in the head
position of the user. These signals can be used to control
a variety of communication, robotic, mobility, and
recreational devices. This clinical evaluation explored the
use of the UHCU for powered wheelchair control by
quadriplegic individuals.

Key words: *evaluation/trials, quadriplegic, Rehabilitation
Evaluation Unit (REU), sensor, VA Technology Transfer
Section (TTS), UHCU, UHCW, ultrasonic head control-
ler unit, ultrasonic head controller wheelchair.*

INTRODUCTION

The results of years of research and develop-
ment have lead to a product that promotes func-
tional wheelchair mobility and independence in
activities of daily living for veterans with high level
spinal cord injury and similar neurological disabili-
ties. The Ultrasonic Head Controller for Powered
Wheelchairs was developed to provide an alternative
to currently available human/machine interfaces for
severely disabled individuals. The dissimilarity of
the Ultrasonic Head Controller Unit (UHCU) to
other currently available control systems makes the
UHCU unique; it operates without physical contact
between the system and the user.

Earlier models of the UHCU have successfully
demonstrated its use as an interface for powered
wheelchairs used by persons with quadriplegia.
Subsequently, a successful pilot study (1991) of one
precommercial model led to further refinements and
a resolution to questionable wet weather perfor-
mance, indicating that the Ultrasonic Head Control-
ler Wheelchair (UHCW) was ready for a multicenter
clinical evaluation. A geographically diverse multi-
center evaluation was conducted between June
1993 and September 1994. The primary motives
of the evaluation were to assess the acceptance
of the UHCW by veterans; identify prescriptive
(performance) criteria; and to determine what fur-
ther modifications, if any, were needed to improve
the product for optimal use by the targeted popula-
tion.

Product Description and Function

The UHCW is an electrically powered wheelchair controlled by an attached head position sensing electronic interface unit (**Figure 1a** and **1b**). The unit consists of two ultrasound transducers, an on-off switch, and an associated electronics package housed in derin plastic and mounted on a main support beam constructed of heavyweight painted aluminum (**Figure 1b**). The UHCU attaches to the wheelchair, functionally replacing the joystick. The user's head position becomes a joystick equivalent, controlling the speed and direction of the wheelchair.

During operation, the transducers emit inaudible ultrasonic pulses which propagate through the air until reflected by the user's head. The transducers provide raw data that are used to calculate the user's head position in a two-dimensional plane (**Figure 2**). The user tilts his/her head off the neutral vertical axis (same action as tilting a proportional
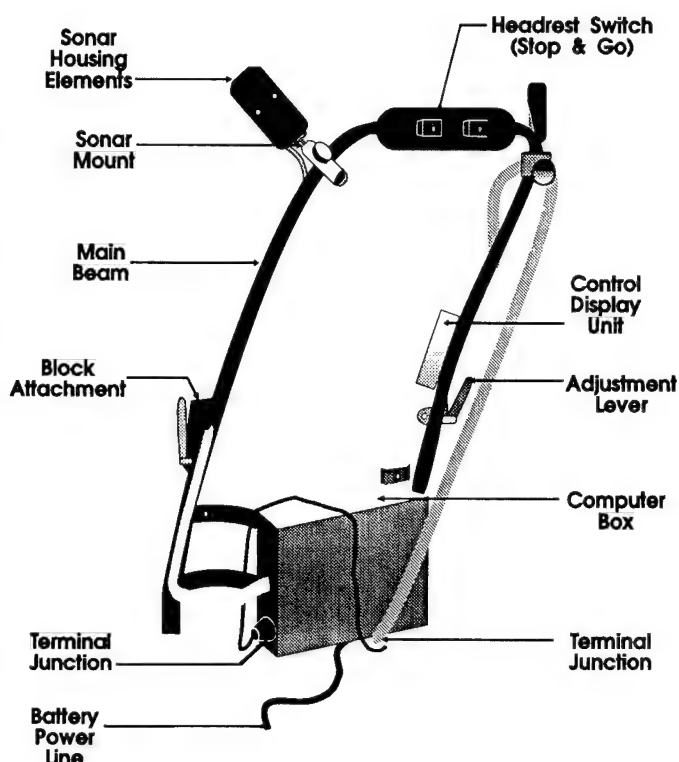
Figure 1b.
Head position sensing electronic interface unit.

joystick) in the forward/backward or left/right direction to accomplish the driving tasks desired.

BACKGROUND

The initial research and development of the first generation prototypes was accomplished by the Palo Alto VA Rehabilitation Research and Development (Rehab R&D) Center, which is supported by VA Rehabilitation Research and Development Service with additional support from the Paralyzed Veterans of America (PVA). These VA prototype UHC units were installed on E&J model 3P and Invacare Rolls electric wheelchairs. A series of design iterations driven by clinical requirements have, over the years, resulted in a model that demonstrated a need to continue efforts toward development for commercial marketing. The second generation models (4 E&J Marathons) were purchased by the VA Rehabilitation Evaluation Unit (REU, currently TTS) from Eureka Laboratories, delivered to the Rehab R&D Center, Palo Alto, CA, in October, 1988 and immediately submitted to acceptance testing. This
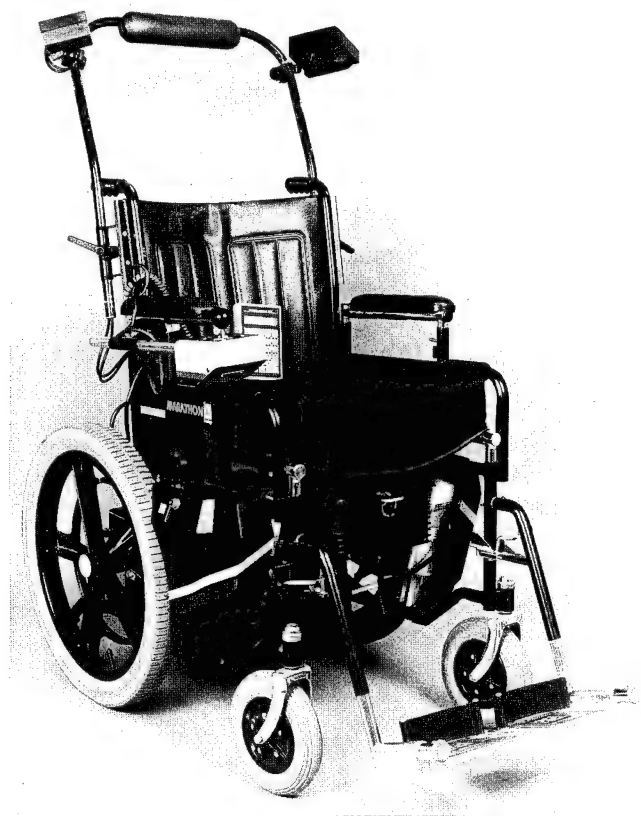
Figure 1a.
Ultrasonic head controlled wheelchair.
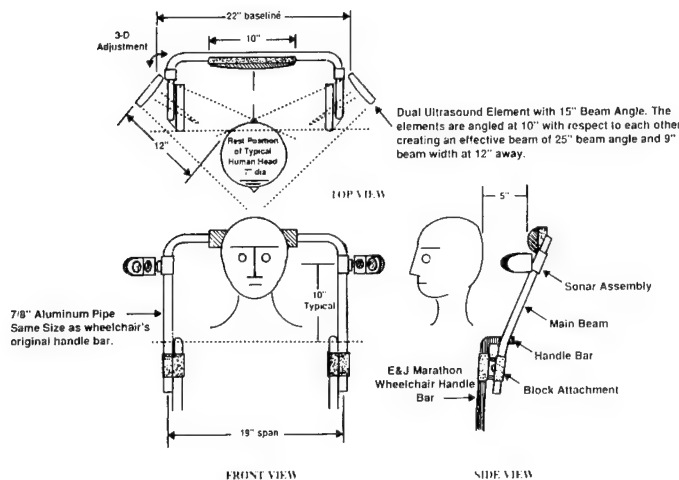
Figure 2.
Orthogonal drawings showing the overall dimensions of the new design in proportion to a typical human head.

acceptance testing raised concerns that required changes to the new models and verified the need for a pilot evaluation. Incorporation of recommended modifications and good results of the pilot evaluation primed the way for TTS to initiate a multicenter clinical evaluation. The initial phase of the multicenter evaluation, halted by poor performance in inclement weather, required resolution by the manufacturer. The manufacturer, Eureka Laboratories Inc., responded with a system which included: 1) environmentally sealed Polaroid sensors (able to withstand water immersion for 24 hours with no effects when housed in a Polaroid enclosure; 2) covers enclosed the top, sides, and back of the sensors (which eventually narrowed the sonar beams to a smaller range); and 3) a software design for rain filtration (that canceled any effects of raindrop reflection); thus enabling the trials to continue.

EVALUATION PROCEDURE AND METHODOLOGY

The clinical trials were conducted at the Spinal Cord Injury Service of six VA Medical Centers. Twenty male subjects (inpatient/outpatients) from among active and first-time users of varied types of wheelchair controllers were recruited with similar levels of spinal cord injury (Quadriplegia C_3, C_4, C_5, and C_6) dysfunction. To operate or facilitate training on the UHCW, whether rated as difficult or easy, subjects reported the need for modifications or

required added appliances (i.e., seat belts, chest straps, Roho cushions, and so forth). Training time for this group of subjects was not distinctive when compared to the pilot study group wherein no subjects were experienced in other control systems. Subjects and Principal Investigators (PIs) for this evaluation were asked to scrutinize specific areas; such as, usage requirements for target population, operation, sonar orientation, adjustments (sensor and driving parameters), environment (attendant) effects, driving safety, adequacy of instructions and controllability (speed/acceleration), straight-line driving, turns, and stopping. Most subjects completed training in one day and had unrestricted use of the UHCW for the remainder of the trial period. Seventeen subjects completed the evaluation over a cumulative period of 14 months.

CLINICAL FINDINGS

After spending sufficient time to become familiar with operating the UHCW, PIs and subjects reported on the operating parameters of the UHCW during clinical trials.

In spite of the many incidents of malfunctions/repairs, subjects rated the UHCW's usefulness favorably during and after their trials. Application of selected parameters with reference to the UHCW's operation, control, and overall performance when correct adjustment was possible were rated as "good." Using the scale in **Table 1**, subjects indicated their assessment of the functions listed in the table.

The comments/opinions of subjects were reviewed at the completion of the trials to aid in the determination of overall acceptance or rejection of the UHCW for the targeted population. The following opinions surfaced:

• Advantages: Better all around visibility, non-contact components and hands-free operation with less fatigue
• Disadvantages: Assistance of caregiver always required, set-up and adjustments difficult, and position of on/off switch impossible for kyphotic subjects
• Recommendation for desired changes: On/off switch positioned within reach of subject's head, reclining back chair and positive locking mechanism

Table 1.
Subjects rating of operation/control/performance parameters.

Parameter	Very Good	Good	Poor	Very Poor	N/A
Stability of design to function	6%	65%	18%	12%	0%
Placement of sonar units	0%	65%	18%	18%	0%
Forward speeds	12%	47%	18%	24%	0%
Reverse speeds	6%	35%	12%	24%	6%
Brake response to head position	6%	53%	18%	18%	6%
Negotiating ramps/inclines	12%	12%	12%	0%	59%
Negotiating turns	6%	47%	29%	12%	0%
Straight-line driving	12%	59%	12%	18%	0%
Uneven terrain	6%	24%	12%	0%	59%
Use in inclement weather	0%	0%	0%	0%	100%
Use in hot weather	0%	6%	12%	0%	82%
Safety	12%	18%	29%	24%	18%
Ease of operation	12%	41%	24%	24%	0%
Design appearance	6%	59%	12%	18%	0%
Ease of transport	0%	0%	0%	6%	88%

%Subjects N = 17

to prevent sensor movement, and location of sensor and design of main support beam to decrease range of motion (ROM) required to operate system.

Daily use of the UHCW during clinical trials was not without problems. The clinical trials at various sites produced more than average reports of technical and/or control malfunctions by subject users. A detailed analysis of subjects' and participating investigators' responses (data) indicated the UHCW's high rate of malfunction (adjustments), unsatisfactory design, and sometimes unpredictable performance parameters identified, and focused these problems in four areas (these problems can be attributed to the changes recommended by the pilot study):

1. The wet weather system covers distorted the sonar beams and blocked the holes that are critical to effective alignment of the sensors with the orifice of the user's ear.
2. The ball joint tightening knob (sensor locking mechanism) was not a positive lock and required continuous adjustments.
3. The distance of the sensors from the user's head often proved too great. The 8° bend on the wheelchair back coupled with an additional 8° of recline on the sensor mount support bracket far exceeded the sensor's effective operating limits and makes it impossible for subjects to reach the on/off switch mounted on the support bracket.
4. The seating system E&J standard low back chair proved to be an obstacle during transfers and offered no upper torso support as would be commonplace on a high back recliner.

DISCUSSION

The UHCW, in retrospect (pilot evaluation 1991), is fully operational and functioning as designed. The deficiencies of the pilot are believed to have been satisfactorily addressed by the manufacturer incorporating recommended changes for improvement of future models. TTS found that the UHWC had met its technologic objective of being an acceptable concept for the target population.

A consensus of evaluating participants all agree that the UHCW has at times proved to be troublesome, not only in function but in sitting position as well. These problems were encountered by all sites throughout the trials and proved to be primary factors in concluding that the UHCW at this juncture requires a review of the recommended changes made after the pilot study, including the wet weather system. It is clearly indicated by the less

than optimal performance and expressed comments of subjects and PIs on the UHCW (when compared to the pilot study) that these changes have negatively influenced the performance of the models used in the multicenter evaluation.

The reported data are mixed and offer both positive and negative viewpoints on performance. The consistency of recurring operating/performance malfunctions are pointed out in each of the data instruments throughout the final report. At the conclusion of the pilot study, the UHCW worked nearly perfectly (a few exceptions noted) as designed. Subjects and PIs of the multicenter evaluation were not apprised of the modifications made after the pilot study and, therefore, did not have the opportunity to compare the "before-and-after" performance of the UHCW. However, if they had been, the conclusions of the data would have been totally different. At this point, it is believed that there are other systems readily available on the market which are immediately superior in reliability and ease of use. Moreover, it is believed by therapists and subjects alike that the benefits that were supposed to have been achieved by the UHCW were not realistic for this model. Furthermore, the refinements recommended by the pilot study and the subsequent changes (wet weather system) can readily be revisited by the manufacturer. The problems identified by this evaluation can be overcome and addressed in a timely manner by the manufacturer. The recommendations on the multicenter evaluation should prove useful toward guiding this effort.

Finally, the manufacturer, with these recommendations, should seek continuous involvement and feedback from the targeted population and clinicians to ensure that the UHCW commercial product development is competitive with existing technology and products designed for similar application in order to be successfully marketed.

CONCLUSION

The precommercial prototypes used in the multicenter evaluation must revisit and recoup the functionality and reliability of the pilot unit that proved to be successful and acceptable to the targeted population. Moreover, if the recommendations of the multicenter evaluation are considered, the problems that surfaced in this evaluation can be readily addressed and implemented by the manufacturer into a commercially viable product.

ABSTRACTS OF RECENT LITERATURE

Joan Edelstein, M.A., P.T.
Director, Program in Physical Therapy, Columbia University, New York, NY
and
Jerome D. Schein, Ph.D.
Professor Emeritus of Sensory Rehabilitation, New York University, New York, NY

Abstracts are drawn primarily from the orthotics, prosthetics, and sensory aids literature. Selections of articles were made from these journals:

American Journal of Speech Language Pathology
American Rehabilitation
Archives of Physical Medicine and Rehabilitation
Journal of Orthopaedic and Sports Physical Therapy
Journal of Prosthetics and Orthotics
Journal of Speech and Hearing Research
Medizinisch Orthopädische Technik
Physical Therapy
Prosthetics and Orthotics International
Rehabilitation Psychology

PROSTHETICS, ORTHOTICS, AND RELATED TOPICS

Biobehavioral Factors Affecting Pain and Disability in Low Back Pain: Mechanisms and Assessment.
Feuerstein M, Beattie. Reprinted from *Phys Ther* 75:267-280, 1995.

Patients with recurrent or persistent low back pain (LBP) and disability represent a formidable challenge to physical therapists. Classic models of disease and pain mechanisms do not adequately explain the commonly observed discrepancies between the extent of pathology and reported pain, or the level of pain and disability. Research over the past decade that considers the interactive role of biological, environmental, and psychological processes in pain and disability has supported the involvement of a number of biobehavioral factors in these conditions. Physical therapists and other health care providers have become more aware of these factors and their impact on the evaluation, treatment, and management of LBP. Despite this recognition, little information is available that translates the implications of this research to direct care within physical therapy practice. The purposes of this article are (1) to provide an operational definition of biobehavioral factors; (2) to review the role of these factors in the clinical presentation of LBP, functional limitation, and disability; (3) to identify commonly used approaches for their recognition and quantification; (4) to illustrate how an understanding of biobehavioral factors can assist the physical therapist in evaluation and treatment of patients with LBP; and (5) to identify certain gaps in current knowledge of the role of biobehavioral factors and their application in physical therapy. Given the central role assumed by many physical therapists in the management of LBP, acknowledging and addressing these factors in clinical practice should assist in the prevention of chronic LBP and disability, as well as potentially improve physical therapy interventions and management. [JEE]

A Biomechanical Comparison of the SACH, Seattle and Jaipur Feet Using Ground Reaction Forces.
Arya AP, Lees A, Nirula HC, et al. Reprinted from *Prosthet Orthot Int* 19:37-45, 1995.

The Jaipur prosthetic foot was developed in India in response to specific socio-cultural needs of Indian amputees. It is being used extensively in India and several other developing countries. Its claim of being a cheaper and satisfactory alternative to other prosthetic feet has not been investigated biomechanically. The present study was undertaken to compare its biomechanical properties with the SACH and Seattle feet, using ground reaction forces.

Three trans-tibial amputees participated in the experiment which measured the ground reaction force data using a Kistler force plate. Subject's normal foot was used as a reference. Six variables

from the vertical and anteroposterior components of ground reaction forces were quantified. Their statistical analysis showed that the normal foot generates significantly larger ground reaction forces than the prosthetic foot. The shock absorption capacity of the SACH foot was found to be better when compared with the other two feet, while the Jaipur foot allowed a more natural gait and was closer in performance to the normal foot. None of the prostheses significantly influenced the locomotor style of the amputees. [JEE]

Clinical Applicability and Test-Retest Reliability of an External Perturbation Test of Balance in Stroke Subjects. Harburn KL, Hill KM, Kramer JF, et al. Reprinted from *Arch Phys Med Rehabil* 76:317-323, 1995 (©1995 by the American Congress on Rehabilitation Medicine and the American Academy of Physical Medicine and Rehabilitation).

We address the test-retest reliability and clinical applicability of an adapted external perturbation balance assessment, ie, the Postural Stress Test (PST). Repeated-measures were designed to assess the clinical features of a component of balance disorder in stroke. Twenty ambulatory stroke patients and 20 age-, gender-, height-, and weight-matched healthy control subjects participated in this study. Stroke patients were tested (using the adapted PST) on 4 separate days; matched control subjects were tested on one occasion. With the subject standing, backward perturbation forces were applied at the level of the center of gravity. Postural reactions to the test were scored in real-time and from videotape, from two different viewing angles, ie, 45° and 90° to the saggital plane. Scores (out of a maximal of 81) were ascertained using a 10-point subjective-observational scale. None of the control subjects fell during testing; four of the hemiplegic subjects fell. Subjects were protected from potential injury by a custom-designed safety harness system. For the hemiplegic subjects, intraclass correlation coefficients (ICCs), calculated as the reliability of any one occasion, ranged from 0.71 to 0.77, whereas those calculated as the reliability of the mean of the first two occasions ranged from 0.83 to 0.93. Although scores on the fourth occasion were significantly greater than those on the third occasion, both being significantly greater than those on the first and

second test occasions ($p < .05$), differences were less than 5 points on the 81-point scale. Results suggested a learning effect over time, beginning on the third occasion, and indicated that data acquired over the first two occasions could provide a suitable baseline. Whether the 5-point difference might be clinically meaningful, is currently unclear. Data averaged over the four occasions for the stroke subjects were used to compare hemiplegic and control subjects. The two angles of viewing for the videotaped assessment produced similar scores for the stroke ($t = 1.38$; $p > .05$) and the healthy ($t = 0.65$; $p > .05$) subjects. Similarly, real-time and videotaped scores (at the 90° observation angle) were similar for the stroke ($t = 0.56$; $p > .05$) and control subjects ($t = 0.13$; $p > .05$). However, videotaped ($p < .01$) and real-time scores ($p < .01$) (both at the 90° observation angle) were significantly lower for the stroke in comparison with the control subjects. Left (n = 10) and right (n = 10) hemiplegic subjects did not exhibit a difference in adapted-PST scores (at 90° observation angle and using videotaped data; $p > .05$). The adapted-PST was reliable when data were averaged for the stroke patients over at least two test occasions. It differentiated between a high-functioning stroke group and a healthy elderly group. Both angles of viewing produced similar results indicating that clinicians may choose their preferred patient observation angle. The assessment can be scored in real-time, eliminating the need for expensive videotaping equipment for assessment. [JEE]

Complexities of Foot Architecture as a Base of Support. Saltzman CL, Nawoczenski DA. Reprinted from *J Orthop Sports Phys Ther* 21:354-360, 1995.

The human foot is a unique structure in the animal kingdom, as it is capable of supporting sustained bipedal gait. The foot facilitates upright walking in several ways: 1) load bearing, 2) leverage, 3) shock absorption, 4) balance, and 5) protection. In this article, we discuss the specialized architecture that enables the foot to accomplish these functions. [JEE]

A Device for Long Term Ambulatory Monitoring in Trans-Tibial Amputees. Stam HJ, Eijskoot F, Bussmann JBJ. Reprinted from *Prosthet Orthot Int* 19:53-55, 1995.

Long term monitoring of walking in trans-tibial amputees (TTA) is considered important for prosthetic prescription and therapy evaluation.

The purpose of this study was to develop a device with the following design criteria: lightweight, easy attachment to the prosthesis, energy and memory capacity for five days and practical in clinical use.

The prototype (CAMP: Continuous Ambulatory Monitoring of Prosthetic walking) consists of a cylindrical unit containing an accelerometer, a miniature computer and six batteries. Specifications, data acquisition and processing, instructions for users and first results are presented and discussed.

The CAMP prototype proved to be a useful device for measuring relevant aspects of prosthetic use for up to five days.   [JEE]

Dreidimensionale dynamische Untersuchung zum Effekt der orthesenversorgung bei vorderer Knieinstabilitat unter sportfunktioneller Belastung. Sommerfeld FP, Geyer M, Siebert WE. Reprinted from *Med Orth Tech* 155:14-21, 1995.

To assess qualitative and quantitative knee-instability in athletes submitted to sport specific stress, a 3-dimensional motion analyses was performed, both pre- and post-operatively to 18 athletes of Hannover Olympic Training Center, who were previously evaluated by reference examinations (clinically, KT-1000, Cybex). Knee-instability (ap-shift) was provoked by a sports specific manouver (One-Leg-Square-Hop-Test) and recorded by a 3-dimensional Video-analyses-system (VAS). Synchronously muscle activity was assessed by EMG. A Don-joy-4-point ACL brace was tested on all athletes. A positive correlation was observed between the 3-dimensional VAS and the reference tests used. While the ap-shift was shown to be present pre- and post-operatively, it was significantly lower postoperatively. Brace support lead also to a remarkable reduction of the ap-shift. EMG recorded muscle imbalance in instable knees that was not affected by brace support.   [JEE]

Dysvascular Amputees: What Can We Expect? Anderson SP. Reprinted from *J Prosthet Orthot* 7:43-50, 1995.

The medical records of 385 amputees were studied to determine if the trends of high occurrence of death and second amputation for patients with vascular disease still exist and if so, to what degree. All the subjects experienced their first amputation between Jan. 1, 1982, and Dec. 31, 1987. Their patient charts were followed for a five- to 10-year period, as applicable, from the date of first amputation until the last entry prior to Dec. 31, 1992.

Multiple amputations occurred in 59 percent of the patients. Thirty-five percent of the subjects underwent a revision to the original amputation within an average of 6.5 months. Contralateral amputation was performed on 30.9 percent of the subjects. Contralateral amputation occurred an average of 24.9 months following the first amputation. Eighteen percent of all patients studied died within the time frame of this study. The average time between contralateral amputation and death was 18 months.   [JEE]

The Effect of Prosthetic Rehabilitation in Lower Limb Amputees. Christensen B, Ellegaard B, Bretler U, et al. Reprinted from *Prosthet Orthot Int* 19:46-52, 1995.

The objectives of this project were to ascertain whether, to date, the views concerning the determination of prosthetic candidacy have been optimal and whether the training methods applied have been effective and have resulted in constant use of the prosthesis after conclusion of the training programme. Secondly it was intended to set up guidelines for future budgeting as well as providing a reference framework for the process of rehabilitation.

An inquiry based on questionnaires was the first phase in a quality assurance project carried out among 29 amputees trained in 1990 and 1991.

The result of the inquiry was that rehabilitation using PTB prostheses for 19 trans-tibial amputations in 18 cases (one patient was a bilateral trans-tibial amputee) led to constant use of the prosthesis and that advanced age was no hindrance to constant use in this group. For 10 trans-femoral amputees the inquiry revealed that advanced age combined with problems of donning the prosthesis was a hindrance to constant use in two cases.

It is concluded that there is a need for testing/developing new types of femoral prostheses. The patients' evaluation of the rehabilitation process and their prostheses stresses the need for communication

between the team of professionals and the patients in the decision process concerning the provision of a prosthesis as well as the provision of complete information on the patients' future functional possibilities. Qualitative measurements must include the kind and number of medical complications and the social conditions of the amputee as well as tests of physical and mental resources.   [JEE]

Energy Expenditure of Below-Knee Amputees During Harness-Supported Treadmill Ambulation. Hunter D, Smith Cole E, et al. *J Orthop Sports Phys Ther* 21:268-276, 1995.

Traditional rehabilitation of amputees is primarily aimed at strengthening remaining musculature necessary for prosthetic use and gait training. Available gait training time, however, is often limited by pain, residual limb skin tolerance, and the patient's cardiovascular endurance. Harness-supported treadmill ambulation is a rehabilitation technique being used by physical therapists to decrease an individual's body weight by a given percentage during exercise. This, theoretically, allows an amputee to ambulate on a prosthesis at a lower energy cost. The purpose of this study was to compare the energy expenditure of healthy below-knee amputee volunteers with healthy able-bodied volunteers during harness-supported treadmill ambulation in order to determine if energy conservation is achieved. Subjects were tested on a treadmill, walking at .67 m/sec (1.5 mph) and 1.34 m/sec (3.0 mph) during each of the following randomized harness-supported treadmill ambulation situations: full body weight, 20% body weight supported, and 40% body weight supported. During the last minute of each trial, rate of perceived exertion, heart rate, and standardized indirect calorimetry oxygen consumption (VO_2, ml/kg/min) measures were collected. Caloric expenditure (kl/min) was calculated using metabolic conversion equations. Peak heart rate, peak VO_2, and peak kl/min were measured after the conclusion of the last walking trial by taking each subject to volitional fatigue. Data were analyzed for each harness-supported treadmill ambulation situation and group using analysis of variance (ANOVA). The researchers identified significantly lower ratings of perceived exertion, heart rates, and VO_2s for able-bodied subjects vs. below-knee amputees for all trials. Both groups demonstrated significantly lower

heart rates, VO_2s, and kl/min at 1.34 m/sec with 40% body weight supported. Additionally, significantly lower VO_2s and kl/min were found for able-bodied subjects vs. below-knee amputees at 1.34 m/sec for 20% body weight supported. The results of this study provide preliminary justification for physical therapists to utilize harness-supported treadmill ambulation with amputees when energy expenditure savings would be advantageous.   [JEE]

Erfahrungen mit der dynamischen Bewegungsanalyse zur Beurteilung einer Knieorthese (Clinical Evaluation of Functional Brace by Means of Dynamic Motion Analysis). Weisskopf M, Nosir HR, Siebert WE. Reprinted from *Med Orth Tech* 115:103-108, 1995.

This study evaluates the role of the functional knee brace MOS Genu in unstable knees. The muscle restraint is not enough to prevent the extremes of APT. 10 patients with isolated ACL tear are evaluated by Lachman test, arthrometer KT 1000 with load of 69 N and 87 N, ultrasound evaluation, one-leg-square-hop-test and motion gait analysis with running speed 2, 4, 6 m/sec. Those are done with and without braces. The reduction by KT 1000 with a load of 67 N is 43% from 9,2 mm to 5,2 mm, by 87 N is 35% from 11,8 mm to 7,7 mm, by sonography is 69% from 8,3 mm to 3,7 mm, by one-leg-square-hop-test is 47% from 4,7 mm to 2,5 mm, and by motion gait analysis is 21% at 2/sec from 4,3 to 4,7 mm, 40% at 4 m/sec from 4,5 mm to 2,7 mm and 20% at 6 m/sec from 4,5 mm to 3,6 mm. Functional knee brace do reduce the APT by offering a strain sheilding effect of the ACL at certain examined load. The dynamic evaluation is better than static one since physiologic conditions are more likely to be encountered due to the developing muscle restraint under loading conditions.   [JEE]

Evaluation and Management of Foot and Ankle Disorders: Present Problems and Future Directors. McPoil TG, Hunt GC. Reprinted from *J Orthop Sports Phys Ther* 21:381-388, 1995.

Recent research has raised serious concerns regarding the reliability and validity of the evaluation and treatment scheme proposed by Root et al. Although the Root et al theory is widely referenced

in the physical therapy literature and commonly taught in continuing education courses, current issues of concern include: 1) measurement technique reliability, 2) the criteria proposed for normal foot alignment, and 3) the position of the subtalar joint between midstance and heel-off during walking. The intent of this paper is to review these three problem areas which have been identified with the Root et al theory as well as to propose the use of a "tissue stress model" which the authors have found to be an effective alternative for evaluating and treating foot disorders.   [JEE]

Footwear and Foot Orthotic Effectiveness Research: A New Approach. Cornwall MW, McPoil TG. Reprinted from *J Orthop Sports Phys Ther* 21:337-344, 1995.

Measurement of calcaneal inversion and eversion during walking is limited when subjects wear shoes. The authors of this study propose the use of transverse tibial rotation as a viable alternative measurement when barefoot assessment is not possible. The purpose of this study, therefore, was to: 1) determine the relationship between transverse tibial rotation and rearfoot motion during the stance phase of normal walking and 2) demonstrate the usefulness of measuring transverse tibial rotation when evaluating the effect of footwear and insole foot orthotic devices. Part 1 consisted of eight volunteers (five women, three men) whose rearfoot and transverse tibial motion was videotaped while they walked along a 12-m walkway. The results of this study showed that although absolute values were not comparable, the two motion patterns are related to each other. The correlation between the mean rearfoot and tibial motion patterns of all 16 feet was $r = .953$. Part 2 investigated the effect of footwear and orthotics on transverse tibial rotation using two case presentations. A video camera was positioned in front of each subject as they walked at a self-selected speed under various footwear or orthotic conditions. The results of the case studies revealed that footwear or foot orthotics decrease maximum tibial internal rotation compared with barefoot walking. In addition, internal tibial rotation velocity and acceleration were decreased by the use of shoes, an accommodative orthosis, and an inflatable medial longitudinal arch support. A rigid orthotic produced a slight increase in transverse

tibial rotation and a dramatic increase in transverse tibial acceleration. It is felt that measurement of transverse tibial rotation may prove useful in evaluating footwear and orthotic effectiveness.   [JEE]

Functional Reach in Wheelchair Users: The Effects of Trunk and Lower Extremity Stabilization. Curtis KA, Kindlin CM, Reich KM, et al. Reprinted from *Arch Phys Med Rehabil* 76:360-367, 1995 (©1995 by the American Congress on Rehabilitation Medicine and the American Academy of Physical Medicine and Rehabilitation).

Our purpose was to compare the effects of using wheelchair trunk and lower extremity stabilization on sitting trunk mobility and functional reach of wheelchair users. Seven subjects with paraplegia who averaged 35.6 years of age and nine able-bodied control subjects with an average age of 26.0 years participated in this study. Each subject's functional reach in the transverse and sagittal planes was video-recorded in each of three conditions, randomized in order: (1) without a belt; (2) with a neoprene chest belt; and (3) with a webbing thigh belt. The area circumscribed by each subject's functional reach under each condition was processed using the Motion Analysis Expert Vision Flextrak program. Functional reach in each belting condition was compared within each subject and between able-bodied controls and subjects with high and low thoracic levels of paraplegia. This study showed that in the sagittal plane, subjects with both high and low thoracic levels of paraplegia were able to substantially increase the area of their functional reach when using a chest belt when compared with the thigh belt or no-belt condition. The mean area of their sagittal plane functional reach increased by over 50% by stabilizing the chest to the wheelchair using a neoprene belt. However, in the transverse plane, only those individuals with lower thoracic paraplegia (T8 to L1) gained substantial benefit from chest strapping, increasing the area of their functional reach by a mean of 24%. In contrast, able-bodied control subjects gained no benefit in functional reach from either belting condition. These results demonstrate that wheelchair users with motor levels L-1 and above who use a chest belt gain a distinct advantage in functional reach. This information has clinical implications for optimal trunk stabilization in wheelchair seating and for perfor-

mance enhancement in wheelchair athletic competition.   [JEE]

A High-Performance, Variable-Suspension, Transradial (Below-Elbow) Prosthesis. Radocy R, Beiswenger WD. Reprinted from *J Prosthet Orthot* 7:65-67, 1995.

The Variable Suspension Prosthesis (VSP) is a transradial (below-elbow) design that combines the proven effectiveness of supracondylar (modified muenster) suspension with new silicone socket technology.

The prosthesis is unique and versatile. It can be worn either as a supracondylar socket with a sock or without a sock using a silicone suspension-type sleeve with an internal forearm interlock. The combination of the supracondylar socket and silicone sleeve provides superior suspension for improved performance in rigorous activities like windsurfing and weight lifting. The prosthesis' ability to be functionally and securely worn with a three-ply sock provides more traditional comfort and added convenience to the user for regular daily activities.

Design and fabrication of the prosthesis follow standard procedures with certain modifications recommended to ensure proper fit and function.

The VSP is applicable to most transradial amputees and is especially valuable to active prosthetic wearers. Field testing indicates the VSP is sound technology and a viable prosthetic alternative for the profession.   [JEE]

Knieorthesenwirkung bei vorderer Kreuzbandinstabilitat. Grifka J, Jutka H. Reprinted from *Med Orth Tech* 155:22-28, 1995.

In examinations of the function of knee orthoses against ventral instabilities, regularly the same problems are evident. Patients practicing sports especially complain about pressure spots, slipping of the splint and a restraint of motion. A principal problem is, that even with most dificult mechanical joints orthoses can not imitate the complicated natural movement of the knee joint.

Moreover there is the danger, that such orthoses don't only have any protection, but develop compulsory forces on the already damage knee, due to their unpropriate joint mechanism.

In order to avoid these problems, a completely new type of knee orthoses ("ACI-Support") has been developed, which is functioning without any mechanical axis for the knee. Due to slightly dorsal attached telescops the knee can move according to its individually determined, variable pattern of motion. The only effect of the orthoses is a stabilisation against ventral translation of the upper tibia, in order to avoid a giving-way phenomenon.

For clinical routine a check up of the orthoses' function is adviced after a few days and after 6 weeks of wearing.   [JEE]

Limitations of Kinematics in the Assessment of Wheelchair Propulsion in Adults and Children with Spinal Cord Injury. Bednarczyk JH, Sanderson DJ. Reprinted from *Phys Ther* 75:281-289, 1995.

Background and Purpose. Recently, there has been a trend for designers to reduce the weight of wheelchairs. Wheelchair performance is frequently evaluated in clinical as well as laboratory settings by kinematic motion analysis. The purpose of this study was to examine the effect of weight on the kinematics of wheelchair propulsion in nonathletic adults and children with spinal cord injury. Subjects and Methods. The weight of identical new lowweight test chairs (9.3 kg) was manipulated by adding weight (5 and 10 kg) in two matched groups ($n = 10$) of adults and children with spinal cord injury. The three-dimensional coordinates of reflective markers were obtained as the subjects performed level wheeling at a speed of 2 m/s. Results. The pediatric group was found to have significantly lower wheeling speeds than the adult group. The addition of weight, however, did not alter the wheeling speeds in either group. Neither the proportions of the wheeling cycle spent in propulsion (24%) nor the angular (shoulder flexion-extension, elbow flexion-extension, shoulder abduction, and trunk flexion-extension) kinematics of wheeling changed with additions of weight in either group. The angular kinematics of the pediatric group, however, were different than those of the adult group. Conclusion and Discussion. These results indicate that adding weight in the range of 5 to 10 kg did not affect wheeling style under the levelwheeling, low-speed conditions of the study. It is possible that performance in wheelchair propulsion

may be more appropriately determined by kinetic and energetic outcome measures than by kinematic measures. [JEE]

New Concept of Spinal Orthosis for Weakened Back Muscles. Watanabe H, Kutsuna T, Asami T, Inoue E. Reprinted from *Prosthet Orthot Int* 19:56-58, 1995.

An anterior bending posture of the trunk during walking is often seen among the elderly commonly due to weakened thoraco-lumbar and gluteal muscles. For the management of this debilitating condition, the authors have developed a modified design of thoraco-lumbo-sacral orthosis (TLSO). Incorporated in this device are pockets for the accommodation of lead weights, which are located posteriorly at the level of the lumbar region and an elasticated anterior abdominal band. The results and level of patient acceptance achieved with the use of this brace have both been excellent. [JEE]

Physical Determinants of Independence in Mature Women. Posner JD, McCully KK, Landsberg LA, et al. Reprinted from *Arch Phys Med Rehabil* 76:373-380, 1995 (©1995 by the American Congress on Rehabilitation Medicine and the American Academy of Physical Medicine and Rehabilitation).

The purpose of this study was to determine the relationship in mature women between muscle strength and whole body oxidative capacity and the ability to perform activities of daily living (ADL). Sixty-one women (mean age 69 years) without major disease or disability were recruited from either a community exercise center or a personal care facility. Physiological measurements consisted of peak oxygen consumption on a cycle ergometer (VO_2 peak) and one repetition maximum strength of nine muscle groups (1-RM). Ability to perform ADL was measured with a balance and gait test, "Bag Carrying Test", and ADL questionnaires. Significant correlations were found with VO_2 peak and calf muscle strength and ability to perform ADL, with weaker or no correlations for other muscle groups. For some relationships, it was possible to identify the minimum level of physiological functioning associated with successful performance of independence tasks. In summary, physiological capacities,

particularly VO_2 peak and strength of the calf muscles, predicted ability to perform activities needed for functional independence in healthy mature women. [JEE]

The Rehabilitation of Gait in Patients with Hemiplegia: A Comparison between Conventional Therapy and Multichannel Functional Electrical Stimulation Therapy. Bogataj U, Gros N, Kljajic M, et al. Reprinted from *Phys Ther* 75:490-502, 1995.

Background and Purpose. Gait Rehabilitation in patients with severe hemiplegia requires substantial effort. Preliminary studies indicate potential beneficial effects of using multichannel functional electrical stimulation (MFES) for gait rehabilitation in these patients. In this study, a new method of gait rehabilitation for nonambulatory patients with hemiplegia by means of MFES added to conventional therapy was introduced. The results of the method's application were evaluated by comparing it with conventional therapeutic methods. Subjects. The proposed rehabilitation method was tested on a group of 20 patients with severe hemiplegia secondary to cerebrovascular accident. Subjects were randomly assigned to one of two groups. One group received 3 weeks of MFES followed by 3 weeks of conventional therapy. The other group received 3 weeks of conventional therapy followed by 3 weeks of MFES. Methods. The effects of each therapeutic method were evaluated by measurements of temporal-distance variables and ground reaction forces and by assessment of each subject's physical status according to the Fugl-Meyer evaluation scale. Results. There was improved performance of the subjects during MFES combined with conventional therapy as compared with conventional therapy alone. Conclusion and Discussion. The superiority of the MFES method as compared with conventional therapy was mainly attributed to the enhanced motor learning accomplished by application of MFES. These results, however, are preliminary, and further research is needed. [JEE]

Screening for Balance and Mobility Impairment in Elderly Individuals Living in Residential Care Facilities. Harada N, Chiu V, Damron-Rodriguez J, et al. Reprinted from *Phys Ther* 75:462-469, 1995.

Background and Purpose. The rapid growth of the elderly population has resulted in a corresponding rise in the number of elderly individuals who experience disability during their lifetimes. The purpose of this study was to test the usefulness of four established clinical measures of balance, gait, and subjective perceptions of fear of falling as screening methods for referring community-dwelling elderly individuals living in residential care facilities for detailed physical therapy evaluation and possible intervention. Subjects. The subjects were a convenience sample of 53 elderly individuals living in two residential care facilities for the elderly. Methods. Subjects were tested on each of four clinical measures of balance and mobility. Their performance on these measures was compared with a physical therapist's brief evaluation of disability and appropriateness for more detailed evaluation. The usefulness of these tools as screening methods was determined by calculating sensitivity and specificity levels using the physical therapist's evaluation as a standard. Results. The sensitivity and specificity levels of the four clinical measures in their application as screening tests for referral to physical therapy were as follows: Berg Balance Scale, 84% and 78%; balance subscale of the Tinetti Performance-Oriented Mobility Assessment, 68% and 78%; gait speed, 80% and 89%, and Tinetti Fall Efficacy Scale, 59% and 82%. The combination of two tests, Berg Balance Scale and gait speed, yielded the highest sensitivity of 91% and the highest specificity of 70% when a subject tested positive on at least one test. Conclusion and Discussion. These findings indicate the feasibility of developing screening methods for referring community-dwelling elderly individuals for a detailed physical therapy evaluation based on established clincal assessment measures, with a combination of tests measuring balance and gait demonstrating the most promising results. [JEE]

Seating Orthosis Design for Prevention of Decubitus Ulcers. Carlson JM, Payette MJ, Vervena LP. Reprinted from *J Prosthet Orthot* 7:51-60, 1995.

Decubitus ulcers can lead to very serious medical consequences for nonambulatory people who have impaired sensation. Associated medical treatment can be extremely expensive. Factors contributing to the formation of ulcers are discussed. Seating orthosis design characteristics that can reduce ulcer-generating factors are presented. Particular attention is given to design features and custom fabrication techniques related to redistributing pressure away from at-risk locations and to minimizing shear. [JEE]

Sensitivity and Specificity of Platform Posturography for Identifying Patients with Vestibular Dysfunction. DiFabio RP. Reprinted from *Phys Ther* 75:290-305, 1995.

Sensitive and specific measures are needed to identify patients with vestibular impairments. The purpose of this clinical perspective is to describe the sensitivity and specificity of dynamic and static platform posturography for detecting vestibular disorders. The sensory organization test (SOT) of dynamic posturography (EquiTest), the motor "perturbation" test, and Romberg's tests on a static (fixed) force platform each had over 90% specificity. This finding means that nearly all of the subjects who should have tested negative, did test negative on each type of assessment. The sensitivity of the SOT was evaluated across five studies involving a total of 836 patients with peripheral vestibular deficits (PVDs). Abnormalities in the SOT were detected in only 40% ($n = 338$) of the cases. Static platform posturography sensitivity was evaluated across six studies involving a total of 571 patients with PVDs, and abnormalities were detected in 53% ($n = 302$) of these cases. Tests of spontaneous and positional nystagmus and the horizontal component of the vestibuloocular reflex (VOR), by comparison, detected PVDs in 48% of 798 patients with suspected vestibular impairment. For patients with vestibular deficits associated with central nervous system disease, a total of 389 cases were identified in five studies and SOT abnormalities were found in 54% ($n = 209$) of these cases. The motor perturbation test was abnormal in 35% ($n = 41$) of 119 patients with central vestibular disease. In conclusion, the sensitivity of static posturography appeared to be slightly better than that of dynamic posturography for detecting PVDS, but the level of sensitivity for each posturography test, as well as for tests of horizontal VOR function, was considered to be low. Combining either type of posturography with other tests of vestibular function, however, increased the overall sensitivity of detecting

vestibular deficits to 61% to 89%. It was concluded that dynamic and static platform posturography as well as tests of VOR function lack adequate sensitivity to detect vestibular impairment when applied in isolation. Posturography appears to detect vestibular deficits in some patients who had normal VOR assessments and, therefore, provides supplemental rather than redundant information about vestibular dysfunction. [JEE]

Der Stellenwet von Orthesen bei der Therapie der meniskoligamentaren Kniegelenksverletzung. Scherer MA. Reprinted from *Med Orth Tech* 115:7-12, 1995.

A survey among 320 surgical units showed an increasing tendency towards early functional postoperative treatment. Following ACL-reconstruction roughly 1/3rd still use plaster of paris immobilization, after meniscus surgery patients are allowed to freely move their joints right away in 75% of all cases. A wide variety of braces are available. They are capable of reducing pathological translation and limiting p.op. range of motion. Nevertheless no convincing scientific data are available that would deem necessary the p.op. use of braces in order to obtain an excellent result. [JEE]

The Subtalar Joint: Anatomy and Joint Motion. Rockar PA. Reprinted from *J Orthop Sports Phys Ther* 21:361-372, 1995.

To fully understand the research literature on the efficacy of various clinical procedures, the physical therapist must be knowledgeable in the anatomy and biomechanics of the synovial joints. This paper presents detailed information on the bony, ligamentous, muscular, and vascular anatomy of the subtalar joint. In addition, there is a discussion of the joint axis as well as the joint motions about this axis. This information will prove valuable to the clinician as new examination and treatment procedures are considered for inclusion in the management of patients with foot-ankle dysfunction. [JEE]

Survey Research and Measurement Error. Nolinske T. Reprinted from *J Prosthet Orthot* 7:68-78, 1995.

Survey research involves looking at the relationships between sociological and psychological variables and relies on various methods of data collection, including in-person and telephone interviews and questionnaires that are mailed or used with an interview or group administration. Each method has the potential for error or inaccuracy. This article introduces various types of survey research while focusing on questionnaire development and use. Recognizing and accounting for survey measurement error when using questionnaires also is discussed. [JEE]

Use of an In-Shoe Pressure Measurement System in the Management of Patients with Neuropathic Ulcers or Metatarsalgia. Mueller MJ. Reprinted from *J Orthop Sports Phys Ther* 21:328-336, 1995.

Many injuries to the foot appear to be caused by repeated, excessive plantar pressures. In-shoe pressure systems are capable of measuring pressures at the interface between the shoe or orthotic and the plantar foot during a given functional activity. The purpose of this article is to describe the use of an in-shoe pressure system as a tool to aid physical therapists in the management of patients with foot problems as a result of excessive plantar pressures. Case histories are provided that describe the application of an in-shoe pressure device in the management of one patient with neuropathic ulcer and one patient with metatarsaigia. A discussion of the primary clinical and equipment considerations of using this type of device is included. [JEE]

COMMUNICATION AIDS

HEARING

Comparison of Procedures for Obtaining Thresholds and Maximum Acceptable Loudness Levels with the Nucleus Cochlear Implant System. Skinner MW, Holden LK, Holden TA, Demorest ME. *J Speech Hear Res* 38:677-689, 1995.

Based on testing of 11 adults with cochlear implants, researchers conclude that ascending loudness judgments with knob determines maximum-

acceptable-loudness levels more efficiently than knob and keyboard detection.   [JDS]

Speechreading Supplemented by Single-Channel and Multichannel Tactile Displays of Voice Fundamental Frequency. Waldstein RS, Boothroyd A. *J Speech Hear Res* 38:690-705, 1995.

To study tactile representations of fundamental frequency (Fo) contributions to speechreading, 12 normally hearing adults participated in 2 experiments. The results show "The findings are consistent with the hypothesis that subjects were not taking full advantage of the (Fo) variation information available in the outputs of the two experimental tactile displays." [JDS]

PSYCHOLOGY

The Effect of Cognitive Rehabilitation on the Neuropsychological Status of Patients in Drug Abuse Treatment who Display Neurocognitive Impairment. Fals-Stewart W, Lucente S. *Rehabil Psychol* 39:75-94, 1994.

Seventy-two court-mandated drug-treatment patients were randomly assigned to one of four treatments: (a) computer-assisted cognitive rehabilitation, (b) progressive muscular relaxation, (c) learning to type on a computer, or (d) no additional treatment. Patients in (a) had a faster rate of cognitive recovery in the first 2 months, more efficient cognitive functions over the first 4 months in treatment, and were rated highest by clinical staff for appropriateness of their participation. Authors hypothesize that the computer training improves attention, which generalizes to daily functioning. [JDS]

Predicting Life Satisfaction Among Adults with Spinal Cord Injuries. Coyle CP, Lesnik-Emas S, Kinney WB. *Rehabil Psychol* 39:95-112, 1994.

Structured interviews with 91 adults with spinal cord injury suggest the most significant predictor of life satisfaction is leisure satisfaction, which accounted for 43 percent of the variance in life-satisfaction scores. Self-esteem and health satisfaction accounted for an additional 16 percent of the variance. [JDS]

SPEECH

Comparing Recognition of Distorted Speech Using an Equivalent Signal-to-Noise Ratio Index. Gordon-Salant S, Fitzgibbons PJ. *J Speech Hear Res* 38:706-713, 1995.

Forty paid subjects were divided among (a) normally hearing listeners, 18-40 years; (b) normally hearing listeners, 65-76 years; (c) persons 18-40 years with mild to moderate hearing loss; or (d) persons 65-76 years with mild to moderate hearing loss. Age and hearing loss affected distorted speech, with age effects primarily evident in the most distorted conditions. Recognition of distorted speech in noise was affected by hearing status but not age. Authors conclude that "increased age produces a reduction in the functional S/N ratio." [JDS]

Dynamic Aspects of Lower Lip Movement in Parkinsonian and Neurologically Normal Geriatric Speakers' Production of Stress. Forrest K, Weismer G. *J Speech Hear Res* 38:260-272, 1995.

Studies of alternating production of stress contrasts by nine males with Parkinson's disease (P) and eight age-matched, neurologically normal males (N) revealed Ps "reduced displacement and peak velocity . . . during opening and closing gestures for both the stressed and unstressed syllables." Ps movement durations were significantly shorter during closing gestures. Other quantitative measures did not differ significantly between P and N. [JDS]

Identifying the Onset and Offset of Stuttering Events. Ingham RJ, Cordes AK, Ingham JC, Gow ML. *J Speech Hear Res* 38:315-326, 1995.

Four sophisticated listeners' judgments of precise onset/offset of stuttering in samples of spontaneous speech demonstrated "the potentially poor reliability of a measurement procedure that is currently widespread in stuttering research." Investigators suggest directions for development of more reliable measures. [JDS]

Increased Postoperative Posterior Pharyngeal Wall Movement in Patients with Anterior Oral Cancer: Preliminary Findings and Possible Implications for Treatment. Fujiu M, Logemann JA, Pauloski BR. *Am J Speech-Lang Pathol* 4:24-30, 1995.

The swallows of 7 of 11 patients with resection of anterior tongue and/or buccal floor showed substantial increase in anterior bulge of the posterior pharyngeal wall (PPW). The authors envision "a possible treatment approach to increasing PPW contraction in dysphagic individuals with reduced BOT [bottom of the tongue]-to-PPW contact during BOT [bottom-of-tongue]-to-PPW contact during the pharyngeal swallow." [JDS]

Voice Intelligibility in Patients Who Have Undergone Laryngectomies. Miralles JL, Cervera T. *J Speech Hear Res* 38:564-571, 1995.

Recorded reading of 24 Spanish 2-syllable words by 30 laryngectomized males—20 tracheoesophageal-esophageal shunt (TES) and 10 without shunt (NES)—was presented to 140 listeners, along with recordings of 10 age-sex-matched, normal-voiced controls. Differences in intelligibility between normal and laryngectomized patients were significant; all laryngectomized patients revealed difficulties producing voicing distinctions. Within patient differences were not significant, though TES had the most errors with fricative consonants, and NES had the most errors with nasals. [JDS]

VISION

Independent Living Services for Older Individuals Who Are Blind: Issues and Practices. Moore JE, Stephens BC. *Am Rehabil* 20:30-35, 1994.

Discusses the prevalence of visual impairment and blindness in persons 65 years and older (estimated to be one in six of the general population), models of service delivery, and numbers receiving services—16 references. [JDS]

BOOK REVIEWS

Jerome D. Schein, PhD, and Sal J. Sheredos

Sociolinguistics in Deaf Communities. Edited by Ceil Lucas. Washington, DC: Gallaudet University Press, 1995. $39.95.

by Jerome D. Schein, PhD
Professor Emeritus of Sensory Rehabilitation, New York University, New York, NY

In three decades, linguists' views of American Sign Language (ASL) have changed from considering it as an inferior substitute for speech to recognizing it as a language independent of English. The leader of that cognitive revolution, William Stokoe, laid a solid foundation in scientific methodology—a foundation that has served subsequent generations of researchers of local sign languages throughout the world. This collection of 10 essays validates the soundness of Stokoe's initial assault on then-traditional thinking.

The current linguistic foray contains essays on sign language in Quebec (QSL), the Philippines (PSL), on a Navajo reservation (NSL), and Spanish variations of ASL (S-ASL). The other six essays probe a variety of sociological aspects of ASL.

Dominique Machabée studies the impact of spoken French on QSL, beginning with the reasonable proposition that deaf people are typically bilingual, having some degree of competence in their locale's spoken language as well as the local sign language. Analyzing videotapes of 10 native signers and interviews with additional informants, Machabée focuses on a single characteristic of sign, initialization. These investigations lead her to several provocative conclusions about the results of QSL-French contact, conclusions further complicated by QSL-ASL contacts. The findings have implications for all language contacts, regardless of mode of expression.

Observations of a Navajo family, 6 of whose 11 members are congenitally deaf, reveals the rule-governed nature of sign-language development, which in turn supports the innateness of human language. This report by Jeffrey Davis and Samuel Supalla illustrates many additional points of general interest, supporting other research on the modifications one language undergoes when it comes into contact with other languages.

While most deaf children are bilingual, some are trilingual. Barbara Gerner de Garcia describes three Hispanic deaf children and their families' school experiences. Her detailed examination of this limited sample prompts her to offer a series of recommendations stemming from her basic observation, "Deaf children in linguistically diverse families may be at a disadvantage, not because they are dealing with three languages but because the schools do not accommodate the needs this creates" (p. 243).

In "Conversations with Deaf Filipinos," Liza Martinez presents data from a wide range of conversational dyads. She finds two patterns of turn-taking that are based on gender. In cross-sex dyads, males sign more than females, but in same-sex dyads, utterances are about equal between the participants. Martinez notes that these gender-specific findings are also observed generally in spoken exchanges. However, the eye-gaze data suggest cultural differences between PSL and ASL, a phenomenon she urges be more intensively studied.

The remaining six studies involve ASL and English. They examine relations between the two languages, between the disproportionate number of users of each, and within ASL. Political, social, and cultural influences come under scrutiny and yield much material for future volumes in this series to consider. If the publisher holds to the annual publication of this series, sociolinguists will certainly profit. What should be equally clear is that adjacent disciplines—anthropology, linguistics, psychology, sociology, and more—will also gain from these diverse contributions that, while centering on manual communication, generally, and sign language, specifically, have broad implications for all language-dependent aspects of human behavior.

The American Sign Language Dictionary on CD-ROM. by Martin L.A. Sternberg. New York: HarperCollins Publishers, 1994, Compact disc and manual, with separate versions for IBM and Mac computers. $69.95.

by Jerome D. Schein, PhD
Professor Emeritus of Sensory Rehabilitation, New York University, New York, NY

Students of sign language know that it cannot be learned from books alone. The two-dimensional page is inadequate to illustrating signs' three-dimensional motion-configurations. Particularly difficult to illustrate are constructs compounding two or more signs: *mother* as "female who holds the baby" or *brother* as "male like me." On paper, the flowing of one sign—for *male* or *female*—into the other—for *holding baby* or *like me*—creates nearly insurmountable problems for the artist who endeavors to draw them. Nor do photographs, singly or in multiples, overcome the difficulties. Now comes a long-awaited solution: filmed examples of persons signing that can be viewed on a computer.

The huge capacity of compact discs enables these slender bits of plastic to hold vast stores of information. The one under review contains nearly 2,200 video clips of signs, along with their glosses in five languages, cross references, mnemonic hints, and supplementary printed and voiced descriptions. A brief history of sign languages, answers to some common questions about signs, suggestions for learning them, and pointers on signing (etiquette, body language, and so forth) add to the understanding of American Sign Language (ASL).

The author has anticipated the disc's use as a self-instructional tool. He provides exercises for practice and for self-testing. Students often recall how they quickly became embarrassed when they had to ask signers to repeat a particular sequence again and again. But a computer disc requires no apologies: students can review signs as often as they desire. What is more, on this disc they can enlarge the image, slow it, or speed it—great advantages to learning.

Since it is based on the author's *American Sign Language Dictionary* (HarperCollins, revised 1994) which contains 4,400 signs, the question naturally arises: How adequate is the vocabulary's range? Before concluding that 2,200 signs do not constitute a large linguistic corpus, one should recall that the functional extent of a single sign increases in context. *Slow, slowly, slower* partake of the same root sign, as holds for words in spoken languages. Should they be counted as one or three signs? How signs are made can greatly alter their meaning; the single sign indicating *size,* for example, can vary in meaning from minuscule to gigantic. On the other hand, some English words require more than one sign for their translation: ASL has three different

signs for *about:* as adjective, adverb, and preposition. So questions about the size of the vocabulary boil down to whether or not users find what they need. For most, this dictionary will provide sufficient entries for most purposes.

Is the CD-ROM difficult to use? No, not for anyone with a modicum of computer literacy. Accessing a particular sign requires nothing more than typing its name. The disc can be used as a thesaurus, by browsing its 21 categories (e.g., Adjectives & Adverbs, Home & Garden, Business & Finance, Family Life). Or one can scroll rapidly through the alphabetical list of entries to jog one's memory for a particular word or concept. The practice exercises permit the student to choose the amount and type of practice exercise desired; they make time fly, as users try their hands at the various games and lessons.

Does this mean that this CD-ROM will eliminate the need for live instruction? For many persons, no. However, it is an invaluable supplement, encouraging the amount of practice that acquiring competence in any language demands. As a dictionary, its ease of access, color, animation, and the cogency of its illustrations carry it head and shoulders above any print version. For rehabilitators who may have been reluctant to prescribe sign language for late-disabled patients because of the difficulties in obtaining adequate instruction and practice for them, this CD-ROM should ease their doubts and enhance appropriate patients' communication options. For professionals who do learn to sign, it provides an attractive means of sustaining this acquired skill and expanding it over time.

If It Weren't For The Honor—I'd Rather Have Walked. Jan Little. Bloomington, IL: Cheever Publishing, 1995, 262 pp.

by Sal J. Sheredos
Program Manager, Technology Transfer Section, VA Rehabilitation Research and Development Service

True to her style, Jan Little humorously provides an information packed, real-life documentary of people, places, events, and milestones that, over the last 40 and more years, have challenged and produced positive results on the social, political, and medical/rehabilitation arenas, leading us into the twenty-first century.

The story, told through her life, unveils the many trials, tribulations, joys, successes, and lessons of hundreds of people, people, and more people, who did not have in their vocabulary "can't," "insufficient (or no) funds," or "not in my mandate." Her personal experiences have great relevance to anyone who is, or is in any way associated with, a person with disabilities (PWD).

Our government agencies and rehabilitation programs have all been attempts to catch up with real needs, making available to all what had already been demonstrated by the pioneering few. Jan provides an historical overview of official milestones, such as the public laws that emphasized protection of rights, as well as the funding of research, development, education and training, and vocational rehabilitation.

Jan, in real-life language, presents the human spirit and ingenuity to deal with and solve challenges by PWDs, and the response of others. This highly readable book would be helpful to anyone who is interested in people and life; those who are involved in any way with rehabilitation will relate to, identify, and remember the people and occurrences in this story.

PUBLICATIONS OF INTEREST

This list of references offers *Journal* readers significant information on the availability of recent rehabilitation literature in various scientific, engineering, and clinical fields. The *Journal* provides this service in an effort to fill the need for a comprehensive and interdisciplinary indexing source for rehabilitation literature.

All entries are numbered so that multidisciplinary publications may be cross-referenced. They are indicated as *See also* at the end of the categories where applicable. A listing of the periodicals reviewed follows the references. In addition to the periodicals covered regularly, other publications will be included when determined to be of special interest to the rehabilitation community. To obtain reprints of a particular article or report, direct your request to the appropriate contact source listed in each citation.

BIOENGINEERING

1. Action Potentials of Curved Nerves in Finite Limbs. Xiao S, McGill KC, Hentz VR, *IEEE Trans Biomed Eng* 42(6):599-607, 1995.
Contact: Shaojun Xiao, Rehabilitation Research and Development Center, VA Medical Center, Palo Alto, CA 94304-1200

BIOMATERIALS

2. Deformation and Stress Analysis of Supported Buttock Contact. Dabnichki PA, et al., *Proc Instn Mech Engrs—Part H: J Eng* 204(H4):263-266, 1995.
Contact: P.A. Dabnichki, Bioengineering Unit, University of Strathclyde, Glasgow

3. Shock-Absorbing Effect of Shoe Insert Materials Commonly Used in Management of Lower Extremity Disorders. Shiba N, et al., *Clin Orthop* 310:130-136, 1995.
Contact: Harold B. Kitaoka, MD, Mayo Clinic, 200 First St., SW, Rochester, MN 55905

BIOMECHANICS

4. Soft Tissue Biomechanics. Smeathers JE, Wright V, *Proc Instn Mech Engrs—Part H: J Eng* 208(H4):191-193, 1995.
Contact: J.E. Smeathers, BSc, PhD, Rheumatology and Rehabilitation Research Unit, University of Leeds, Leeds, UK

COMMUNICATION AIDS—HEARING

5. Method for Determining the Driving Currents for Focused Stimulation in the Cochlea. Rodenhiser

KL, Spelman FA, *IEEE Trans Biomed Eng* 42(4):337-342, 1995.
Contact: Kristin L. Rodenhiser, Dept. of Electrical Engineering, Center for Bioengineering, and Regional Primate Research Center SJ-50, University of Washington, Seattle, WA 98195

6. Study Surveys Views of Nurses on Hearing Aids, Hearing Aid Wearers. Johnson CE, et al., *Hear J* 48(2):29-31, 1995.
Contact: Dr. Johnson, Dept. of Communication Disorders, Auburn University, 1199 Haley Center, Auburn, AL 36849-5232
See also 8

COMMUNICATION AIDS—VISION

7. OPTONET: Neural Network for Visual Field Diagnosis. Accornero N, Capozza M, *Med Biol Eng Comput* 33(2):223-226, 1995.
Contact: Prof. Neri Accornero, Dipartimento di Scienze Neurologiche, Viale dell'Universita 30, 00185 Roma, Italia

8. Study of the Tactual Reception of Sign Language. Reed CM, et al., *J Speech Hear Res* 38(2):477-489, 1995.
Contact: Charlotte M. Reed, Research Laboratory of Electronics, Massachusetts Institute of Technology, Cambridge, MA 02139

9. Visual Neuroprosthetics—Functional Vision for the Blind. Normann RA, *IEEE Eng Med Biol Mag* 14(1):77-83, 1995.
Contact: Richard A. Normann, Dept. of Bioengineering, The University of Utah, Salt Lake City, Utah 84112

FUNCTIONAL ASSESSMENT

10. Functional Performance Measure for Persons with Alzheimer Disease: Reliability and Validity. Carswell A, et al., *Can J Occup Ther* 62(2):62-69, 1995.
Contact: Anne Carswell, PhD, OT(C), Occupational Therapy Programme, Faculty of Health Sciences, University of Ottawa, 451 Smyth Rd., Ottawa, Ontario, K1H 8M5, Canada

11. Treatment-Based Classification Approach to Low Back Syndrome: Identifying and Staging Patients for Conservative Treatment. Delitto A, Erhard RE, Bowling RW, *Phys Ther* 75(6):470-489, 1995.
Contact: Anthony Delitto, PhD, PT, Dept. of Physical Therapy, School of Health and Rehabilitation Sciences, University of Pittsburgh, 101 Pennsylvania Hall, Pittsburgh, PA 15261

FUNCTIONAL ELECTRICAL STIMULATION

12. Diaphragm and Accessory Respiratory Muscle Stimulation Using Intramuscular Electrodes. Dunn RB, Walter JS, Walsh J, *Arch Phys Med Rehabil* 76(3):266-271, 1995.
Contact: Robert B. Dunn, PhD, Rehabilitation R&D Center (151L), VA Hines Hospital, P.O. Box 20, Hines IL 60141

13. Dynamic Response of the Cat Ankle Joint During Load-Moving Contractions. Zhou BH, et al., *IEEE Trans Biomed Eng* 42(4):386-393, 1995.
Contact: Bing He Zhou, Bioengineering Laboratory, Dept. of Orthopaedic Surgery, Louisiana State University Medical Center, New Orleans, LA 70112

14. Machine Learning in Control of Functional Electrical Stimulation Systems for Locomotion. Kostov A, et al., *IEEE Trans Biomed Eng* 42(6):541-551, 1995.
Contact: Aleksandar Kostov, Division of Neuroscience, University of Alberta, Edmonton, Alberta, T6G 2S2, Canada

GAIT ANALYSIS

15. Electromyograph Analysis of the Popliteus Muscle in Level and Downhill Walking. Davis M, Newsam CJ, Perry J, *Clin Orthop* 310:211-217, 1995.
Contact: Craig J. Newsam, MPT, Rancho Los Amigos Medical Center, Pathokinesiology Laboratory, 7601 E. Imperial Hwy., Downey, CA 90242

16. Surface vs. Fine-Wire Electrode Ensemble-Averaged Signals During Gait. Jacobson WC, Gabel RH, Brand RA, *J Electromyograph Kinesiol* 5(1):37-44, 1995.

Contact: Richard A. Brand, Dept. of Orthopaedic Surgery, 2430 Steindler Bldg., The University of Iowa, Iowa City, IA 52242

GENERAL

17. 1994 Edward R. Stitt Lecture Award—Organizational Analysis of The Veterans Administration Decentralized Hospital Computer System: The Challenge of Innovation in a Bureaucratic Setting. Ginsburg RE, *Milit Med* 160(4):161-167, 1995.
Contact: Ronald E. Ginsburg, MD, Stratton VA Medical Center, Dept. of Pathology and Laboratory Medicine, 113 Holland Ave., Albany, NY 12208

18. Conservative Options in the Management of Spinal Disorders, Part II: Exercise, Education, and Manual Therapies. Reitman C, Esses SI, *Am J Orthop* 25(3):241-250, 1995.
Contact: Charles Reitman, PT, MD, Baylor College of Medicine, 1333 Moursund Ave., Houston, TX 77030

19. Foot Injuries Caused by Anti-Personnel Mines. Wertheimer B, et al., *Milit Med* 160(4):177-179, 1995.
Contact: Borna Wertheimer, MD, Orthopedic Surgeon, Dept. of Orthopedics, University Hospital Osijek, Radiceva 23, 54000 Osijek, Croatia

20. From the Veterans Health Administration: The Health of Persian Gulf Veterans. Kizer KW, *JAMA* 273(23):1817, 1995.
Contact: Kenneth W. Kizer, MD, MPH, Under Secretary for Health, Dept. of Veterans Affairs, 810 Vermont Ave. NW, Room 800, Washington, DC 20420

21. Heterotopic Ossification: Treatment of Established Bone with Radiation Therapy. Schaeffer MA, Sosner J, *Arch Phys Med Rehabil* 76(3):284-286, 1995.
Contact: Julian Sosner, MD, Dept. of Rehabilitation Medicine, St. Vincent's Hospital and Medical Center, 153 West 11th St., New York, NY 10011

22. Hospitalization Charges, Costs, and Income for Firearm-Related Injuries at a University Trauma Center. Kizer KW, et al., *JAMA* 273(22):1768-1773, 1995.

Contact: Kenneth W. Kizer, MD, MPH, Dept. of Veterans Affairs, 810 Vermont Ave. NW, Room 800, Washington, DC 20420

23. NIH Consenus Conference: Total Hip Replacement. NIH Consensus Development Panel-Total Hip Replacement, *JAMA* 273(24):1950-1956, 1995.
Contact: Office of Medical Applications of Research, Federal Bldg., Room 618 National Institutes of Health, 7550 Wisconsin Ave. MSC 9120, Bethesda, MD 20892

24. Physical Activities of Nonistitutionalized Dutch Elderly and Characteristics of Inactive Elderly. Van Den Hombergh CE, et al., *Med Sci Sports Exerc* 27(3):334-339, 1995.
Contact: Carla E. J. Van Den Hombergh, Dept. of Epidemiology and Public Health, and Dept. of Human Nutrition, Wageningen Agricultural University, 6700 AE Wageningen, The Netherlands

25. Physical Medicine and Rehabilitation. Brandstater ME, *JAMA* 273(21):1710-1712, 1995.
Contact: Murray E. Brandstater, MBBS, PhD, FRCPC, Loma Linda University, Loma Linda, CA 92354

26. Quantitative Analysis of Research in Physical Therapy. Robertson VJ, *Phys Ther* 75(4):313-327, 1995.
Contact: Valma J. Robertson, PhD, School of Physiotherapy, La Trobe University, Locked Bag 12, Carlton South, Victoria, Australia 3053

27. Serial Casting of the Lower Extremity to Correct Contractures During the Acute Phase of Burn Care. Johnson J, Silverberg R, *Phys Ther* 75(4):262-266, 1995.
Contact: Joanne Johnson, PT, Dept. of Rehabilitation Medicine, New York Hospital Cornell Medical Center, Box 142, 525 E. 68th St., New York, NY 10021

28. Superimposition of Analogue Data Onto a Video Image: A New Technique. Tarrant SC, et al., *J Med Eng Technol* 18(6):218-223, 1994.
Contact: S.C. Tarrant, Medical Physics Group, Dept. of Physics, University of Exeter, Exeter EX4 4QL, UK

29. Towards the Realization of an Artificial Tactile System: Fine-Form Discrimination by a Tensorial Tactile Sensor Array and Neural Inversion Algorithms. Caiti A, et al., *IEEE Trans Syst Man Cybern* 25(6):933-946, 1995.
Contact: A. Caiti, Dept. of Communications, Computer and System Sciences, University of Genova, 16145 Genova, Italy

GERIATRICS

30. Falls: Epidemiology and Strategies for Prevention. Mosenthal AC, et al., *J Trauma* 38(5):753-756, 1995.
Contact: Anne C. Mosenthal, MD, Dept. of Surgery, UMDNJ-New Jersey Medical School, 185 South Orange Ave., Newark, NJ 07103

31. Prevention of Falls Among the Community-Dwelling Elderly: An Overview. Steinmetz HM, Hobson SJG, *Phys Occup Ther Geriatr* 12(4):13-29, 1994.
Contact: Helena M. Steinmetz, BSc(OT), OT(C), Dept. of Occupational Therapy, The University of Western Ontario, Elborn College, London, Ontario N6G 1H1, Canada

32. Prevention of Fractures in the Elderly: A Review. Johnell O, *Acta Orthop Scand* 66(1):90-98, 1995.
Contact: Olof Johnell, Dept. of Orthopedics, Malmo General Hospital, Lund University, S-214 01 Malmo, Sweden

33. Screening for Balance and Mobility Impairment in Elderly Individuals Living in Residential Care Facilities. Harada N, et al., *Phys Ther* 75(6):462-469, 1995.
Contact: Nancy Harada, PhD, PT, Health Services Research Assoc., Geriatric Research, Education, and Clinical Center (11G), VA Medical Center-West Los Angeles, Los Angeles, CA 90073

HEAD TRAUMA AND STROKE

34. Intervention Design for Rehabilitation at Home After Stroke: A Pilot Feasibility Study. Holmqvist LW, et al., *Scand J Rehabil Med* 27(1):43-50, 1995.

Contact: L. Widen Holmqvist, RPT, Division of Neurology, Dept. of Clinical Neuroscience and Family Medicine, Huddinge Hospital, Karolinska Institute, Huddinge, Sweden

35. Neuropharmocological Therapy and Motor Recovery After Stroke. Hassid EI, *Milit Med* 160(5):223-226, 1995.
Contact: Eric Isaac Hassid, MD, Resident in Neurology, Madigan Army Medical Center, Fort Lewis, WA 98431-5000

36. Pilot Project for Group Cognitive Retraining with Elderly Stroke Patients. Thomas KS, Hicks JJ, Johnson OA, *Phys Occup Ther Geriatr* 12(4):51-66, 1995.
Contact: Karen S. Thomas, MS, OTR, Albuquerque VA Medical Center, 2100 Ridgecrest Dr., SE, Albuquerque, NM 87108

37. Rehabilitation of Gait in Patients with Hemiplegia: A Comparision Between Conventional Therapy and Multichannel Functional Electrical Stimulation Therapy. Bogataj U, et al., *Phys Ther* 75(6):490-502, 1995.
Contact: Uros Bogataj, PhD, Laboratory of Biocybernetics, Dept. of Biocybernetics, Automation, and Robotics, Jozef Stefan Institute, Jamova 39, 61111 Ljubljana, Slovenia

MUSCLES, LIGAMENTS AND TENDONS

38. Electric Field Stimulation of Excitable Tissue. Plonsey R, Barr RC, *IEEE Trans Biomed Eng* 42(4):329-336, 1995.
Contact: Robert Plonsey, Dept. of Biomedical Engineering, Duke University, Durham, NC 27708-0281

ORTHOPEDICS

43. Ambulatory Ability After Hip Fracture: A Prospective Study in Geriatric Patients. Koval KJ, et al., *Clin Orthop* 310:150-159, 1995.
Contact: Kenneth J. Koval, MD, Dept. of Orthopaedic Surgery, Hospital for Joint Diseases Orthopaedic Institute, 301 E. 17th St., New York, NY 10003

44. Application of Computer Graphics for Assessment of Spinal Deformities. Vandergriend B, et al., *Med Biol Eng Comput* 33(2):163-166, 1995.
Contact: B. Vandegriend, University of Alberta, Dept. of Electrical Engineering, 238 Civil/Electrical Bldg., Edmonton, Alberta, T6G 2G7 Canada

45. Determination of Fracture Healing by Transverse Vibration Measurement: A Preliminary Report. Flint AJ, Nokes LDM, Macheson M, *J Med Eng Technol* 18(6):205-207, 1994.
Contact: A.J. Flint Medical Systems Engineering Research Unit, School of Electronic and Electrical Systems Engineering (ELSYM), University of Wales College of Cardiff, Cardiff, Wales, UK

46. Effect of Implant Material Properties on the Performance of a Hip Joint Replacement. Rotem A, *J Med Eng Technol* 18(6):208-217, 1994.
Contact: A. Rotem, Faculty of Mechanical Engineering, Technion-Israel Institute of Technology, Haifa 32000, Israel

47. HYOMEX: A Miniature Universal Testing Machine for In Vivo Biomechanical Studies. Hult E, et al., *J Med Eng Technol* 18(5):169-172, 1995.
Contact: E. Hult, Dept. of Orthopaedics, University of Sahlgren Hospital, S-413 45 Goteborg, Sweden

PROSTHETICS

48. Performance of Above Elbow Body-Powered Prostheses in Visually Guided Unconstrained Motion Tasks. Doeringer JA, Hogan N, *IEEE Trans Biomed Eng* 42(6):621-631, 1995.
Contact: Joseph A. Doeringer, Dept. of Mechanical Engineering, Massachusetts Institute of Technology, Cambridge, MA 02139

49. Prosthetic Fitting and Ambulation in a Paraplegic Patient with Above-Knee Amputation. Herman T, David Y, Ohry A, *Arch Phys Med Rehabil* 76(3):290-293, 1995.
Contact: Talia Herman, BPT, Dept. of Neuro-Rehabilitation, Sheba Medical Center, Tel Hashomer 52621, Israel

SPINAL CORD INJURY

50. Upper Extremity Neuropathies in Patients with Spinal Cord Injuries. Nemchausky BA, Ubilluz RM, *J Spinal Cord Med* 18(2):95-97, 1995.
Contact: Rodrigo M. Ubilluz, MD, 17 A. Kingery Quarter 202, Hinsdale, IL 60521

51. Urinary Tract Infection in Persons with Spinal Cord Injury. Cardenas DD, Hooton TM, *Arch Phys Med Rehabil* 76(3):272-280, 1995.
Contact: Diana D. Cardenas, MD, Dept. of Rehabilitation Medicine (RJ-30), University of Washington Medical Center, Seattle, WA 98195

WHEELCHAIRS and POWERED VEHICLES

52. Lifestyle Implications of Power Mobility. Miles-Tapping C, MacDonald LJ, *Phys Occup Ther Geriatr* 12(4):31-49, 1995.
Contact: Carole Miles-Tapping, PhD, OTM, OT Dept., Rehabilitation Services, Victoria General Hospital, 2340 Pembina Highway, Winnipeg, Manitoba, R3E 2E8, Canada

53. Limitations of Kinematics in the Assessment of Wheelchair Propulsion in Adults and Children with Spinal Cord Injury. Bednarczyk JH, Sanderson DJ, *Phys Ther* 75(4):281-289, 1995.
Contact: Janet H. Bednarczyk, MPE, RPT, 260 Sherbrook St., New Westminister, British Columbia, V3G 3M2 Canada

WOUNDS and ULCERS

54. Instrument to Measure the Dimensions of Skin Wounds. Jones BF, Plassmann P, *IEEE Trans Biomed Eng* 42(5):464-470, 1995.
Contact: Bryan F. Jones, Dept. of Computer Studies, University of Glamorgan, Pontypridd, Mid Glamorgan CF37 1DL, UK

55. Maggot Therapy for Treating Pressure Ulcers in Spinal Cord Injury Patients. Sherman RA, Wyle F, Vulpe M, *J Spinal Cord Med* 18(2):71-74, 1995.
Contact: Ronald A. Sherman, MD, Division of Infectious Disease and Geriatrics, Medical Service,

111-GE, VA Medical Center 5901 E. Seventh St., Long Beach, CA 90822

56. Reaction of Skin and Soft Tissue to Shear Forces Applied Externally to the Skin Surface. Zhang M, Turner-Smith AR, Roberts VC, *Proc Instn Mech Engrs—Part H: J Eng* 208(H4):217-222, 1995.
Contact: M. Zhang, BSc, MSc, Dept. of Medical Engineering and Physics, King's College School of Medicine and Dentistry, London, UK

57. Use of an In-Shoe Pressure Measurement System in the Management of Patients with Neuropathic Ulcers or Metatarsalgia. Mueller MJ, *J Orthop Sports Phys Ther* 21(6):328-336, 1995.
Contact: Michael J. Mueller, PhD, PT, Asst. Prof., Program in Physical Therapy, Washington University School of Medicine, 660 S. Euclid, Box 8502, St. Louis, MO 63110

Periodicals reviewed for
PUBLICATIONS OF INTEREST

Acta Orthopaedica Scandinavica
Advances in Orthopaedic Surgery
American Journal of Occupational Therapy
American Journal of Orthopedics
American Journal of Physical Medicine and Rehabilitation
American Journal of Sports Medicine
American Rehabilitation
Annals of Biomedical Engineering
Archives of Physical Medicine and Rehabilitation
ASHA (American Speech and Hearing Association)
Assistive Technology
Biomaterials, Artificial Cells, and Immobilization Biotechnology
Biomedical Instrumentation & Technology
Canadian Journal of Rehabilitation
Clinical Biomechanics
Clinical Kinesiology
Clinical Orthopaedics and Related Research
Clinical Rehabilitation
CRC Critical Reviews in Biomedical Engineering
DAV Magazine (Disabled American Veterans)
Disability and Rehabilitation
Electromyography and Clinical Neurophysiology
Engineering in Medicine and Biology Magazine

Ergonomics
Gait and Posture
Hearing Journal
Hearing Rehabilitation Quarterly
Hearing Research
Human Factors: The Journal of the Human Factors Society
IEEE Engineering in Medicine and Biology Magazine
IEEE Transactions on Biomedical Engineering
IEEE Transactions in Systems, Man and Cybernetics
IEEE Transactions on Rehabilitation Engineering
International Journal of Rehabilitation Research
JAMA
Journal of Acoustical Society of America
Journal of Applied Biomaterials
Journal of Biomechanical Engineering
Journal of Biomechanics
Journal of Biomedical Engineering
Journal of Biomedical Materials Research
Journal of Bone and Joint Surgery—American Ed.
Journal of Bone and Joint Surgery—British Ed.
Journal of Clinical Engineering
Journal of Electromyography and Kinesiology
Journal of Head Trauma and Rehabilitation
Journal of Medical Engineering and Technology
Journal of Neurologic Rehabilitation
Journal of Orthopaedic and Sports Physical Therapy
Journal of Orthopaedic Research
Journal of Prosthetics and Orthotics
Journal of Rehabilitation
Journal of Speech and Hearing Research
Journal of Spinal Cord Medicine
Journal of Trauma
Journal of Vision Rehabilitation
Journal of Visual Impairment and Blindness
The Lancet
Medical and Biological Engineering and Computing
Medical Engineering Physics
Medical Psychotherapy Yearbook
Medicine & Science in Sports and Exercise
Military Medicine
New England Journal of Medicine
The Occupational Therapy Journal of Research
Orthopaedic Review
Orthopedic Clinics of North America
Orthopedics
Paraplegia

Paraplegia News
Physical and Occupational Therapy in Geriatrics
Physical Medicine and Rehabilitation
Physical Therapy
Physiotherapy
Proceedings of the Institution of Mechanical Engineers—Part H: Journal of Engineering in Medicine
Prosthetics and Orthotics International
Rehab Management

Rehabilitation Digest
Scandinavian Journal of Rehabilitation Medicine
Science
Spine
Sports 'N Spokes
Techniques in Orthopaedics
Topics in Geriatric Rehabilitation
VA Practitioner
Vanguard
Volta Review

CALENDAR OF EVENTS

NOTE: An asterisk at the end of a citation indicates a new entry to the calendar.

1995

September 5-7, 1995
41st Annual Conference of the American Paraplegia Society, Las Vegas, Nevada
Contact: Mario T. Balmaseda, Jr., MD, Program Committee Chairman, American Paraplegia Society, 75-20 Astoria Boulevard, Jackson Heights, NY 11370-1177

September 5-8, 1995
2nd Leeds European Rehabilitation Conference, Neurological Rehabilitation: New Initiatives in Treatment & Measuring Outcome, Leeds, England UK
Contact: Mrs. Carol Would, Conference Secretary, Department of Continuing Professional Education, Continuing Education Building, Springfield Mount, Leeds LS2 9NG; Tel: (0532) 333232; Fax: (0532) 333240

September 8-10, 1995
4th Scientific Meeting of the Scandinavian Medical Society of Paraplegia, Oslo, Norway
Contact: Congress Secretariat, 4th Scientific of SMSOP, c/o Sunnaas Hospital, N-1450 Nesoddtangen, Norway; Tel: +47 66 96 90 00; Fax: +47 66 91 25 76

September 11-13, 1995
First Biennial Conference, Advancing Human Communication: An Interdisciplinary Forum on Hearing Aid Research and Development, Bethesda,Maryland
Contact: NIDCD; Tel: 301-496-7243; TDD 301-402-0252

September 11-19, 1995
10th Asia Pacific Regional Conference of Rehabilitation International, Indonesia

Contact: Secretariat, 10th ASPARERI, H.Hang, jebat II-2 Blok F IV, Kebayoran Baru, Jakarta 12120, Indonesia; Tel: +62 21 717 366

September 19-23, 1995
American Academy of Orthotists and Prosthetists, National Assembly (AAOP), San Antonio, Texas
Contact: Annette Suriani, 1650 King Street, Suite 500, Alexandria, VA 22314; Tel: 703-836-7116

September 20-23, 1995
17th Annual International Conference of the IEEE Engineering in Medicine and Biology Society and 21st Canadian Medical and Biological Engineering Conference, Montreal, Canada
Contact: Robert E. Kearney, PhD, Eng, Department of Biomedical Engineering, McGill University, 3775 University Street, Montreal, Quebec, Canada H3A 2B4; Tel: 514-398-6737; Fax: 514-398-7461; E-Mail: rob@neuron.biomed.mcgill.ca

September 27-30, 1995
American Academy for Cerebral Palsy & Developmental Medicine, 49th Annual Meeting, Philadelphia, Pennsylvania
Contact: AACPDM, 6300 N. River Road, Ste. 727, Rosemont, IL 60018; Tel: 708-698-1635

October 5-8, 1995
International Conference on Aging and Physical Activity: Promoting Vitality and Wellness in Later Years, Colorado Springs, Colorado
Contact: Laura Wilhelm, Human Kinetics, PO Box 5076, Champaign, IL 61825-5076; Tel: 800-747-4457 or 217-351-5076; Fax: 217-351-2674

October 9-12, 1995
Second Australian Conference on Technology for People with Disabilities, Australia
Contact: Rehabilitation Engineering, PO Box 209, Kilkenny SA 5009, Australia; Tel: (08) 243-8261; Fax: (08) 243-8208*

October 9-13, 1995
39th Annual Meeting, Human Factors and Ergonomics Society, San Diego, California
Contact: HFES, PO Box 1369, Santa Monica, CA 90406-1369; Tel: 310-394-1811; Fax: 310-394-2410; E-Mail: 72133.1474@CompuServe.com

November 2-4, 1995
Annual Scientific Meeting of the International Medical Society of Paraplegia, New Delhi, India
Contact: The Secretariat, International Medical Society of Paraplegia, National Spinal Injuries Centre, Stoke Mandeville Hospital, Aylesbury, Bucks HP21 8AL, UK; Tel: 44 296 315866; Fax: 44 296 315286

November 12-16, 1995
11th Congress of the Western Pacific Orthopaedic Association, Hong Kong
Contact: Professor SP Chow, Department of Orthopaedic Surgery, Queen Mary Hospital, Pokfulam, Hong Kong; Tel: 852 855 4258; Fax: 852 817 4392

November 15-18, 1995
National Home Health Expo, Atlanta, Georgia
Contact: Home Health Expo; Tel: 404-641-8181

November 16-20, 1995
American Academy of Physical Medicine & Rehabilitation, Orlando, Florida
Contact: Joan Cahill, AAPM&R, 122 S. Michigan Avenue, Suite 1300, Chicago, IL 60603; Tel: 312-922-9366; Fax: 312-922-6754

November 17-20, 1995
American Speech-Language-Hearing Association (ASHA), Annual Convention, Cincinnati, Ohio
Contact: Frances Johnston, ASHA, 10801 Rockville Pike, Rockville, MD 20852; Tel: 301-897-5700

November 18-22, 1995
American Academy of Physical Medicine and Rehabilitation, Annual Meeting, Orlando, Florida
Contact: AAPM&R, One IMB Plaza, Suite 2500, Chicago, IL 60611-3604; Tel: 312-464-9700

November 30-December 2, 1995
National Conference, The Association for Persons With Severe Handicaps (TASH), San Francisco, California
Contact: Tel: 410-828-TASH

December 6-10, 1995
Sixth International Neural Regeneration Symposium, Pacific Grove, California
Contact: Office of Regeneration Research Programs (151N), VA Medical Center, PO Box 1034, Portland, OR 97207*

1996

February 22-27, 1996
American Academy of Orthopedic Surgeons Annual Convention (AAOS), Orlando, Florida
Contact: AAOS, 6300 North River Road, Rosemont, IL 60018-4226; Tel: 708-823-7186; Fax: 708-823-8031

March 7-9, 1996
Twelfth International Seating Symposium, Vancouver, British Columbia, Canada
Contact: 12th International Seating Symposium, Continuing Education in the Health Sciences, The University of British Columbia, Room 105-2194 Health Sciences Mall, Vancouver, BC, Canada V6T 1Z3; Tel: 604-822-4965; Fax: 604-822-4835*

March 19-23, 1996
Conference on Technology and Persons with Disabilities, California State University, Northridge, Los Angeles, California
Contact: Conference Committee, Center on Disabilities, California State University, Northridge, 18111 Nordhoff Street, Northridge, CA 91330-8340; Tel: 818-885-2578; Fax 818-885-4929; E-Mail: LTM@CSUN.EDU

April 22-May 5, 1996
18th World Congress of Rehabilitation International Equality Through Participation—2000 and Beyond, Auckland, New Zealand
Contact: Mrs. Bice Awan, Accident Rehabilitation & Compensation, Insurance Corporation, PO Box 242, Wellington, New Zealand; Tel: +64 4 4738 775

May 12-16, 1996
The First Mediterranean Congress on Physical Medicine and Rehabilitation, Herzlia, Israel
Contact: Dr. Haim Ring, c/o Ortra Ltd., PO Box 50432, Tel Aviv 61500, Israel; Tel: 972-3-664825; Fax: 972-3-660952

May 18-23, 1996
World Congress on Osteoporosis, Amsterdam, The Netherlands
Contact: Congress Secretariat: CONGREX® Holland bv, Keizersgracht 782, 1017 EC Amsterdam, NL; Tel: +31.20.6261372; Fax: +31.20.6259574

June 7-12, 1996
RESNA '96, Salt Lake City, Utah
Contact: RESNA, 1700 North Moore Street, Suite 1540, Arlington, VA 22209-1903; Tel: 703-524-6686*

June 16-20, 1996
XXIII International Congress of Audiology, Bari, Italy
Contact: Centro Italiano Congressi-CIC Sud, Via C. Rosalba Trav. 47/E n.28, 70124 Bari, Italy*

July 1-5, 1996
9th International Conference in Medicine and Biology, Ljubljana, Slovenia
Contact: Mrs. A. Kregar, Cankarjev dom, Prešernova 10, 61000 Ljubljana, Slovenia; Tel: +386 (0) 61 125 8121, 176 71 00; Fax: +386 61 217 431*

August 7-10, 1996
7th International ISAAC Conference on Augmentative and Alternative Communication, Vancouver, British Columbia, Canada

Contact: ISAAC, PO Box 1762, Station R., Toronto, Ontario, Canada; Tel: +1 416-737-9308

August 16-27, 1996
1996 Atlanta Paralympic Games, Atlanta, Georgia
Contact: Tel: 404-588-1996

September 18-21, 1996
American Academy for Cerebral Palsy & Development Medicine, 50th Annual Meeting, Minneapolis, Minnesota
Contact: AACPDM, 6300 N. River Road, Suite 727, Rosemont, IL 60018; Tel: 708-698-1635

1997

February 13-18, 1997
American Academy of Orthopedic Surgeons Annual Convention (AAOS), San Francisco, California
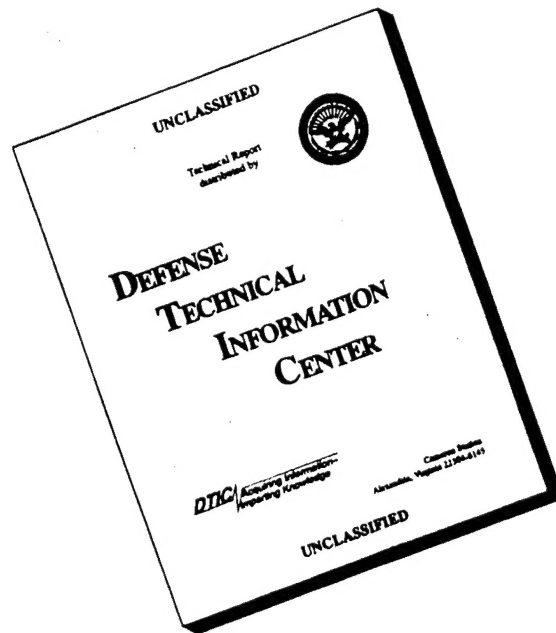*Contact:* AAOS, 1650 King Street, Suite 500, Alexandria, VA 22314; Tel: 703-836-7114

August 31 - September 5, 1997
8th World Congress of the International Rehabilitation Medicine Association IRMA, Kyoto, Japan
Contact: Japan Convention Services, Inc., Nippon Press Center Bldg., 2-1, 2-chome, Uchisaiwai-cho, Chiyoda-ku, Tokyo 100, Japan

DISCLAIMER NOTICE

JRRD On-Line

Selected portions of the *Journal of Rehabilitation Research and Development* (*JRRD*) are being put on-line via CompuServe. Abstracts of scientific articles, Calendar of Events, Publications of Interest and Progress Reports are available to readers through **JRRD On-Line**. They are also available on our BBS: (410)962-2525 or through TELNET/FTP; 199.125.193.50.

USING THE EXISTING VA REHABILITATION DATABASE ON COMPUSERVE

I. **What you need: Access to equipment and software.**
   - Personal computer

   - Modem with communication software

   - Subscription to CompuServe (connect time costs on the standard pricing plan: 2400 baud = $4.80/hour, 14400 baud = $9.60/hour).

II. **What to do:**
   - Type "GO REHAB" (or "GO HUD" and select the "Research and Development" menu option).

III. **You can get help if needed:**
   - VA Rehabilitation Database—write or call
     Scientific and Technical Publications Section
     VA Rehabilitation R&D Service (117A)
     103 South Gay Street
     Baltimore, Maryland 21202-4051
     Phone: 410-962-1800

IV. **Eligibility:**
   - The VA Rehabilitation Database is available for use by all persons interested in rehabilitation research and development.

To place an order for a *JRRD* or *Progress Reports* issue, and/or to be added to the mailing list, you may use Internet Mail: pubs@balt-rehab.med.va.gov.